SYSTEM DESIGN AND FABRICATION FOR MICROSATELLITE RELATIVE NAVIGATION EXPERIMENT

A Thesis

by

ANDREW LEWIS TUCKER

Submitted to the Office of Graduate and Professional Studies of
Texas A&M University
in partial fulfillment of the requirements for the degree of

MASTER OF SCIENCE

Chair of Committee,	Helen L. Reed
Committee Members,	Daniele Mortari
	Darren DePoy
Head of Department,	Srinivas Rao Vadali

May 2021

Major Subject: Aerospace Engineering

ABSTRACT

Satellites are a critical element of the modern world, and designers continue to increase their capability while significantly reducing their size, which has put space missions within the reach of Universities. Microsatellites in the 10-100 kg size class are now able to perform a sizable amount of tasks in a relatively small and inexpensive package. Texas A&M University's second foray into space featured a 50 kg microsatellite designed and manufactured by students within the AggieSat Lab Student Satellite Program.

AggieSat4 was the second satellite fielded by AggieSat Lab under the NASA Low-earth Orbiting Navigation Experiment for Spacecraft Testing Autonomous Rendezvous and docking (LONESTAR) campaign. The LONESTAR campaign's goal was to partner design labs from Texas A&M and the University of Texas at Austin to build pairs of satellites to perform navigation experiments. A series of four missions would culminate with the two paired spacecraft performing autonomous rendezvous and docking.

AggieSat4 was designed and fabricated from 2010 to 2015, delivered to the International Space Station in December 2015, and released into low Earth orbit in January 2016. During this process a great deal of knowledge was gained by the students as to how to design a spacecraft mission to meet a set of requirements, how to design and engineer a spacecraft to carry out this mission, and how to fabricate and assemble

the spacecraft as designed. Many tips, tricks, and lessons from hindsight were learned along the way.

The requirements and mission concept of operations development for AggieSat4 will be presented, along with the engineering design process, resulting configuration, fabrication process, and some of the tips, tricks, and lessons learned. These topics can serve as a starting guide for students and others designing their own space missions, with the goal of helping them identify the processes and items of consideration to help meet their mission requirements.

ACKNOWLEDGEMENTS

I would like to thank Dr. Mortari and Dr. DePoy for sitting on my committee, as well as for their guidance through coursework. I would also like to thank Gail Rowe for helping me navigate all the administrative aspects of the degree process.

I would like to thank my parents and family for providing the resources and preparation for my education, as well as the never ending love and support.

Thanks to Mr. David Kanipe and Mr. Darryl May of NASA's Aeroscience and Flight Mechanics Division and Johnson Space Center for starting and managing the LONESTAR program. Thanks to Mr. Joseph Perez, former AggieSat Lab director for teaching me about hardware development and spaceflight integration. Thanks to Mr. John Graves, AggieSat2 Program Manager and AggieSat Lab Manager for his leadership and for teaching me about spacecraft operations, as well as developing radio hardware for AggieSat4. And thanks to Mr. Zane Singleton for providing the technical interface between AggieSat Lab and NASA.

A great deal of gratitude goes to my friends, co-workers, and classmates who worked at AggieSat Lab on both AggieSat2 and AggieSat4. Without your hard work and dedication, we would never have been able to make these missions happen. We made a great team!

Thanks to everyone who participated at the NASA Johnson Space Center, the United States Department of Defense Space Test Program, MEI Technologies, Oceaneering Space Systems, our colleagues at the University of Texas at Austin, the

University of Houston, ISS astronauts Scott Kelly and Tim Peake, and every amateur radio operator worldwide who made this program possible end-to-end.

Thanks to groups that contributed funds and support to AggieSat4, to the Edward "Pete" Aldridge '60 Professorship, Sinclair Interplanetary, VectorNav, The Aerospace Corporation, and Lockheed Martin for their support. The team is also grateful to Boeing, SpreadSheetWorld, Microhard Systems Inc., Texas Space Grant Consortium, National Science Foundation Research Experiences for Undergraduates Program/Undergraduate Summer Research Grants Program (at Texas A&M), and Sandstorm A&M Mother's Club.

AggieSat4 would not have been possible without the dedication and professional support from Ms. Rebecca Marianno, Ms. Colleen Leatherman, Dr. Kristi Shryock, Mr. Rodney Inmon, Mrs. Yolanda Veals, Mrs. Andrea Loggins, the Physics and Astronomy Machine Shop, Dr. Rodney Bowersox (as Aerospace Engineering Department Head), Mr. David Breeding (Engineering Safety Office), Dr. Gregory Huff and the Electromagnetic and Microwave Laboratory team, and The Battalion.

And most importantly I would like to thank my committee chair Dr. Reed. I can't begin to state just how much support, encouragement, resources, and time she has freely given to me which have shaped me into the person I have become. I have been truly blessed to have had her as a mentor and friend, and any student should be so fortunate to have a teacher like her!

CONTRIBUTORS AND FUNDING SOURCES

Contributors

This work was supervised by a thesis committee consisting of Professor Helen Reed and Daniele Mortari of the Department of Aerospace Engineering. and Professor Darren DePoy of the Department of Physics and Astronomy.

Funding Sources

Graduate study was supported by a Graduate Assistant in Research position from Texas A&M University.

This work was also made possible in part by a Grant (NNJ06HG15G) from the National Aeronautics and Space Administration (NASA), which facilitated the design, manufacture, and launch of AggieSat4. These funds made possible the work of AggieSat4, but were not directed specifically for the purpose of creating this thesis. The contents of this document are solely the responsibility of the author and do not necessarily represent the official views of the NASA.

NOMENCLATURE

1U	Foundational CubeSat "unit", 1U = 10x10x10 cm cube
3U	3x 1U cube volume CubeSat, 3U = 10x10x30 cm block
α_b	Fastener coefficient of thermal expansion
α_j	Joint material coefficient of thermal expansion
Γ	Uncertainty factor
$\Delta T_{hot/cold}$	Maximum/minimum temperature a fastener experiences
A_t	Tensile area (surface area of threads engaged in fastener)
AGSL	AggieSat Lab
AGS2	AggieSat2
AGS4	AggieSat4
B	Signal bandwidth
Baud	Bits per second data rate
Bevo-2	The AggieSat counterpart spacecraft from the University of Texas
ConOps	Concept of operations
Cyclops	Deployment mechanism for releasing payloads from ISS
D	Fastener major diameter
$D_{pmin, ext}$	Heli-Coil® pitch diameter
E_b	Young's modulus for fastener material
Eb/No	Signal to noise ratio
E_j	Young's modulus for joint material

EAF	Experiment attachment fixture for the Cyclops deployment mechanism
f	Transmission frequency
F_{SU}	Joint ultimate shear strength
g	Gravitational acceleration force (9.8 m/s^2)
G_{rms}	Root-mean-square gravitational acceleration
ISIPOD	3U CubeSat canister deployment system
k	Boltzmann constant (1.38E-23 J/K)
K_B	Fastener stiffness
K_j	Joint stiffness
K_{Typ}	Nut factor
L_1	Bonded material length
L_2	Joint material length
L_e	Length of fastener thread engagement
L_{hc}	Heli-Coil® length
L_{pa}	Atmospheric absorption
L_{pp}	Precipitation loss
L_s	Free space loss
m	Mass
Mb	Megabit (10^6 bits)
MB	Megabyte (8 Mb)
MS	Margin of safety

n	Propagation loss
N_S	Number of fasteners
N_0	Noise power
nL_1	Joint force application distance
PA_t	Maximum fastener load
P_b	Axial fastener load
P	Fastener external load
$PLD_{max/min}$	Maximum/minimum fastener preload
PSCAM	The Aerospace Corporation provided camera
R	Link range
RelNav	Relative navigation
RELLIS	Texas A&M satellite campus, formerly Riverside campus
T	Torque
T_0	Noise temperature
T_R	Receiver temperature
T_P	Heli-Coil® locking torque
X, Y, Z	Primary Cartesian coordinate axes in given reference frame

ACRONYMS

ADCS	Attitude determination and control system
AFRL	Air Force Research Lab
AFSK	Audio frequency shift keying
AMP	Amplifier
ARD	Autonomous rendezvous and docking
ARM	Advanced RISC machines
BER	Bit error rate
CAD	Computer assisted drafting
CDH	Command and data handling
CG	Center of gravity
CMG	Control moment gyroscope
COMM	Communications
COTS	Commercial off the shelf
dB	Decibel
dBm	Decibel milliwatt
D/L	Downlink
DoD	Department of Defense
DRAGON	Dual RF Astrodynamic GPS Orbit Navigator
EIRP	Effective isotropic radiated power
ERP	Effective radiated power

EPS	Electrical power system
FCC	Federal Communications Commission
FEM	Finite element method
FHSS	Frequency hopping spread spectrum
FM	Frequency modulation
FSK	Frequency shift keying
GN&C	Guidance, navigation, and control
GPS	Global positioning system
G/S	Ground station
HDR	High data rate radio
HPB	Half power beamwidth
IC	Integrated circuit
IMU	Inertial measurement unit
ISIS	Innovative Solutions In Space
ISS	International Space Station
ITU	International Telecommunications Union
JAXA	Japan Aerospace Exploration Agency
JEM	Japanese Experiment Module
JSC	NASA Johnson Space Center
LDR	Low data rate
LEO	Low Earth orbit
LI-ION	Lithium ion (battery)

LNA	Low noise amplifier
LONESTAR	Low Earth Orbiting Navigation Experiment for Spacecraft Testing Autonomous Rendezvous and Docking
M2O-X	Mission two objective #X
MEI	Merging Excellence and Innovation Technologies
MR-X	Mission requirement #X
MSC-X	Minimum success criteria #X
NAS	National Aerospace Standard
NASA	National Aeronautics and Space Administration
NF	Noise figure
NORAD	North American Aerospace Defense
OA-4	Orbital ATK Cygnus Cargo Vehicle
PBER	Packet bit error rate
PCB	Printed circuit board
PLR	Packet loss rate
PSD	Power spectral density
PSI	Pounds per square inch
RAM	Random access memory
RCS	Reaction control system
RF	Radio frequency
RFIC	Radio frequency integrated circuit
RMS	Root mean square

RPM	Revolutions per minute
RW	Reaction wheel
SD	Secure digital memory format
SMA	Subminiature version A coaxial connector
SMTRS	Structures, mechanisms, thermal, and radiation systems
SNR (Eb/No)	Signal to noise ratio
SOH	State of health
SSIKLOPS	Space Station Integrated Kinetic Launcher for Orbital Payload Systems (now Cyclops)
STARE	Space-Based Telescopes for the Actionable Refinement of Ephemeris
STM	Space Traffic Management
STS	Space Transportation System (Space Shuttle)
TAMU	Texas A&M University
TC	Torque Coil
TNC	Terminal node controller
TPI	Threads per inch
TX/RX	Transmit/receive
UHF	Ultra-high frequency radio band
USB	Universal serial bus
UT	The University of Texas at Austin
UTS	Ultimate tensile strength

UTJ	Ultra triple junction
VDCS	Visual data capture system
VHF	Very high frequency radio band
VNS	Visual navigation system
VSWR	Voltage standing wave ratio

TABLE OF CONTENTS

Page

LIST OF FIGURES

Page

LIST OF TABLES

Page

1. INTRODUCTION

Satellites play a crucial role in modern society, facilitating global communications, entertainment, navigation, security services, and countless other capabilities that most people take for granted on a day-to-day basis. As resources for spacecraft are always constrained, the global trend is toward designing and manufacturing spacecraft that are smaller, while being as capable if not more so than their predecessors. To give some perspective, more traditional spacecraft have been on the order of 1000-5000 kg with dimensions in the 10s of meters, and current thinking is toward spacecraft on the order of 300 kg or less with body dimensions under 2 meters. Leadership at the Defense Innovation Unit and Air Force Research Lab (AFRL) believe that the current market trend is to utilize large constellations of small satellites to provide both government and commercial services [1]. A distributed system of small spacecraft may offer new mission concepts to meet requirements, may offer advantages in economies of scale related to manufacturing and the supply chain, may offer advantages in launch costs and available opportunities, is less prone to single point of failure issues, can be incrementally improved as technology advances, can be replenished in the event of single-unit failures, and is more hardened against adversary actions than a single highly capable relatively large spacecraft.

With recent advances by nations such as China and Russia, the unparalleled advantage that the United States has held in space is being steadily eroded [2]. Moreover, as of today, some 72 nations have a space program, and eight countries

along with the European Space Agency have the ability to launch objects into space [3]. In response, the Department of Defense has adopted a space policy to leverage the unmatched innovation of the American commercial space industry to provide solutions as space becomes more and more congested, contested, and competitive [2, 4, 5]. This strategy requires that the United States engages the best talent. Satellite design labs at universities provide some of the most effective means of training students to be competent engineers, ready to enter the workforce and contribute to the solutions of utilizing space to improve the lives of people around the world, and to challenge the actions of bad actors.

Universities have been leaders in developing small satellites and small satellite technologies. Prior to 2015, the roughly 75% of microsatellites (spacecraft under 100 kg) and nanosatellites (spacecraft under 10 kg) launched and operated were from University programs, and it was not until 2015 that commercial industry began to field the majority of small vehicles [6]. The CubeSat standard developed by California Polytechnic State University (Cal-Poly) San Luis Obispo had a dramatic effect towards standardization in this industry, defining spacecraft by size and mass constraints [7]. This standardization has led to a significant increase in the number of small satellites launched each year [6]. Very common sizes have been "1U" (10x10x10 cm) and "3U" (10x10x30 cm), though larger sizes exist [8].

Texas A&M University's AggieSat Lab (AGSL) has worked with NASA, the AFRL University Nanosatellite competition, and Lawrence Livermore National Labs/Naval Postgraduate School in various projects in small spacecraft design. Under

the NASA program, AGSL produced two small spacecraft to test navigation experiments and train University students on spacecraft design and fabrication [9]. With Lawrence Livermore National Labs, AGSL participated in the design and engineering analysis of the STARE (Space-based Telescopes for the Actionable Refinement of Ephemeris) 3U CubeSats in , an orbital debris tracking demonstration and space traffic management (STM) experiment [10][12][13]. AGSL continues to participate in the AFRL University Nanosatellite competition, with its most recent entry being AggieSat 6 whose planned missions are the demonstration of an on-orbit satellite locator and the collection of radiation data.

AGSL is a student led spacecraft design laboratory, with a focus on developing the skill sets of students. In this endeavor, AGSL has had the opportunity to design, build, launch, and operate two small spacecraft through a partnership with the National Aeronautics and Space Administration (NASA) through the LONESTAR program.

LONESTAR (Low Earth Orbit Navigation Experiment for Spacecraft Testing Autonomous Rendezvous and docking) was a NASA program to partner the student spacecraft labs of TAMU and the University of Texas at Austin (UT) to produce a series of spacecraft that incrementally developed skills, methods, and techniques to culminate in Autonomous Rendezvous and Docking (ARD) between spacecraft from both labs. Both Universities each flew two spacecraft missions as part of the program.

The first pair of spacecraft were AggieSat2 (AGS2) and Bevo-1, both 5 in. DoD standard CubeSats deployed from Space Shuttle Endeavor on STS-127 (deployed July 15, 2009, re-entry March 17, 2010). The purpose of these two spacecraft was to give

each lab experience in building spaceflight hardware, as well as to test a new GPS receiver developed by NASA. Due to a possible stabilizing magnet polarity misalignment and a spring loaded antenna, the two spacecraft did not completely separate after deployment from their spring-loaded canister. While the two did not separate completely, the spring separation mechanism did force them apart sufficiently to remove the AGS2 electrical inhibit and allow for it to activate. Unfortunately, Bevo-1 never turned on. Even though the antenna was unable to fully deploy, reduced ground communication was still possible, and health status and GPS data were able to be recorded and transmitted for much of the flight. The two spacecraft remained conjoined until their re-entry according to NORAD.

Figure 1: Bevo-1 (left) and AGS2 (right)

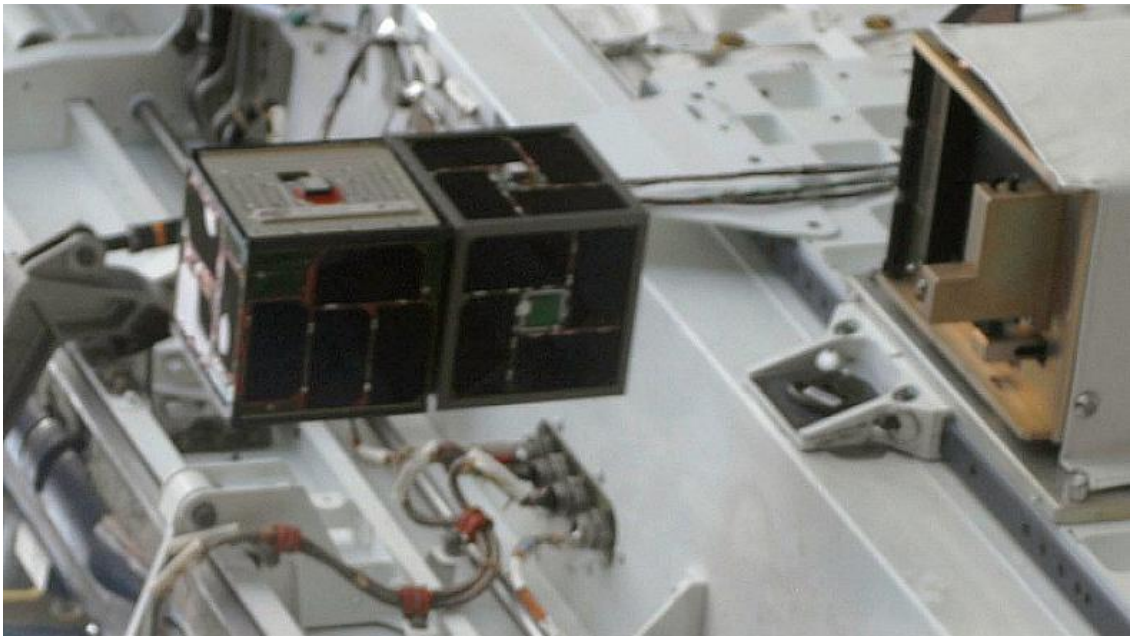

Figure 2: Failure of Separation on Deployment (Photo by NASA)

The second mission consisted of spacecraft named AggieSat4 (AGS4) and Bevo-2. The purpose of this mission was to again test the GPS receiver model, as well as to perform relative navigation and attitude control demonstrations. AGS4 was a larger 50 kg class vehicle, while Bevo-2 was a standard 3U CubeSat to be deployed from AGS4. Both were launched to the International Space Station (ISS) as a combined unit aboard Orbital OA-4, and deployed from the Station on January 29, 2016.

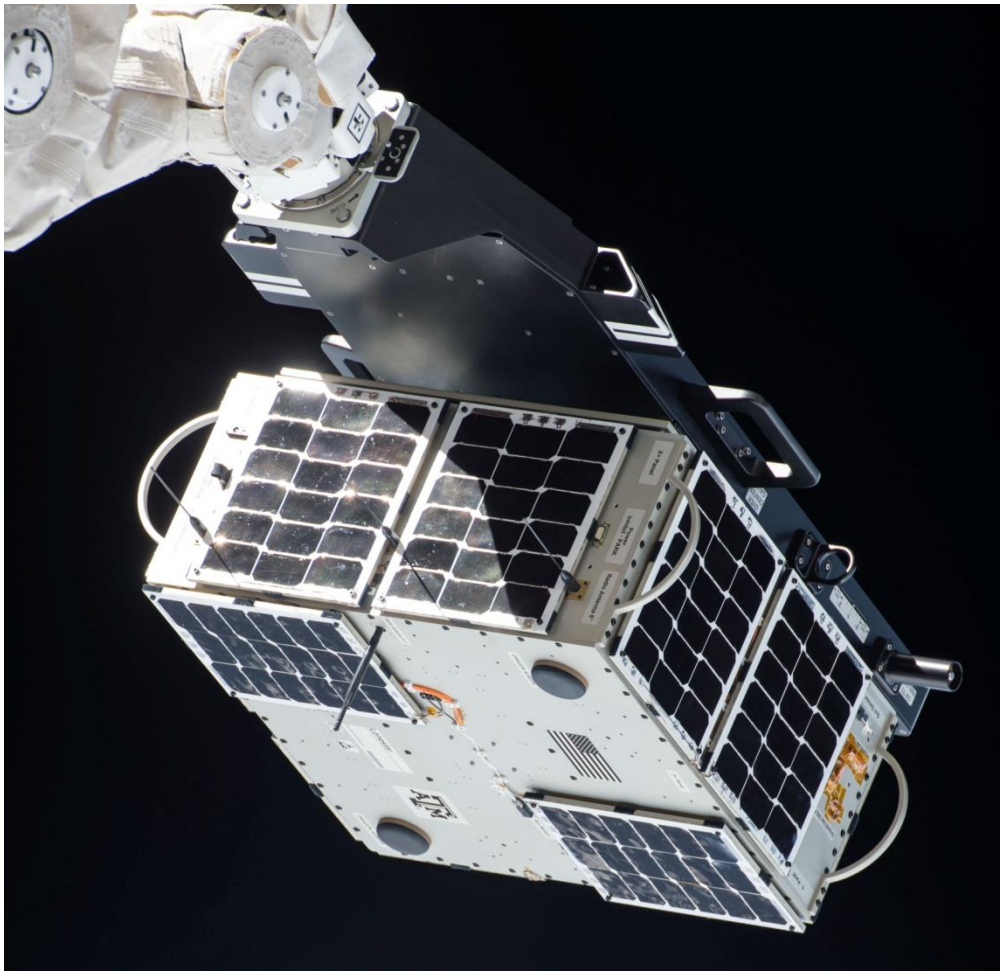

Figure 3: AGS4 Deploying from ISS (Photo by NASA)

Unfortunately, technical problems prevented the mission demonstration from occurring. Bevo-2 was released without being commanded, and two separate objects were tracked by NORAD. As the release system was three fault tolerant and had been tested thoroughly, the suspected cause of this release was mechanism failure with the commercial off the shelf (COTS) payload deployer due to repeated thermal cycles beyond what the deployer had been tested to by the manufacturer. AGS4 also experienced problems in that the computer memory would fill up after ~52 hours,

forcing a reset. Beacons stopped being received after about 7 days after deployment, and this situation was unresolved at the time of re-entry on March 12, 2018.

The subsequent sections of this document detail the design of the mission and spacecraft, assembly, testing, and operation of AGS4. Additionally, many lessons learned and other information are provided that will be helpful to AGSL students as they prepare to design, build, and fly spacecraft of their own.

2. DESIGN PROCESS AND RESULTING CONFIGURATION

2.1. Mission Requirements

Mission requirements are the driving factor shaping the design of any satellite or its mission. They are the means by which the customer (NASA) defines what they want to happen. These definitive requirements are then refined by both the design team and the customer into a set of derived requirements that dictate how the mission is designed, what the spacecraft will do, and how it will be designed to do these things.

One note regarding the verbiage of the requirements is that they use the word "will", where they should instead use "shall". While many may view the words as interchangeable, from personal experience working with the United States government since the end of this project, it has been learned that "shall" is the preferred word as "will" implies some degree of uncertainty to some groups. For the purposes of this thesis, the language in the requirements was left as agreed to at the time by all parties for this project in order to document the requirements as worked to.

2.1.1. NASA Defined Requirements

The requirements provided by NASA were in the form of mission objectives, and are outlined in the table below. These mission objectives applied to both the AGSL and UT teams, as the two were partners for these missions. As the AGS4 mission was the second in the LONESTAR campaign, they were given an M2O designation.

Table 1: AGS4 Mission Objectives

-	**Mission 2 Objectives (M2O)**
M2O-1	Both teams will evaluate sensors including but not limited to: Global Positioning System (GPS) receivers, Inertial Measurement Units (IMU), rate gyros, and accelerometers.
M2O-2	Both teams will evaluate a 1st generation Reaction Control System (RCS).
M2O-3	Both teams will work together to evaluate a 1st generation Guidance, Navigation and Control (GN&C) system including guidance algorithms, absolute navigation, and relative navigation.
M2O-4	Both teams will work together to evaluate communications capabilities between two spacecraft and from each spacecraft to their ground stations.
M2O-5	Both teams will evaluate the capability to take video.
M2O-6	Each University will select two members to create and organize an interface monitoring function in order to maintain robust and productive communications between the university teams and oversight members: NASA and MEI Technologies.
M2O-7	Each spacecraft will have three-axis stabilization.
M2O-8	Both teams will work together to evaluate GN&C system interfaces and compatibility and the testing required for these systems.

Using these mission objectives, the two teams and NASA management derived the following set of mission requirements which were used to shape the design of AGS4 and the mission.

Mission requirements often trace back to the set of customer defined requirements (M2O's) to show that they are being met. In this case, each M2O should have at least one MR tracing to it to show that the requirement is being met. However, some other derived requirements are more operational constraints such as the envelope and mass constraints outlined below, which were dictated by the available NASA resources provided to the program. The table below details the derived mission requirements, and how they trace to the M2O.

Table 2: Derived Mission Requirements

	Mission Requirements	Trace-ability	AGSL Verification Process
-	**Satellite Envelope Requirements**		
MR-1	The entire LONESTAR envelope is not to exceed the maximum dimensions of the NASA deployment system for the Japanese Aerospace Exploration Agency (JAXA) Japanese Experiment Module (JEM) airlock on the International Space Station (ISS).		**Analysis**- evaluate CAD model **Lab testing**- measure assembled structure
-	**Satellite Mass**		
MR-2	The entire LONESTAR mass is not to exceed 100 kg.		**Lab testing**- weigh integrated structures
MR-3	AggieSat4 shall not exceed 50 kg.		**Analysis**- evaluate CAD model **Lab testing**- weigh assembled structure
MR-4	Bevo-2 shall not exceed 35 kg.		-
MR-5	This project will follow the standard project management schedule.		**Documentation**- Integrated project schedule
MR-6	Each University team will select two members to create and organize an interface monitoring function in order to maintain robust and productive communications between the university teams and oversight members: NASA and MEI Technologies.	M2O-6	Enforced by lab management. Email communication and weekly telecoms between both Universities and JSC.

Table 2: Derived Mission Requirements (Continued)

	Mission Requirements	Trace-ability	AGSL Verification Process
-	**GN&C System**		
MR-7	Each spacecraft will have three-axis stabilization capability and demonstrate it.	M2O-1 M2O-2 M2O-7	**Analysis-** simulate space environment and control disturbances in Simulink® **On orbit-** attitude sensor data will be gathered while AGS4 tracks Bevo-2.
MR-8	Both teams will work together to evaluate any GN&C system interfaces and compatibility and the testing required for these systems.	M2O-1 M2O-2 M2O-3 M2O-8	**Lab testing-** Crosslink testing exchanges navigation solutions.
MR-9	Each team will evaluate and test an additional component that will be needed for the next generation of their spacecraft and the final mission.	M4O-1	**Analysis-** Ensure that design includes components to test next generation capability.
MR-10	Each team will evaluate and test portions of their future generation control system algorithms.	M2O-2 M2O-3 M3O-2 M3O-3	**On orbit-** AGS4 will demonstrate active tracking capability.
-	**Communications**		
MR-11	Each spacecraft will communicate with the ground station, both directions.	M2O-4	**Lab testing-** simulate mission communications using ground station hardware **On orbit-** AGS4 will send packets and receive commands from the Ground Support team

Table 2: Derived Mission Requirements (Continued)

	Mission Requirements	Trace-ability	AGSL Verification Process
MR-12	Each spacecraft will communicate with the other when separated.	M2O-4 M2O-8	**Lab testing-** Joint simulated crosslink testing will be done prior to integration **On orbit-** AGS4 will crosslink navigation information with Bevo-2 after the release event
MR-13	Each satellite will exchange its GPS solution with the other satellite.	M2O-1 M2O-4 M2O-8	**Lab testing-** Joint simulated crosslink testing with GPS packets will be done prior to integration **On orbit-** AGS4 will crosslink its GPS solution information with Bevo-2 after the release event
MR-14	Each spacecraft will evaluate the viability and capability of downloading captured visual evidence.	M2O-5	**Lab testing-** AGS4's camera will capture an image with its camera and downlink the image to the ground station hardware **On orbit-** AGS4 will capture visual evidence of the release event and downlink the images to the Ground Support team

Table 2: Derived Mission Requirements (Continued)

	Mission Requirements	Trace-ability	AGSL Verification Process
-	**Payloads**		
MR-15	Each spacecraft will carry a GPS system for use in determining the viability of navigation solutions for the final mission.	M2O-1 M2O-2 M2O-3 M2O-8 M4O-1	**Lab testing-** a GPS system will be used
MR-16	Each spacecraft will downlink GPS data for the NASA team to be able to evaluate the operation of the receiver.	M2O-1 M2O-2 M2O-3 M2O-4	
-	**General Capabilities**		
MR-17	The two spacecraft will separate from each other.		
MR-18	Each spacecraft will take and downlink video or still photographs.	M2O-4 M2O-5	
MR-19	Once separated, each spacecraft will provide Relative Navigation (RelNav) solutions.	M2O-1 M2O-2 M2O-3 M2O-4 M2O-8 M3O-2	

2.1.2. Minimum Success Criteria

With these derived mission requirements agreed to by both satellite teams and NASA management, the two teams then further refined the MR into a series of Minimum Success Criteria (MSC). These are codifications of what each spacecraft will do in order to meet the MR, and define the mission concept of operations. These derived MSC's are outlined in the table below.

Table 3: Minimum Success Criteria

-	**Minimum Success Criteria (MSC)**	**Trace-ability**
MSC-1	The LONESTAR-2 spacecraft will demonstrate the on-orbit performance of the three-axis stabilization systems to an accuracy described by MSC 1.1 and MSC-1.2 for the Bevo-2 and AggieSat4 the spacecraft, respectively.	MR-7
MSC-1.1	Bevo-2 will conduct two different confirmations: image and 3-axis stabilization confirmation. Image confirmation will consist of pointing at an object and capturing an image 150 seconds apart, then downlinking both images. 3-axis stabilization will consist of recording all ADCS data and downlinking all pertinent information.	MSC-1
MSC-1.2	The AggieSat4 spacecraft will demonstrate the on-orbit performance of its three-axis stabilization system to an accuracy adequate to accomplish one of the maneuvers contained within MSC-3.2.	MSC-1
MSC-2	Each LONESTAR-2 spacecraft will demonstrate the on-orbit performance of its "additional component".	MR-9
MSC-2.1	Bevo-2 shall verify basic functionality and characterize the performance of the cold-gas thruster system using GPS and IMU measurements.	MSC-2
MSC-2.2	AggieSat4 will downlink carrier phase GPS data from two onboard GPS antennas. This will enable an accurate RelNav vector between the two antennas to be computed and analyzed on the ground. **-OR-** AggieSat4 will demonstrate enhanced communications speeds for the downlinking of video and image data.	MSC-2
MSC-3	Each LONESTAR-2 spacecraft will demonstrate the on-orbit performance of the future generation control system algorithms.	MR-10

Table 3: Minimum Success Criteria (Continued)

-	Minimum Success Criteria (MSC)	Trace-ability
MSC-3.1	Bevo-2 shall demonstrate minimum success of the future generation control system algorithm by performing one of the following two actions: 1) After initialization, Bevo-2 shall actively point the Visual Navigation System (VNS) towards the AggieSat4 using crosslinked GPS relative position solutions with the performance data downlinked for evaluation. 2) A series of preprogrammed reorientation and translational maneuvers shall be executed with the performance data downlinked for evaluation.	MSC-3
MSC-3.2	AggieSat4 will demonstrate future generation control system algorithms with the successful execution of one of the following maneuvers, with the first being the primary objective: 1) AggieSat4 will actively track Bevo-2 using crosslinked GPS data until Bevo-2 is out of range for crosslink. 2) AggieSat4 will actively track dummy propagated GPS data once every second for a period of time equivalent to Bevo-2 being "out-of-range" based on the release speed and direction. 3) AggieSat4 will hold a target object (such as the Moon and Earth) in the field of view of the spacecraft's camera for a minimum of fifteen (15) seconds. Photographs of the object with timestamps should be downloaded to confirm.	MSC-3
MSC-4	Each LONESTAR-2 spacecraft will be capable of receiving commands, acting upon those commands, and downlinking a response within a reasonable amount of time.	MR-11
MSC-5	Each LONESTAR-2 spacecraft will send to and receive from the other, and then validate a "dummy" DRAGON GPS preloaded data file after separation.	MR-8 MR-12
MSC-6	Each LONESTAR-2 spacecraft will send to and receive from the other, and then assess fifty (50) GPS state solutions.	MR-8 MR-12 MR-13 MR-15 MR-19

Table 3: Minimum Success Criteria (Continued)

-	Minimum Success Criteria (MSC)	Trace-ability
MSC-7	Each LONESTAR-2 spacecraft will collect and downlink images at a minimum resolution of 1024x768.	MR-14 MR-18
MSC-8	Each LONESTAR-2 spacecraft will collect and downlink at least two (2), not necessarily consecutive, orbits' worth of DRAGON GPS data for delivery to the NASA DRAGON GPS development team.	MR-15 MR-16
MSC-9	Each spacecraft will confirm the separation event between the two LONESTAR-2 spacecraft through direct observation.	MR-8 MR-14 MR-17 MR-18
MSC-10	Each LONESTAR-2 spacecraft will exchange 50 RelNav solutions with the other.	MR-8 MR-12 MR-13 MR-15 MR-19
MSC-11	Each LONESTAR-2 spacecraft will downlink complete state of health data to the ground at a rate which constitutes a reasonable amount of time between transmissions.	MR-11 MR-20

2.2. Concept of Operations and Mission Architecture

Using the MR and MSC as the shaping forces, the AGSL and UT teams developed a concept of operations (ConOps) for the mission, outlining what tasks should be performed and in what order. The mission profile begins with AGS4 being launched to the ISS as soft-stowed cargo. After arriving at the ISS, AGS4 would then be unpacked by the astronauts. Using the Cyclops (formerly SSIKLOPS, Space Station Integrated Kinetic Launcher for Orbital Payload Systems) Experiment Attachment Fixture (EAF), AGS4 would be locked onto the Cyclops deployment table, which would release the payload from the end of a robot manipulator arm. Cyclops would exit the

ISS via Japanese JEM airlock, where the robot arm would maneuver it into place before activating the release mechanism.

Upon release, solar power would activate the power system, which would begin the boot-up of the computer system. Additionally, EPS would contain a module that houses three separate timer circuits to prevent Bevo-2 from being released while too close to ISS. All three timers would have to reach or exceed the value in order for the computer to be able to command the Bevo-2 release.

After initial boot up, AGS4 would collect and process telemetry and health status information, and transmit it in a beacon once every six seconds. This data would provide a snapshot of the current status of AGS4 components, as well as provide a location indicator for tracking purposes. Using these beacons, communications would be established by the ground station, and all state of health data downloaded. AGS4 would then be commanded to begin its collection of the two orbits of GPS data per MSC-8 for download at the next ground pass.

After downlinking the GPS data, which would take multiple ground passes to download, both the AGSL and UT teams would prepare to initiate the RelNav experiment. AGS4 would then be commanded to begin the RelNav process. After ensuring that Bevo-2's batteries were topped off, AGS4 would orient to 90° off of the velocity vector and release Bevo-2, as this release vector provides the most time in radio range with each other and several re-contact opportunities. AGS4 would use a camera to image the separation. The operations to this point would take sufficient time that the timers would no longer inhibit the deployment.

After deployment, the inhibit switches on Bevo-2 would close and allow it to boot-up. Crosslink radios would be used to exchange GPS solutions between the spacecraft. As GPS receivers can take several minutes to converge on a navigation solution, especially at orbital speeds, the crosslinked AGS4 solution would be used to "hot start" the Bevo-2 receiver. Once both spacecraft achieve navigation solutions, AGS4 and Bevo-2 would use the location of the other to calculate the relative position of the other with respect to themselves, and point and track the other as they progress through the orbit. This scenario would demonstrate both RelNav and attitude control.

In case something went wrong with the crosslinking, AGSL developed a contingency plan to track a simulated Bevo-2 using a propagated solution, and exercise point-and-hold maneuvers. AGS4 would also image the Earth and Moon for a visual confirmation of pointing stability.

Primary or contingency location data for both spacecraft, and attitude data and imagery from AGS4 would be downloaded over the next several orbits, as the expected data generated would exceed what can be expected in a single pass. The position and pointing data would be used to verify that AGS4 tracked Bevo-2, and the images would verify the separation.

After all RelNav experiment data was downlinked, the remaining life of the spacecraft would be spent downlinking extra captured images, the complete state of health record, and practicing further control maneuvers by imaging Earth and other celestial objects.

2.3. Trade Study Process

A trade study is a means of comparing options for processes, systems, or individual components against others of their type in order to determine a solution that best fulfills the mission requirements. Sometimes the most capability is not best for the job at hand, and "better is the enemy of good".

For all things being compared, the trade study begins by listing all options being considered to fulfill the mission requirements, along with their attributes being compared. A table format can help for visualization.

First, any options that do not meet any of the mission requirements are removed. Then, the attributes of each option are compared to those of the other candidates, and ranked. The designers will need to use the mission requirements as a guide to determine which attributes carry the most weight. Color coding cells can be used if helpful. The option that has the most positives and fewest drawbacks is usually apparent after ranking. However, some subjective factors such as personnel experience with a particular option, or company reputation and past experience should be considered too as they can produce a smoother path to the end goal, which can definitely be worth not going with the "perfect" approach on paper.

The example covered below outlines the process followed to determine in which radio band AGS4 should seek a license to operate. Subsequent trade studies were then performed in the same manner to determine the hardware selection. This same process is equally applicable to all subsystems and other areas of the spacecraft design decision-making process.

The Communications team considered three different frequency bands to use for AGS4. These were Commercial UHF/S-band, Experimental S-band, and Experimental Amateur VHF/UHF. The frequency bands had differing characteristics as laid out in the table below.

Table 4: Comm Frequency Band Trade Study Example

	Commercial UHF/S-band	**Experimental S-band**	**Experimental Amateur VHF/UHF**
License Cost	$50,000+	$65	$65
License Lead Time	6-12 mo.	3-6 mo.	3-6 mo.
Equipment Cost	$100's-$1000's	$100's-$1000's	$100's
Worldwide Receiver Availability	Pay-per-use	Limited	Common, Amateur radio operator volunteers
Dedicated Frequency?	Yes	No, shared with other users	No, shared with other users
AGSL Ground Station Modifications required?	Yes	Yes	Minimal
Encryption Legal	Yes	No	No
Signal Propagation Loss	Low	Low	Very Low
Interference Level at Ground Station	Very Low	Very Low	Very Low

Commercial frequencies, while benefiting from not requiring the sharing of the airwaves with other users, were almost immediately discarded due to the high regulatory cost, which would have placed significant pressure on the program budget. Choosing between the remaining two was not difficult, as the large number of amateur operators worldwide willing to provide communications services, and not needing to modify the AGSL ground station were huge positive factors. The largest drawback to using

frequencies that overlap with Amateur bands is the potential for interference at the receiving station. Experience with AGS2, and measurements in the rural setting of the ground station on the Riverside Campus (now RELLIS) indicated that the risk of interference was unlikely and could be worked around.

In this manner, the AGS4 team determined that using Amateur VHF (144 MHz) and UHF (440 MHz) bands with Experimental authorization would produce a communications system with the greatest chance of successful throughput and mission data retrieval.

2.4. Spacecraft Design

Engineering design is a multi-iteration process to determine a vehicle platform design that meets all MR and MSC. The design is often split into subsystem engineering teams responsible for an aspect of the vehicle. The process is iterative because no subsystem is an island, and any change to one of them can have significant repercussions on all the rest. For instance, if it is determined that a navigation sensor or antenna is located in a position where it will be ineffectual, moving it to a better location could impact the number of solar panels that can be fitted to that face, and as a result every system now has less power with which to accomplish its tasks. Almost every change or adjustment has downstream effects, particularly to the vehicle mass and center of gravity (CG). The following sections outline the six spacecraft subsystems and how they were developed into the final flight configuration.

The decision was made to use U.S. Customary units for the design of mechanical systems and hardware on AGS4, and to use the Metric system for analysis and

calculations. This decision was made because the majority of machine shops and tools available in the United States use Customary units, making it far easier for AGSL to source parts, have pieces machined, and source fasteners. Metric units were used on analyses as students were more familiar with them for engineering calculations from coursework. This arrangement was acceptable to the NASA management as it is commonly implemented at NASA, and was reflected in the documentation and data shared with AGSL. The following sections will present quantities such as mechanical dimensions and fastener torque using Customary units, and results from analyses such as displacements, temperatures, and mesh sizes are in Metric (though sometimes both are indicated for clarity).

2.4.1. Structures, Mechanisms, Thermal, and Radiation Systems (SMTRS)

The main role of the SMTRS team was to design and analyze the AGS4 structure to include bus design and component locations, as well as thermal and loads analysis.

2.4.1.1. Bus Design

AGS4 was designed to host the COTS ISIPOD CubeSat dispenser provided by UT to release Bevo-2 for the RelNav experiment. This design constraint was central to the design process of AGS4, as the bus was practically built around the ISIPOD.

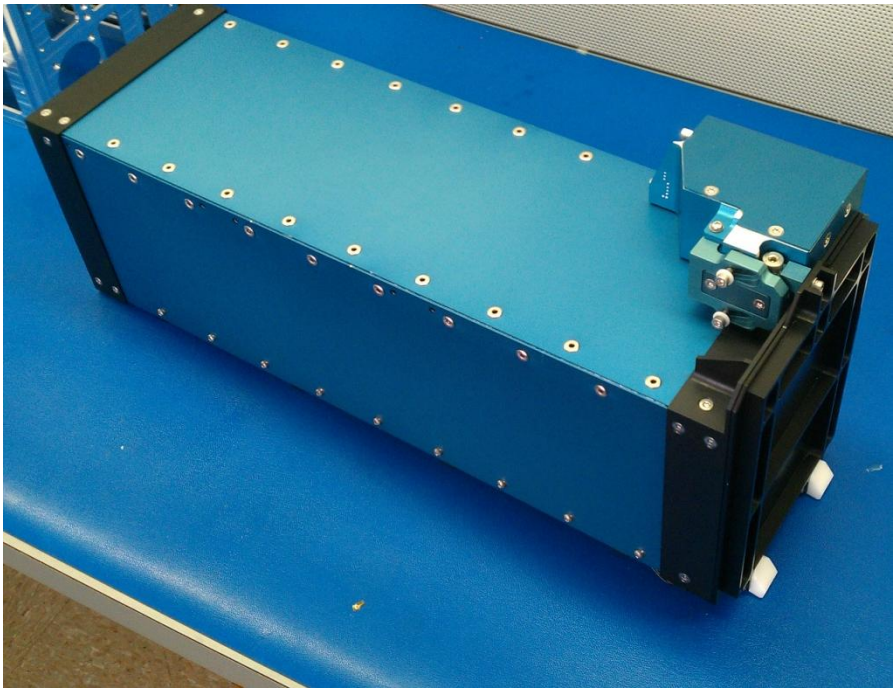

Figure 4: ISIPOD CubeSat Deployment System

Since the beginning of the project, the AGS4 design has been a box shape of the approximate maximum dimensions allowable by the Japanese JEM airlock. There have been several design iterations as subsystem designs mature, all focusing on maintaining the necessary balance for the attitude control system to function properly. This was accomplished by a combination of logic, trial, and error, arranging the subsystem components and wiring in different configurations until the center of gravity (CG) was in the appropriate zone. The Cyclops deployment mechanism required that the AGS4 CG fall within 0.25" from the center of the EAF in the X and Y axes, with no restriction on the Z axis. The figure below outlines the component placement from a top view that achieved this balance.

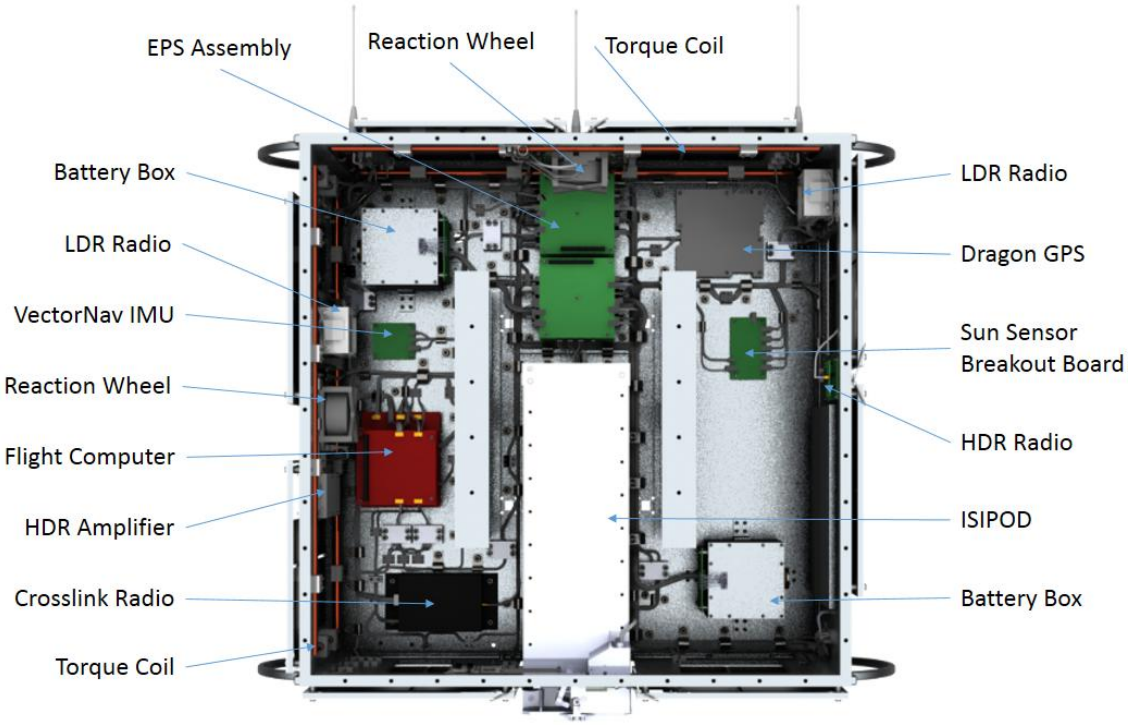

Figure 5: AGS4 Component Placement

It was also important to have the CG close to the center of the force vector created by Bevo-2's release, as being significantly off would impart a torque to AGS4 that could rotate the vehicle such that the camera no longer had Bevo-2 in the field of view. ADCS determined that the AGS4 CG would need to be within 0.5" from the ISIPOD force vector to tolerate the rotational forces. Furthermore, it was desirable to have the spacecraft CG be as close to the geometric center as possible so that the vehicle dynamics changed the least amount after Bevo-2 deployment. In order to achieve this CG location, it was necessary to raise up the ISIPOD launcher such that it met the CG, as lowering the CG was not practical past a certain point. In order to preserve the mass budget and control authority, this elevation block would need to be lightweight. With

significant cut outs, the spacer block was light enough and strong enough to bring Bevo-2 up to the CG line. The spacer block is shown in the figure below.

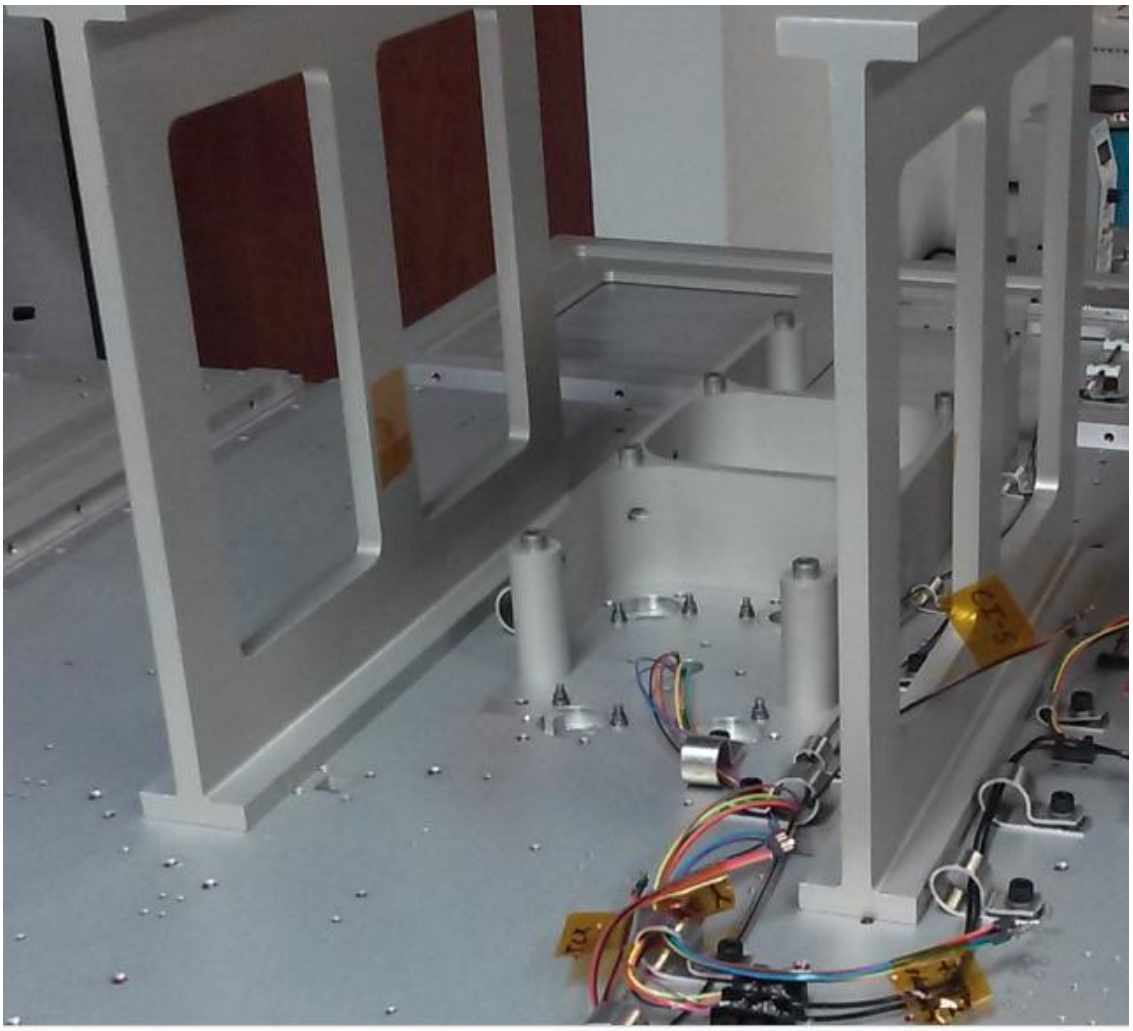

Figure 6: ISIPOD Spacer Block and I-Beams

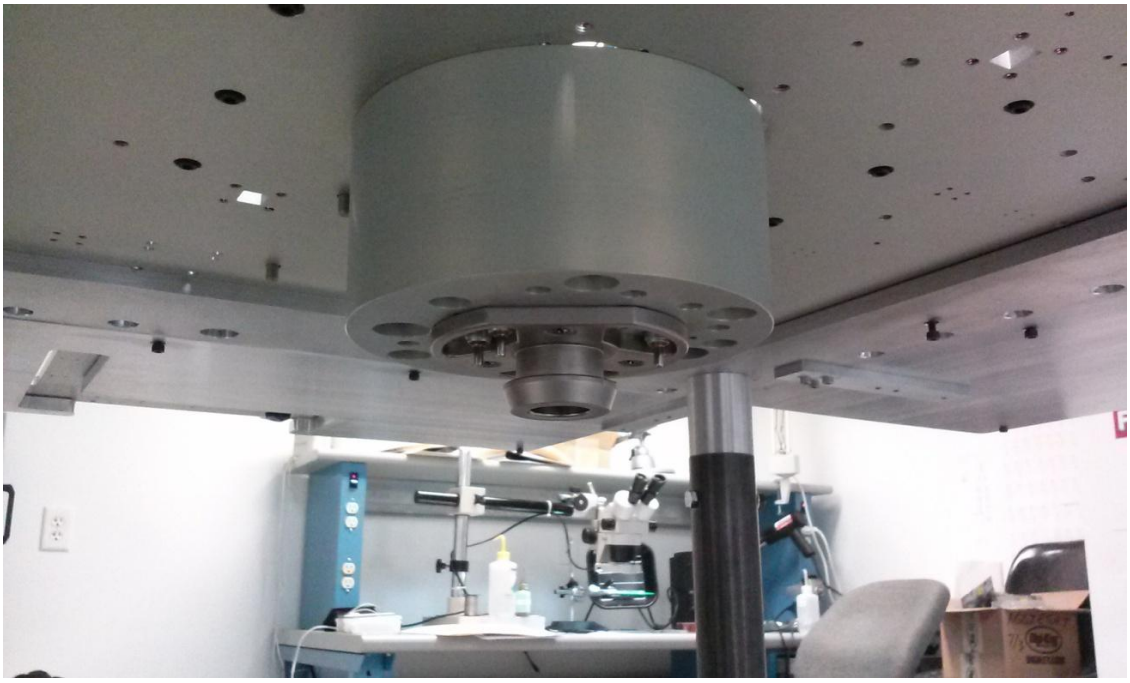

Figure 7: Cyclops EAF and Spacer

Also seen in Figure 6 above are two "I-beam" structural supports. These supports were added to strengthen the vehicle as initial analysis indicated that the +Z face would sag significantly under launch loads, and the natural frequency was closer to that of the launch vehicle.

The final result of AGS4 was a vehicle with a deployment envelope of 32.2" x 29.3" x 20.2" including all protrusions and attachments such as antennas and the Cyclops EAF. The positions of these protrusions were such that they still satisfied the airlock envelope clearance requirements [14]. The motion of the airlock door is such that a box of these dimensions would not fit, but limited protrusions on certain sides do not cause interference. The figures below outline the bus and protrusion dimensions, as well as the

coordinate system directions. In this coordinate system, the panel with the EAF is the -Z face, and the panel with the ISIPOD protruding out is the -X face.

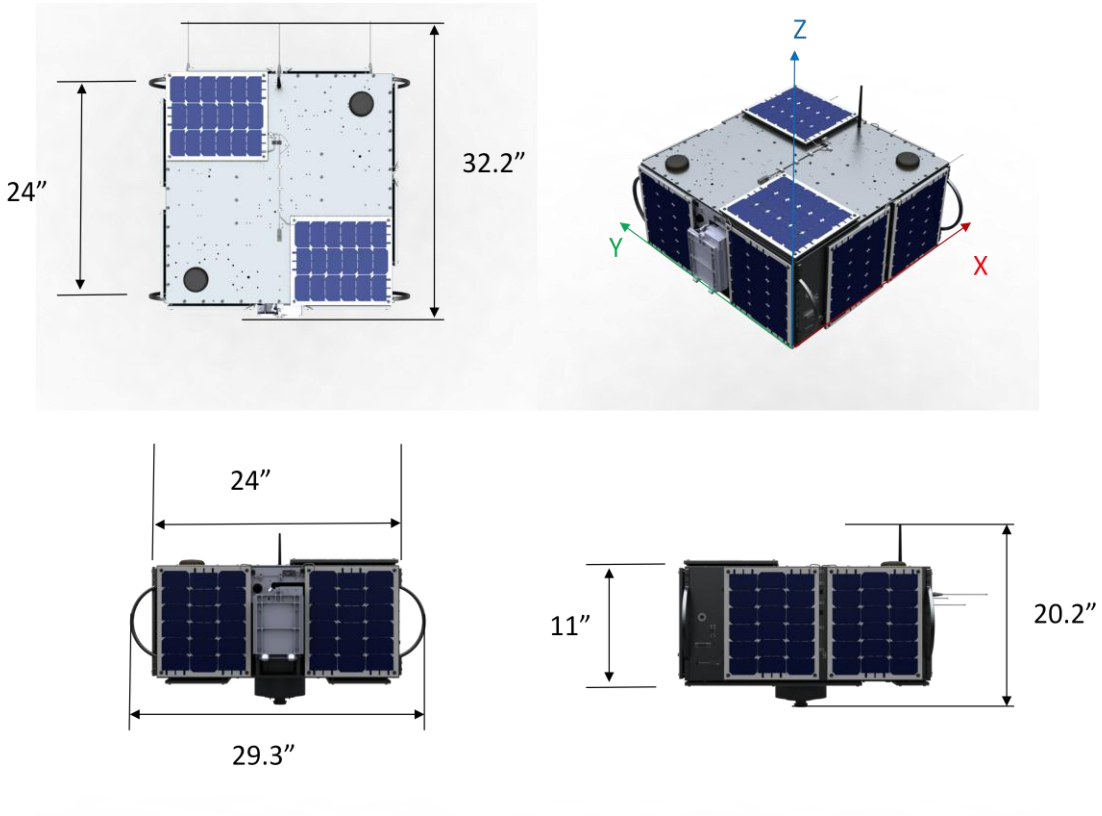

Figure 8: AGS4 Exterior Dimensions and Coordinate Axes

The net result of all this component placement and structural components was a vehicle mass and CG properties as outlined in the tables below. The AGS4 portion of the launch mass was 48.8 kg, satisfying the requirement to remain under 50 kg. This was calculated by creating a mass budget, which is a list of all structures, components, wires, fasteners, and estimates for epoxies and coatings by their quantities and masses to ensure that the project stays under the required amount.

Table 5: Mass Configurations

Mass Configurations		
Launch Configuration	52.25 kg	116.3 lb
Cyclops Deployment Configuration	51.62 kg	113.8 lb
With Solar Panel Covers, without Bevo-2	48.8 kg	107.6 lb
Without Solar Panel Covers, without Bevo-2	47.67 kg	105.1 lb

Four different mass configurations were evaluated to ensure that the requirements were being met, as well as to determine the dynamic properties for active spacecraft pointing control. The first was the launch configuration, which verified that the combined spacecraft mass was under 100 kg. The second was the mass of AGS4 and Bevo-2 without the solar panel covers, as it would be released from the ISS and begin early operations. The third was AGS4 with the solar panel covers to verify that all AGSL hardware going to space was under the 50 kg limit. And fourth was the configuration for AGS4 free flying after Bevo-2 release.

Table 6: Center of Gravity Location

Center of Gravity (Cyclops EAF Coordinates)	
X	-0.082"
Y	0.142"
Z	7.588"

The final component configuration placed the CG within the 0.25" Cyclops requirement for the X and Y axes, and under 0.25" from the calculated ISIPOD force vector, thereby satisfying the CG location requirements.

AGS4 was designed as a series of panels that would fold up into the completed box structure. This approach was helpful as it divided the spacecraft up into regions which was an easy way to designate component locations. A custom assembly jig was developed to keep all the panels in the appropriate relative position and orientation such that wires could be run across the panel gaps to supply power and data to the components on that face. Once all parts were integrated into their panel, the panels would be folded in and attached to one another. The figures below show how the panels were laid out for assembly.

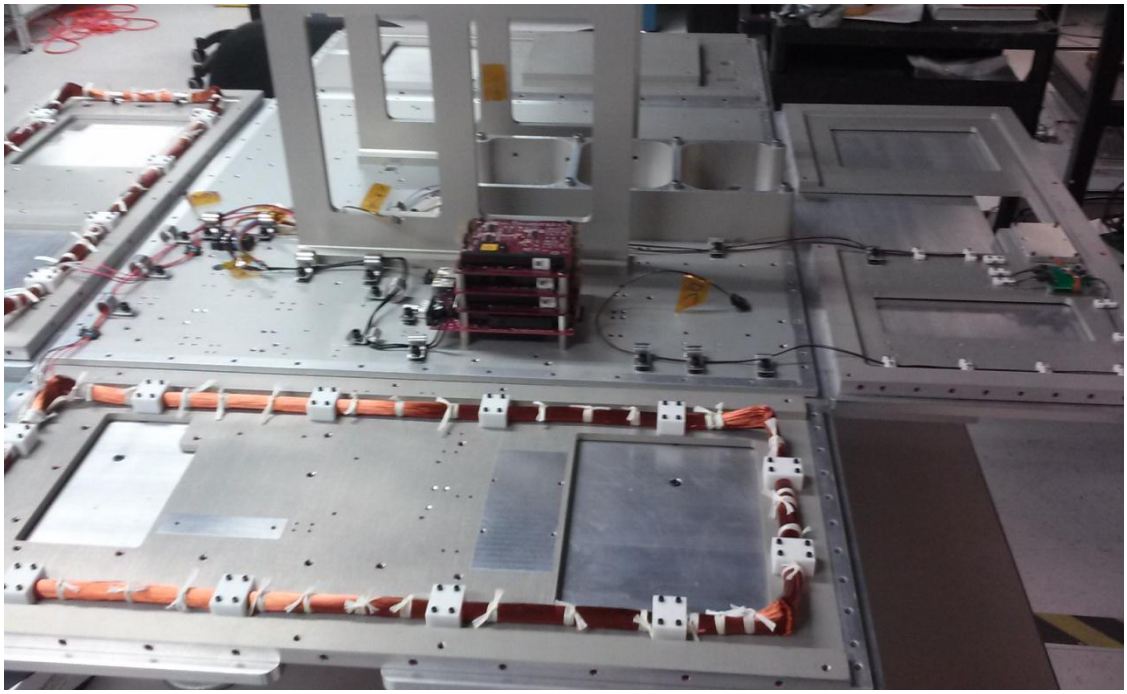

Figure 9: Panel Assembly Configuration

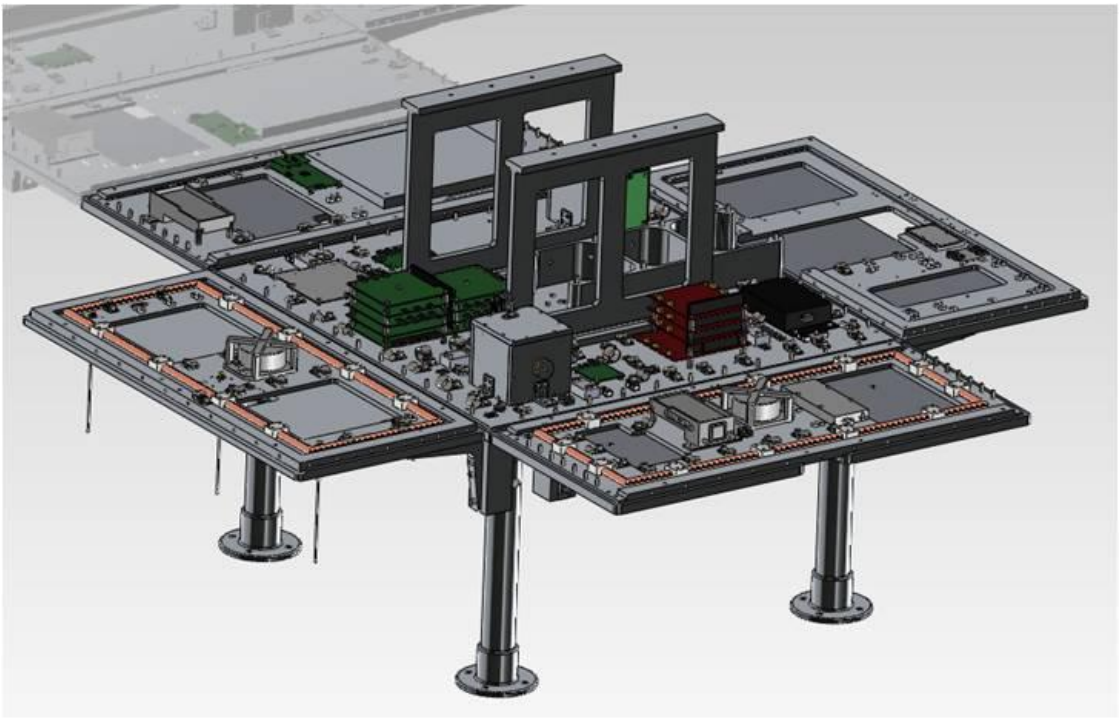

Figure 10: AGS4 Assembly Jig and Panel Layout

All structural materials on the vehicle were made out of 6061-T6 aluminum. This aluminum grade was selected for its weight, and its common use in aerospace applications. As the structural analysis indicated that this material was strong enough to endure the expected loads, the stronger but heavier 7075 series aluminum was not needed. In order to preserve grounding and bonding between all structural elements except the solar panel trusses, Alodine® was applied to all bonding surfaces. Alodine® is a corrosion prevention treatment that maintains electrical connectivity. The remainder of the aluminum surfaces were anodized with Type-II soft coat to prevent electrical conductance in places not desired. Soft coat anodization was chosen over Type-III hard

coat as it is a much simpler process, and the surfaces of AGS4 are not expected to experience high amounts of friction or wear over its lifetime.

Locking inserts are necessary to prevent fasteners from backing out due to the launch vibrations, which could cause pieces to fly apart [15]. There are many approved methods to prevent fastener back-out, but the one favored by the AGS4 team was locking threaded inserts from Heli-Coil®. To use Heli-Coils®, the fastener hole is drilled to a prescribed diameter that is larger than would be for the fastener alone. The hole is tapped with a specific tap and die set, and the Heli-Coil® is inserted using the installation tool, similar to a fastener installation. The Heli-Coil® has specially designed surfaces that cut into the hole material to lock it in place, and similar surfaces on the inside to cut into and lock onto the inserted fastener, preventing back-out. Also recently approved for use was Locktite® epoxy, but this was only used on the #0 size fasteners since Heli-Coils® are not made that small. All of the Heli-Coils® were installed by the AGSL students, as having the machine shop install the hundreds of them would have been costly. The process is not difficult, and previous student experience was leveraged to teach the other lab members how to perform the procedure.

2.4.1.2. Other Structures

In addition to the bus, structural elements were designed for the backing of the solar panels, to prevent them from flexing and cracking the solar cells. Frequently aluminum honeycomb panels are used for this purpose as they are extremely rigid and unbelievably light. Unfortunately this option would produce panels that were too thick and would have clearance issues with the airlock, and so rather than redesign the whole

bus to shrink it down and accommodate the thick panels, AGSL designed thin, lightweight aluminum trusses to support the panels.

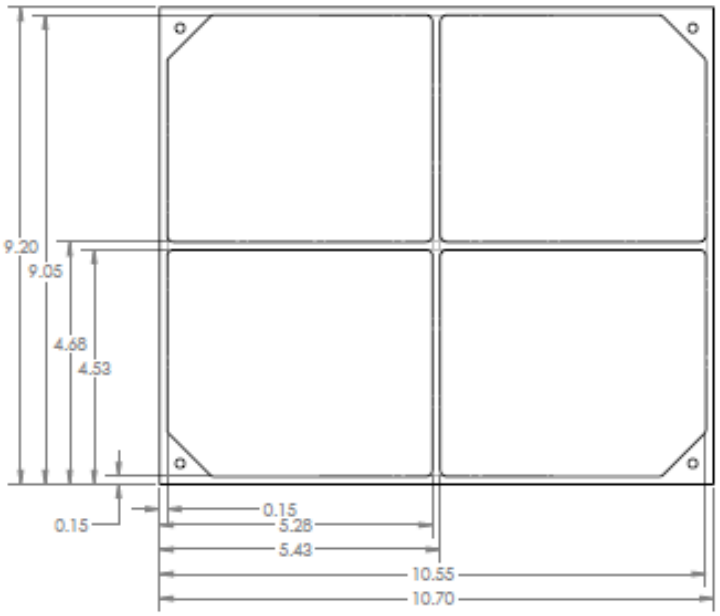

Figure 11: Solar Panel Truss Structure (inches)

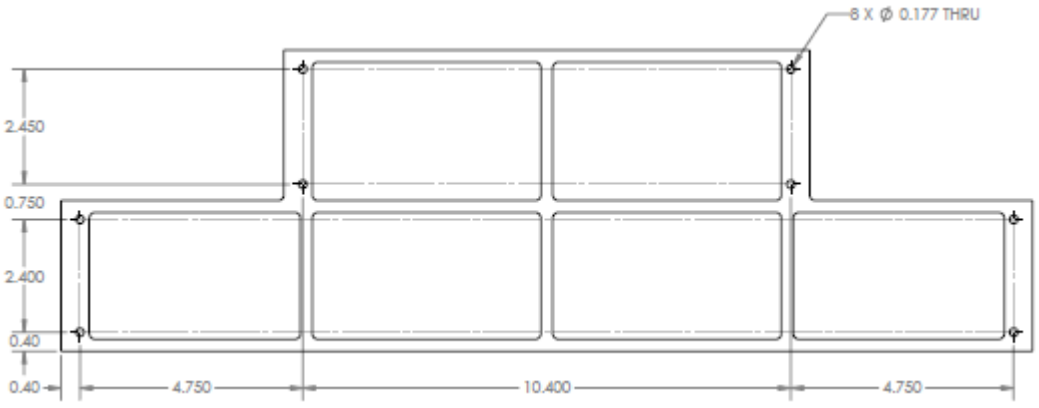

Figure 12: T-Shaped Solar Panel Truss (inches)

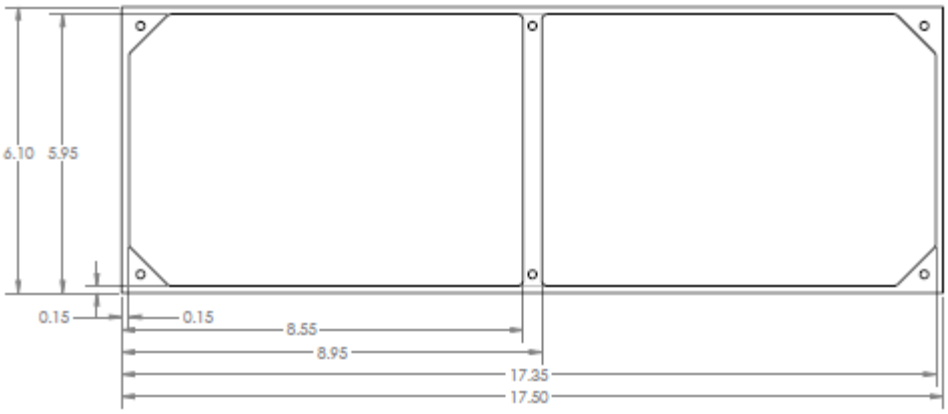

Figure 13: Long Solar Panel Truss (inches)

The solar panels were affixed to these structures using epoxy, and attached to the bus using screws.

Similar to the solar panel structures, the panels required to have some sort of cover to protect them from impact and contain any potential glass fragments that might come loose into the ISS cabin environment [16]. In the micro gravity environment, tiny glass particles will find their way into sensitive equipment or possibly astronauts' eyes. Covers would need to be able to withstand a 25 lb distributed force to protect against accidental astronaut impact, and would need to be see-through so that the cells could be inspected for cracks or breaks before removal. If a crack were to be discovered, the cover for that panel would be left in place to prevent cabin contamination.

The initial thought was to use polycarbonate sheet as the cover since it is strong enough to withstand the impact, clear to see through, and relatively lightweight. Unfortunately, there was not enough room in the mass budget to fly this design, so the team had to get creative. Instead of a solid sheet, a waterjet was used to cut triangular

holes in the sheet to retain strength but lose weight. Another polycarbonate sheet would be cut to provide a 1/4" standoff between the grid sheet and the cells. A Mylar® plastic film was epoxied to the inside of the grid to retain visibility but provide containment. The result was a cover with a mass of just 122 g. Velcro® strips were epoxied to the cover frame, and a mating piece was epoxied to the solar panel/truss combination in order to secure the cover. Astronauts would pull on these Velcro® tabs to remove the covers. The figure below shows the finished square panel covers.

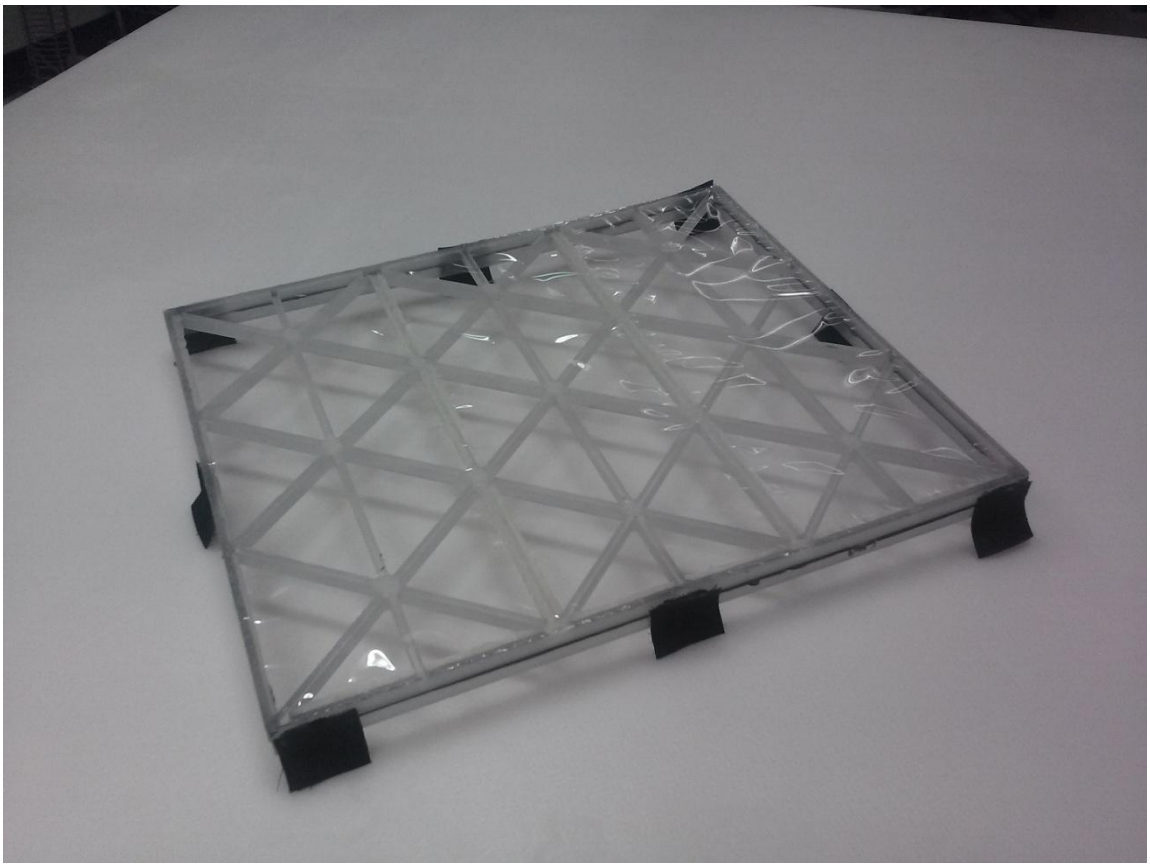

Figure 14: Solar Panel Cover

There was not enough clearance on the bottom of the spacecraft for it to be attached to the Cyclops table if any of the cells broke and required the cover to stay on. To prevent contamination risk, Mylar® covers were cut for each of the bottom panels and held in place with Kapton® tape. This would provide no impact protection, but would provide containment. If all cells were intact after install onto Cyclops, the tape tabs could be pulled and the Mylar® slid off.

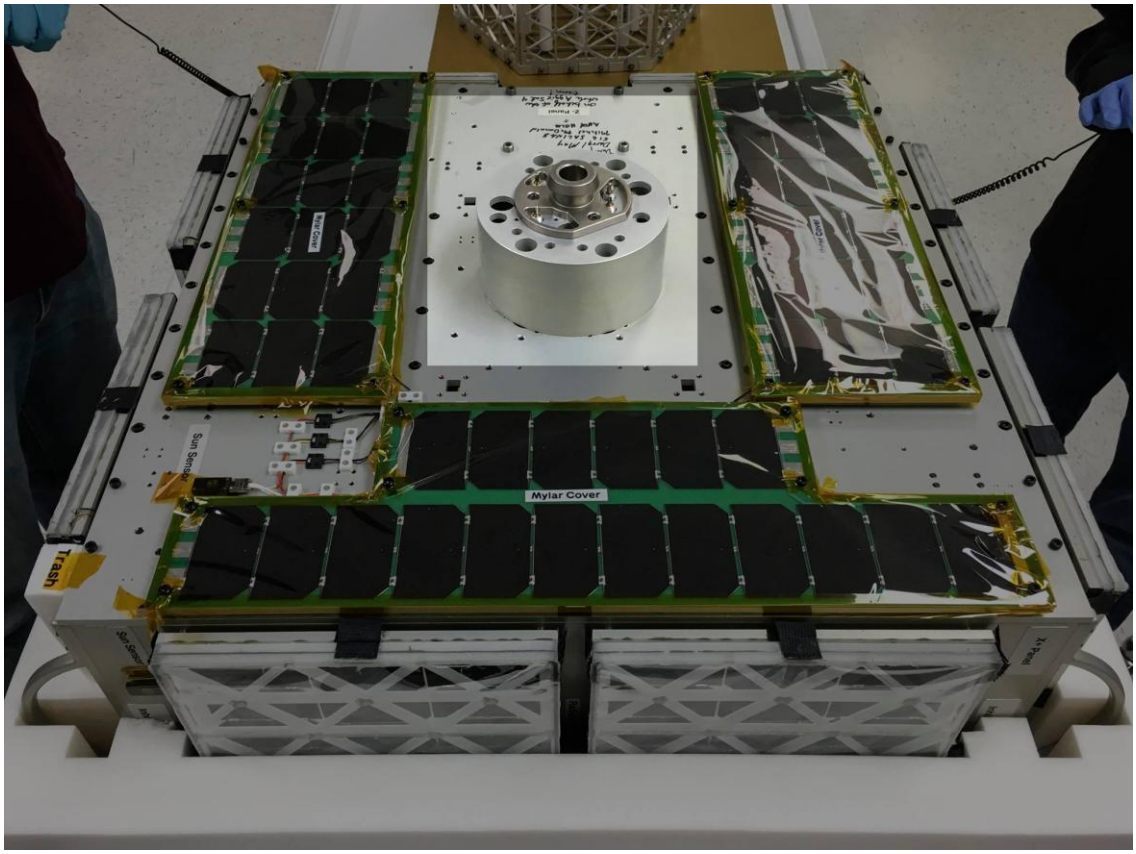

Figure 15: Bottom Panel Mylar® Covers

One other item that was developed, and that AGSL was a pioneer of, was the use of 3D printed materials in spacecraft. After learning that polycarbonate was an

acceptable material for both inside and outside ISS from a temperature and outgassing standpoint, it was decided to be used for brackets to secure wires. AGS2 had used Teflon® for a similar purpose, but this required expensive material and machining. The TAMU Aerospace Engineering department machine shop had high end 3D printers that could print in polycarbonate, and thus AGSL was able to create custom wire brackets for less than a dollar a piece. These brackets not only were of the correct custom size and so therefore did not require shimming to prevent wire wiggle, but they do not have sharp edges like metal brackets that require covering. Some of these brackets can be seen in the above image in the lower left quadrant, the white blocks with the wires passing through them. They can also be seen clearly in the figure below.

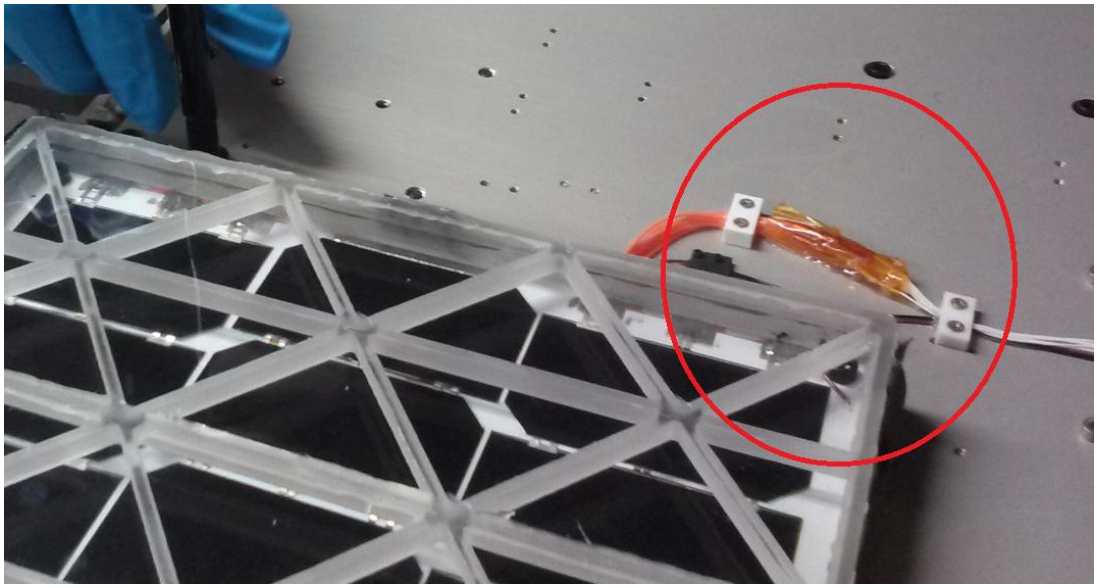

Figure 16: Polycarbonate Wire Brackets

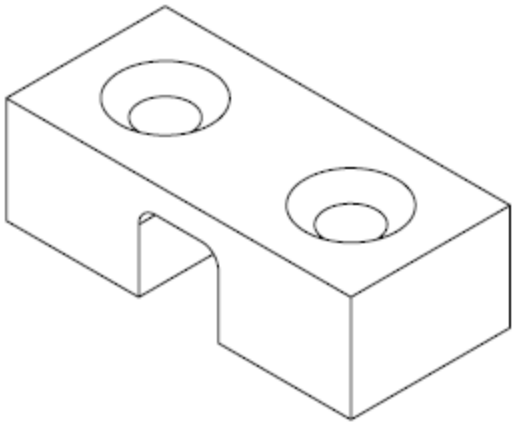

Figure 17: Polycarbonate Wire Bracket Model

2.4.1.3. Wire Modeling

All of the component wires were modeled in SolidWorks®. While a tedious and difficult process, it was necessary in order to determine the correct length for each wire, and the correct size for each wire bracket. Proper bend radius for the gauge wires used was implemented, which also determined the paths that the wires would take from one component to another. Wire "corridors" began to develop, where all the wires going in a general direction were clustered together to keep them organized. This modeling also served to more accurately model the mass and center of gravity of AGS4.

2.4.1.4. Foam Packaging Enclosure

In order to protect AGS4 as soft stow cargo for the launch, NASA cut and assembled approximately 2" thick LD45FR foam padding in the form of two clamshell halves. This was based on the AGS4 exterior CAD model. The foam was designed to

fit snugly, prevent damage from impacts, and dampen the vibrations from the launch vehicle.

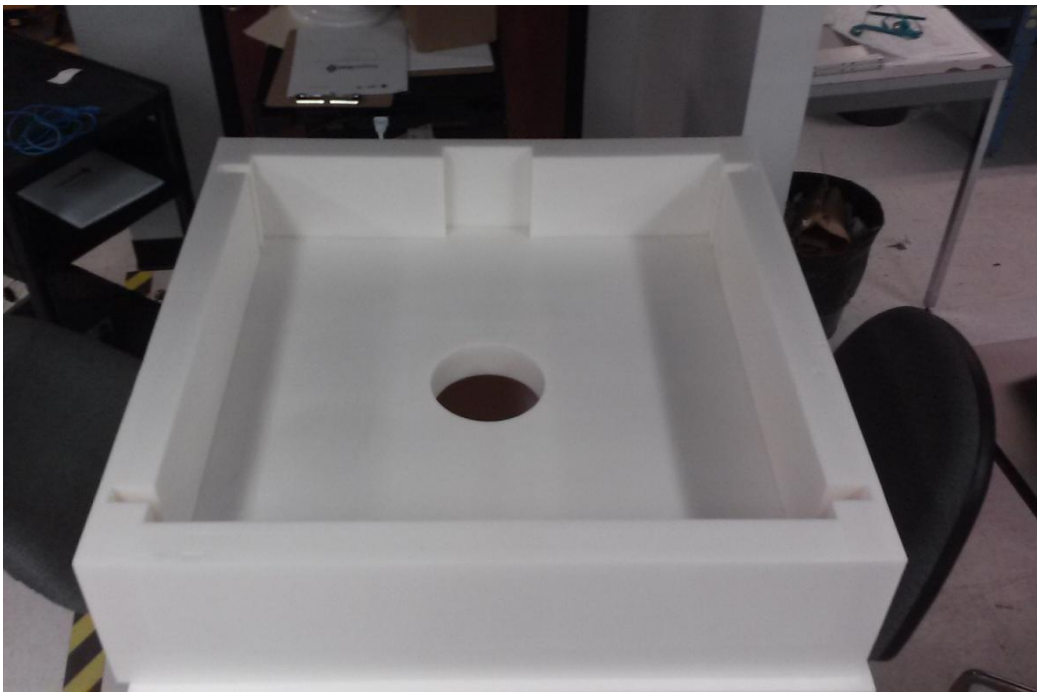

Figure 18: Clamshell Foam Lower Half

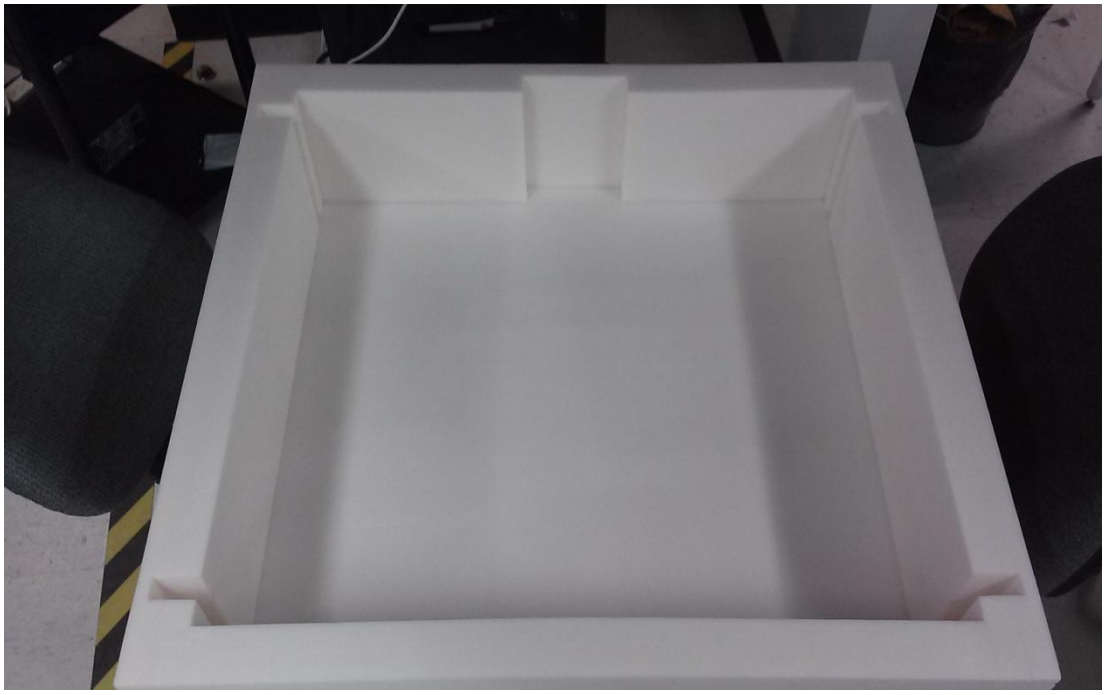

Figure 19: Clamshell Foam Upper Half

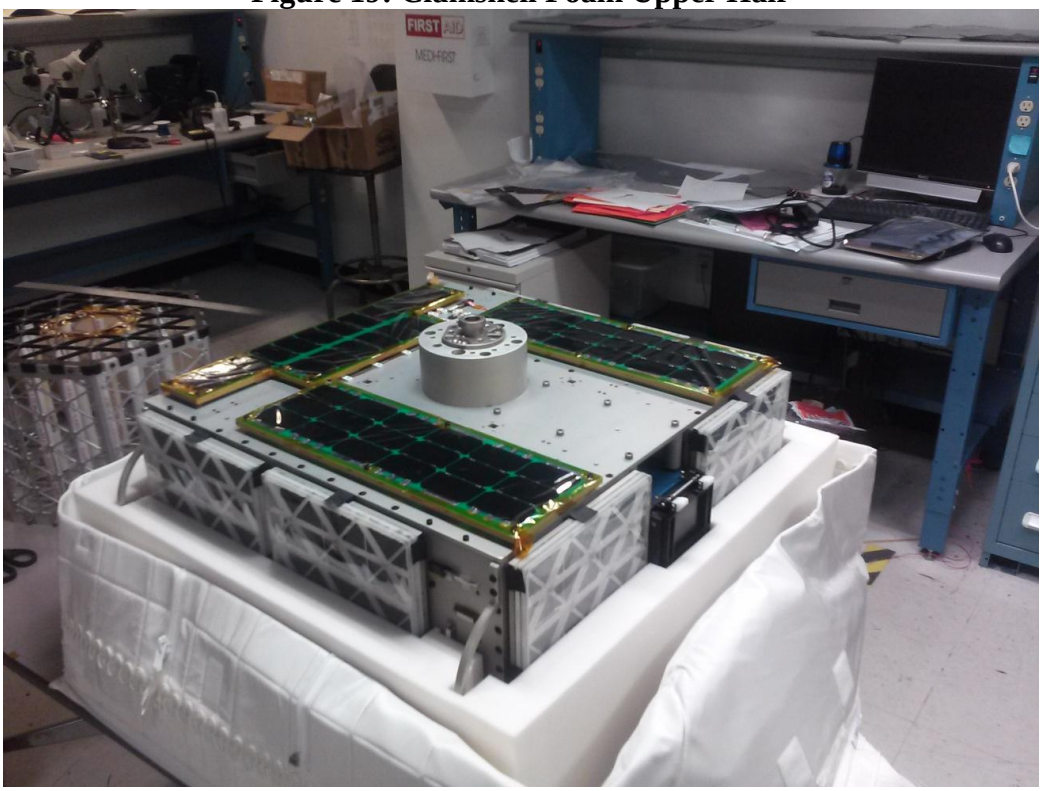

Figure 20: Foam Packaging Housing AGS4

2.4.1.5. Structural Analysis

In order to ensure that the design would survive the acceleration and vibration loads of the launch vehicle, a structural analysis was performed [17]. Using SolidWorks®, gravitational loads were applied to mirror the a Falcon-9's acceleration, and a dynamic random vibration power spectral density (PSD) curve was applied to mirror the vibrations from the engines.

Before any analysis can begin, the boundary conditions must be defined. These were derived from the method by which AGS4 would be strapped to the launch vehicle inside the foam packaging. The figure below details how the package would be attached to the vibration testing table and the launch vehicle.

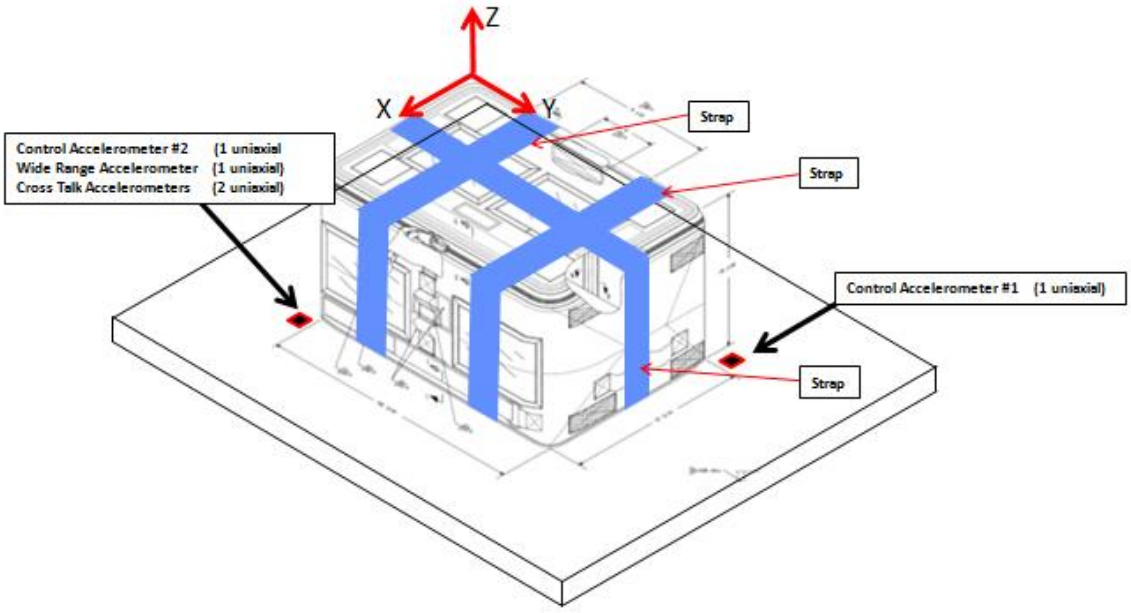

Figure 21: AGS4 Launch Restraint Configuration (Image by NASA)

As the foam packaging was designed to provide open space for the solar panels and other features to not experience any contact, the weight of the structure was focused on a few structural points. These points were modeled as fixed geometry in SolidWorks®, and are at the bus corners and the Cyclops spacer as shown in the figures below.

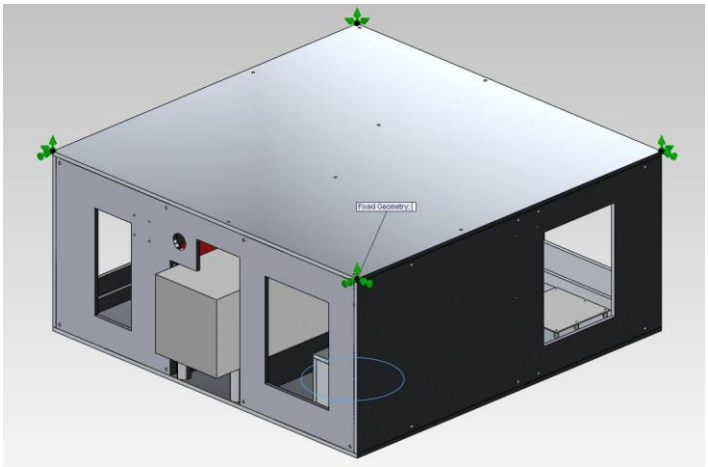

Figure 22: Top Fixed Constraints

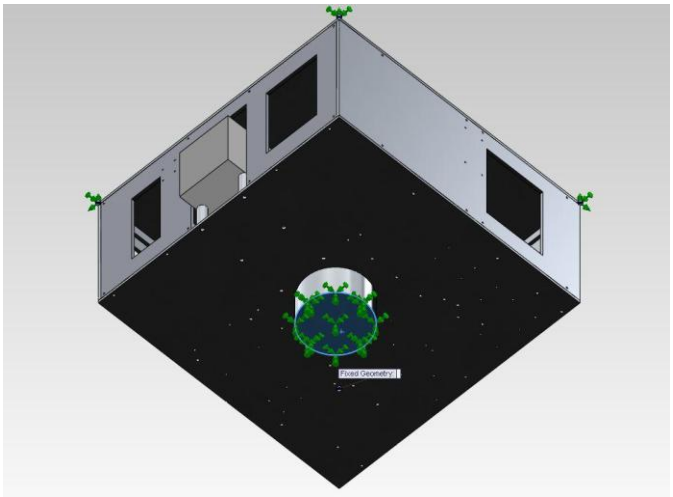

Figure 23: Bottom Fixed Constraints

Without the resources of a supercomputer, modeling the entire model to the highest degree of fidelity would not be possible. Simplification to the components was needed to cut down the model complexity. Electronics boards were simplified down to just the FR4 plastic boards with the appropriate density to account for the surface components that were suppressed. The ISIPOD model was simplified, and Bevo-2 replaced with a simple block of the same mass. Wires and fasteners were omitted as their complexity was far too great, and they will likely experience significant amounts of low amplitude oscillation between mounting brackets which would make simulation impossible with the high end computers available to the lab.

SolidWorks® uses finite element method (FEM) analysis to determine the stresses and deflection a structure experiences under load. FEM divides the model into a mesh of roughly equal size pieces, and uses the conditions of the neighboring pieces as the boundary conditions for the piece in question. Structural stress and deformation calculations are performed on the piece in question. Then, the piece that was just examined is used as the boundary condition for the next piece in its new deformation state. This process is continued across the entire mesh and repeated using the results of each piece in the next iteration until convergence is reached, and the results do not change significantly from one iteration to the next.

With the simplified model developed, the next step was to determine the appropriate mesh size to perform the analyses. Too coarse an analysis will yield inaccurate results, while too fine a mesh will spend orders of magnitude more time for an unimproved result. A convergence analysis was performed using the SolidWorks®

natural frequency calculation function. The analyses started with coarse meshes and progressively increased the number of nodes in the system until the 1st mode natural frequency did not change significantly with more nodes. As shown in the table of results below, this occurred at a 1.5 cm mesh.

Table 7: Frequency Modes for Mesh Sizes

Mesh Size (cm)	2.5	2.25	2	1.75	1.5	1.25	1
# of Model Nodes	238032	277943	306549	352220	433309	552024	762143
Frequency Mode #1 (Hz)	**311.08**	**307.08**	**301.86**	**298.26**	**288.53**	**284.21**	**281.1**
Frequency Mode #2 (Hz)	317.66	315.93	313.15	310.59	303.87	299.97	297.63
Frequency Mode #3 (Hz)	335.44	332.1	324.68	319.38	309.57	305.53	303.22
Frequency Mode #4 (Hz)	378.41	373.45	370.91	365.17	355.76	350.53	351.89
Frequency Mode #5 (Hz)	398.30	395.47	394.38	392.06	383.73	378.26	371.55
Run Time	00:08:32	00:09:24	00:10:04	00:12:04	00:40:28	00:51:01	01:13:48

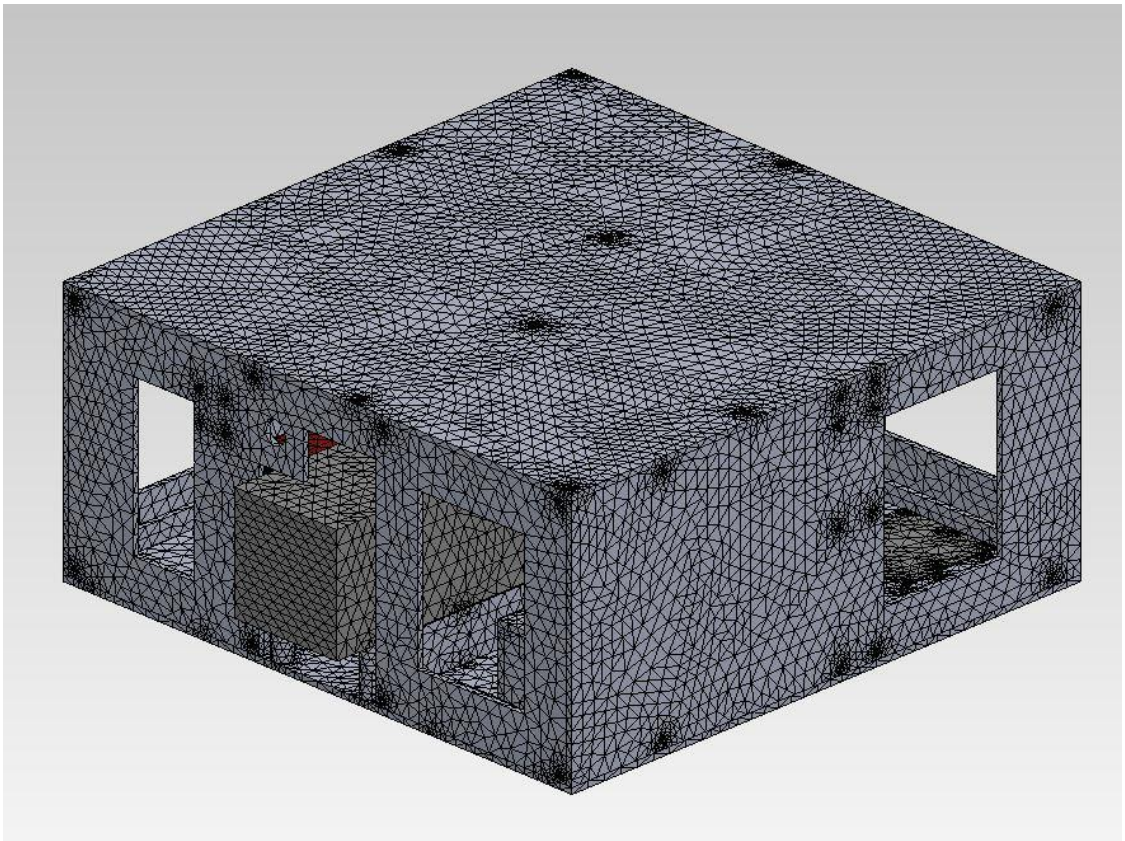

Figure 24: 1.5 cm Analysis Mesh

Since the 1st mode natural frequency is above 280 Hz, it is not expected to experience resonance with the launch vehicle that would induce structural failure. A natural frequency above 100 Hz is desired to prevent resonance. The items that are most susceptible to vibrations are the electronics boards.

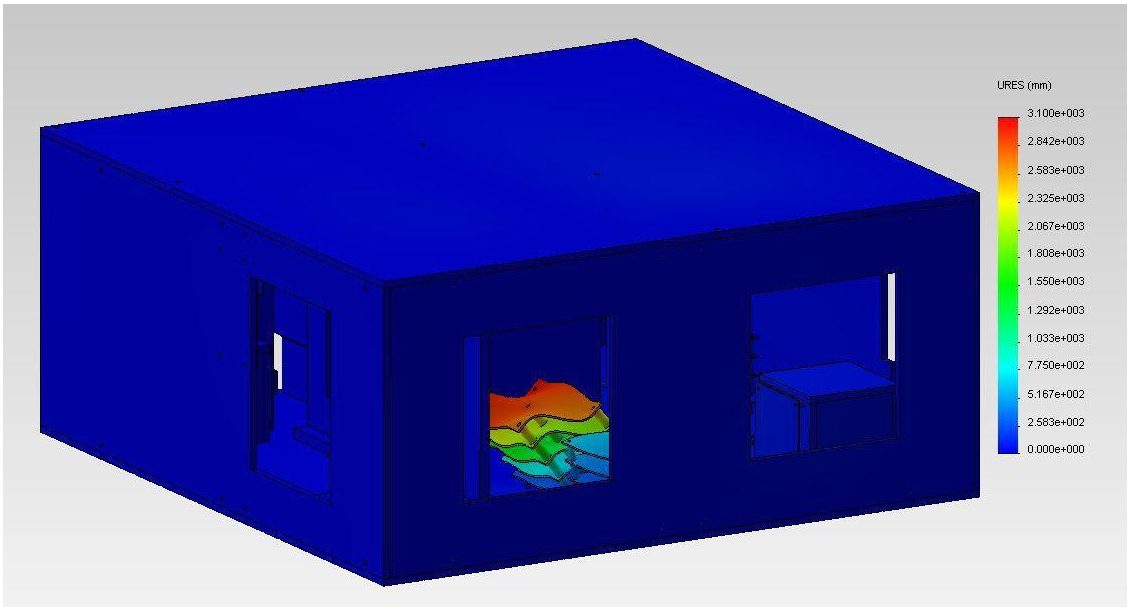

Figure 25: 1st Mode Natural Frequency Response

In order to perform the random vibration analysis, the launch environment needs to be known. Since at the time of the analysis it was unsure whether OA-4 would fly on an Atlas V or Falcon-9 rocket, the NASA management had AGSL perform the analysis with the Falcon-9 environment as this was the more harsh of the two [16]. The random vibration environment of the vehicle is outlined in the table below, and the PSD curve in the following figure.

Table 8: Falcon-9 Random Vibration Environment

Frequency (Hz)	Level (g^2/Hz)
20	0.057
153	0.057
190	0.099
250	0.099
750	0.055
2000	0.018
Composite	9.47g rms
Duration	60 seconds/axis

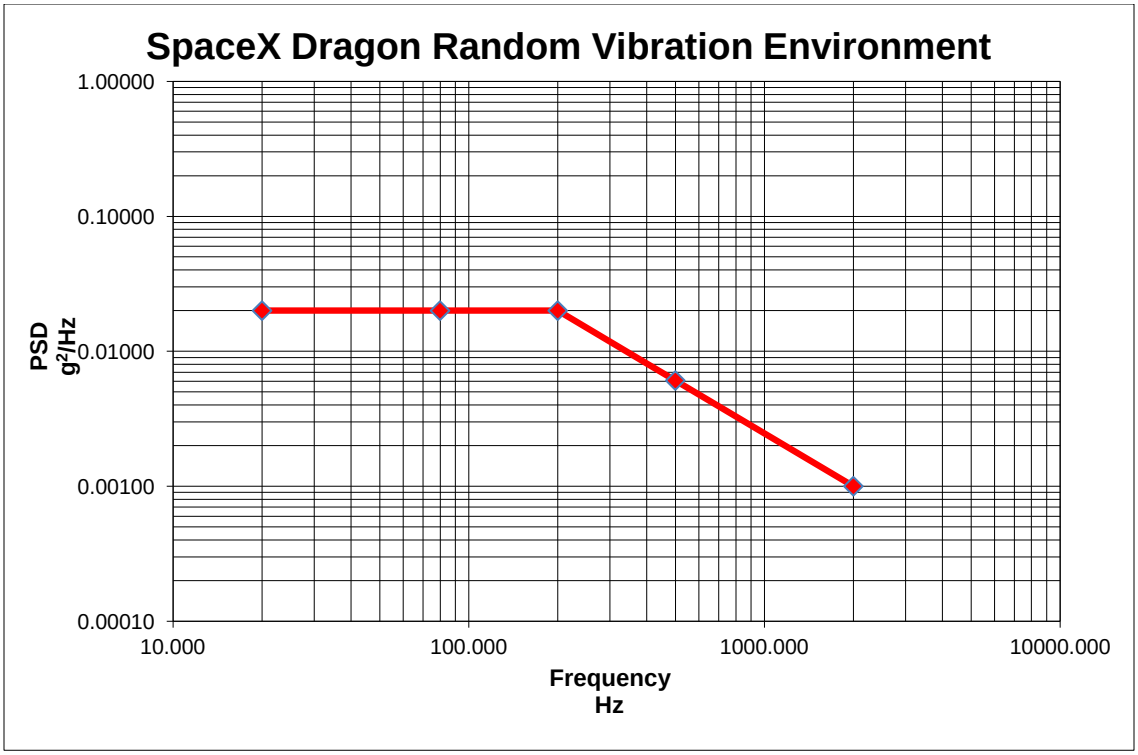

Figure 26: Falcon-9 PSD Function

However, in order to determine that the payload is safe to experience these loads, NASA tests to +3 dB, or double the power. Fortunately for soft stowed payloads like AGS4, the foam packaging attenuates a great deal of this vibration power. Since foam can have non-linear properties, including it in the simulations would increase the complexity by orders of magnitude beyond AGSL computing capabilities. Fortunately, NASA provided the "Cargo Tool" [18] which utilizes the surface area of the spacecraft in contact with the foam to determine the attenuation so that it can be left out by testing with an adjusted curve. Two inches of LD45FR foam was used in the Cargo Tool to produce the attenuated +3 dB PSD curve shown in the figure below. The 0.7 psi curve applies to the X and Y axes, and the 0.2 psi curve applies to the Z axis. These psi values are determined

based on the mass of the spacecraft and the surface area of foam in contact with the faces on that axis to distribute the weight.

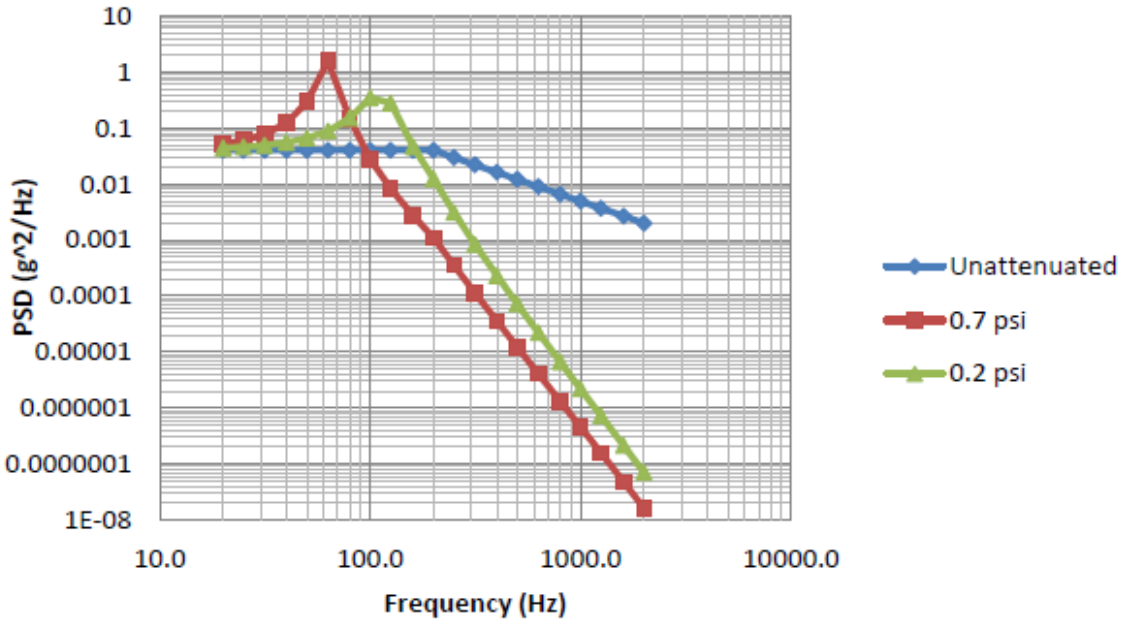

Figure 27: Attenuated +3 dB PSD Function

The analysis was run using these curves for each axis. This produced a calculation of maximum instantaneous acceleration and stress at each point in the model. The results calculated were that the lowest factor of safety anywhere in the model under these loads was 565 at the location that the Cyclops attachment fixture attaches to the standoff spacer. This is a good indicator that none of the materials will fracture due to the vibration environment. Unfortunately, there are things that cannot be properly modeled such as wiring, soldered connections, and integrated circuit silicon wafers which can break due to vibrations, and while they do not pose an imminent safety

hazard, they do harm the ability to meet the mission objectives. Adherence to workmanship standards [15] and proper soldering techniques [19] reduce this risk.

This same analysis was applied to the solar panels (with structural truss backing) and solar panel covers. As the bottom face panels do not have structural covers, they were analyzed as just the panels with their truss backing.

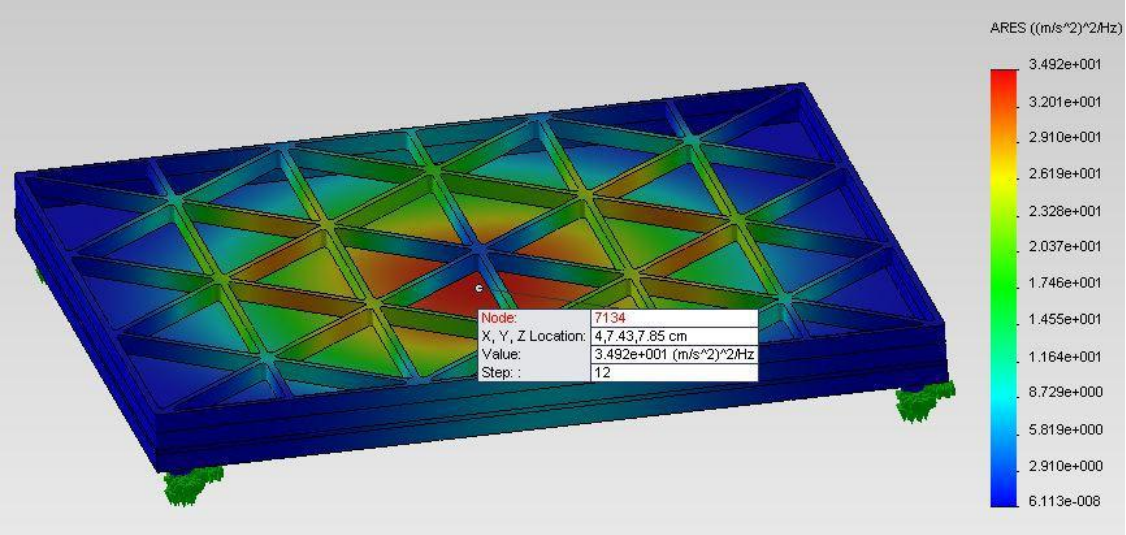

Figure 28: Solar Panel Vibration Analysis

The results of this analysis indicate that these structures are not at risk of fracturing due to vibration loads.

Table 9 : Solar Panel Vibration Factor of Safety

Panel	1 sigma acceleration (g)	Stress (Pa)	Factor of Safety
T-Shaped	2.2596	11567	23775
Long	2.1767	7424.4	37040
Square with Cover (X/Y-Axis)	2.711	19966	13773
Square with Cover (Z-Axis)	7.074	119599.4	1438

With confidence that the vehicle and components will not fracture due to vibrations and resonance, the analysis of stresses and deflections due to acceleration are analyzed in a similar fashion. SSP 50835 [16] states that the maximum acceleration load that the SpaceX Dragon is capable of experiencing is 9.0 g's, though actual loads are much less, and that payloads should be analyzed to this value in all axes. Additionally, payloads should be able to withstand rotational accelerations of the launch vehicle of up to 13.5 rad/sec^2. The specification also requires that all payloads have a factor of safety of at least two.

This analysis was setup the same way as the vibration analysis. An acceleration of 9.0 g was applied to each axis, both positive and negative directions, while a rotational acceleration equal to 13.5 rad/sec^2 was applied as if the payload were mounted to the outside wall 1.8 m away from the center. This was to simulate any of the six spacecraft faces being in the vertical position during launch, while the rocket performs the rotation maneuver. The resulting maximum displacements and minimum factor of safety per axis are detailed in the table below.

Table 10: Axial and Rotational Acceleration Results

	Factor of Safety	Displacement (mm)	Max. Displacement Location
X-axis	4.04	0.02768	EPS Boards Assembly
Y-axis	3.3	0.04522	EPS Boards Assembly
Z-axis	2.38	0.04277	CDH Assembly

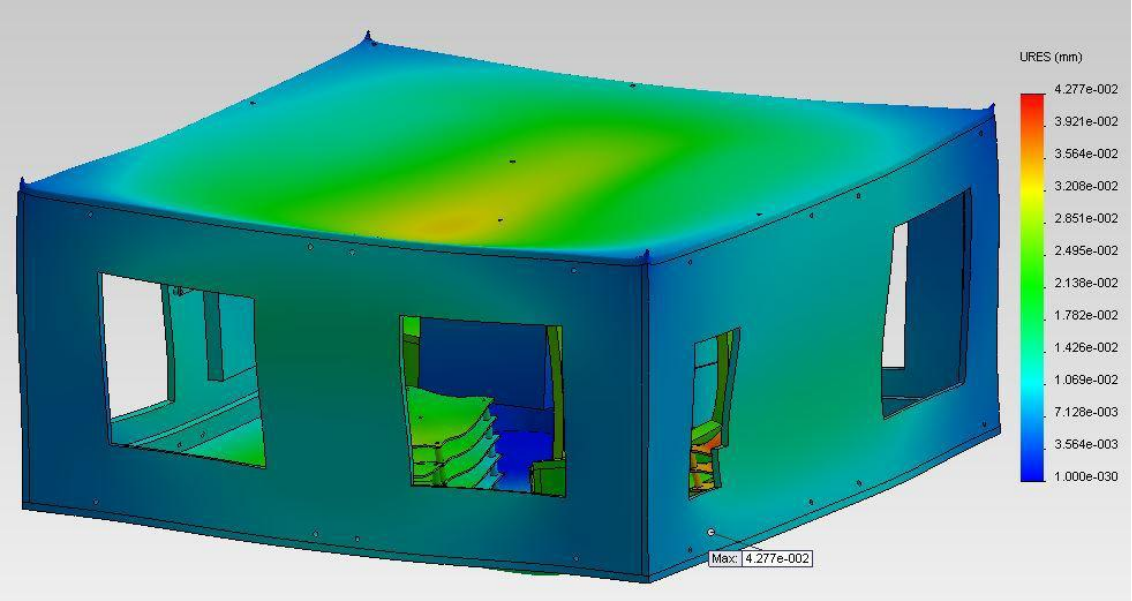

Figure 29: +Z Axis and Rotational Acceleration Displacement

This same analysis was also applied to the solar panel structures and solar panel covers. Under their own weight due to the accelerations, as expected the highest stress and displacements of the panels occurred when they were oriented perpendicular to the axis of acceleration.

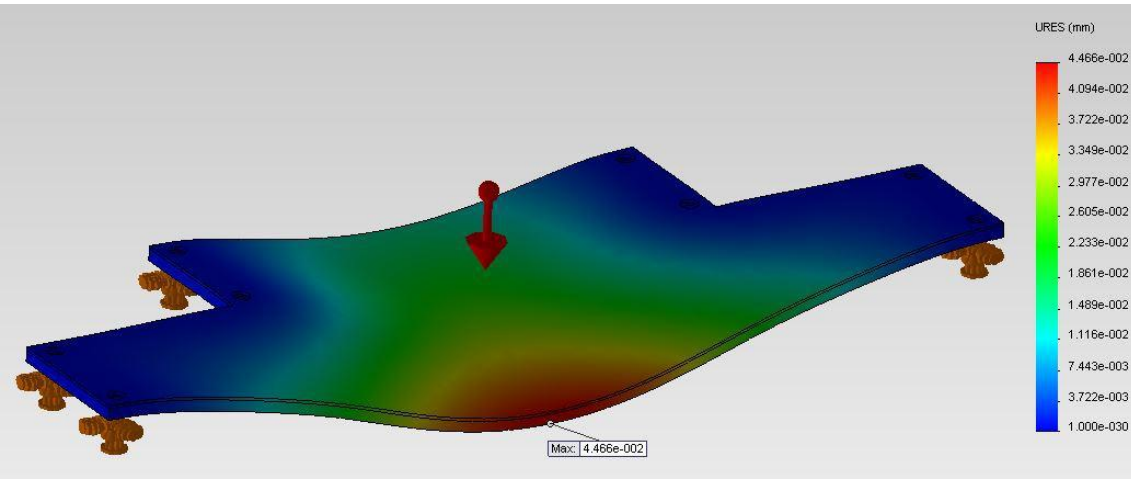

Figure 30: T-Shaped Panel Displacement

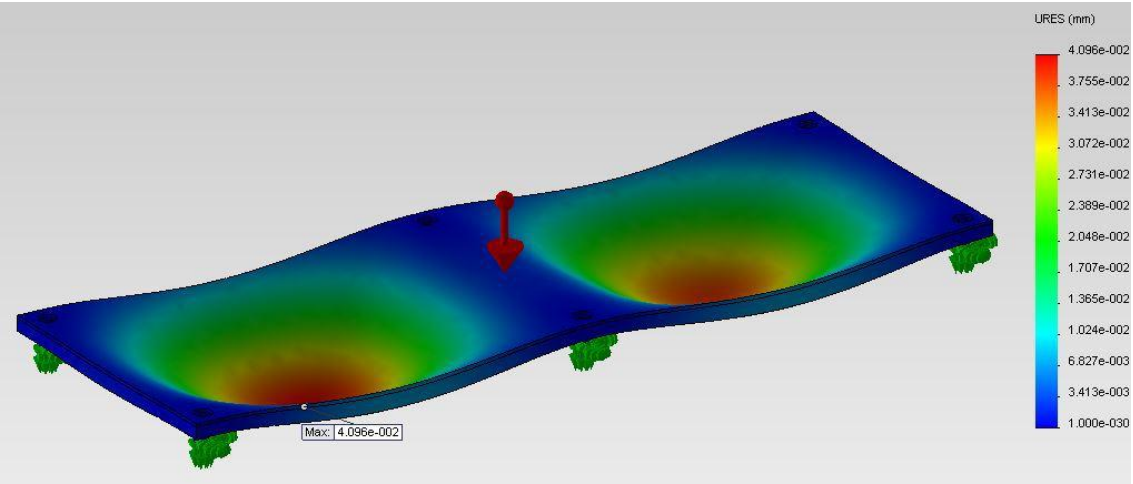

Figure 31: Long Panel Displacement

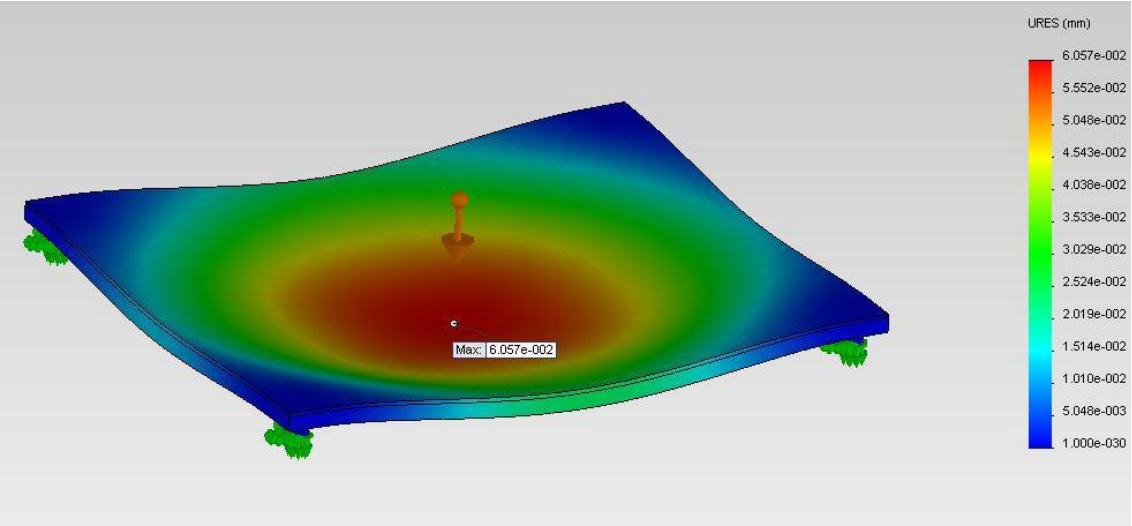

Figure 32: Square Panel Displacement

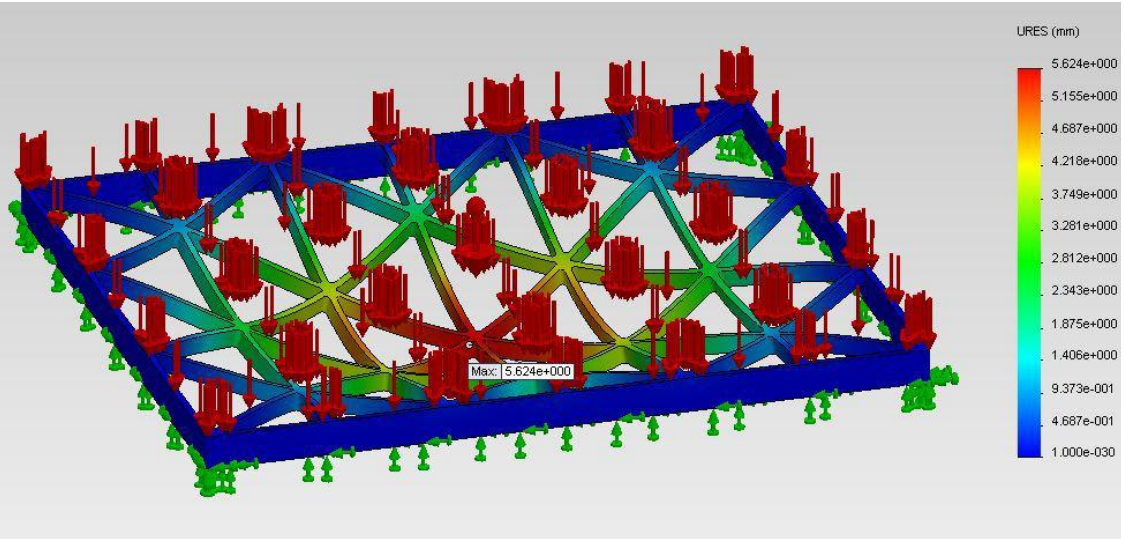

Figure 33: Panel Cover Displacement

Table 11: Panel Acceleration Stress and Displacement

	Minimum Factor of Safety	Maximum Displacement (mm)
T-Shaped Panel	7.70	0.04466
Long Panel	53.45	0.04096
Square Panel	19.29	0.06057
Panel Cover	2.63	5.624

Since all factor of safety requirements were satisfied, the next concern was that the maximum displacement would be enough to crack or damage the solar cells fixed to them, or that the panel covers would deflect far enough that they would make contact. A simple test was done on a sample solar cell and it was found that the cell could flex by roughly 1 mm without cracking the cover glass, more than enough to tolerate these displacements. The solar panel covers on the other hand were a much closer call. The grid structure sits 1/4", or 6.35 mm off the face of the solar cells. Given the maximum displacement of 5.6 mm, there is only a small amount of margin under maximum load.

Still, this was sufficient to protect the cells, and maximum loads were unlikely to be experienced.

This structural analysis indicated that the AGS4 configuration would survive launch and reach the ISS as a viable payload, without posing a hazard to the crew or station.

2.4.1.6. Thermal Analysis

A thermal analysis [20] was required to verify that AGS4 could withstand being outside the ISS for up to 10 hours while coming out of the airlock and being manipulated by the robotic arm. Unlike the structural analysis, which could leave out components such as the solar panels which do not significantly contribute to the dynamic response, a thermal analysis requires a higher fidelity simulation model which includes these items. This is because these components provide surface shading, which impacts internal temperatures due to their impact on radiant heating. Fortunately including these features does not pose quite as much a computation burden as it does on the structural analysis, since a great deal of the heat transfer is by internal conduction, which results in a larger mesh size being adequate to calculate temperatures. Using the SolidWorks® thermal analysis package, a test case was run as a convergence analysis, and it was found that a mesh of 5 cm is sufficient to accurately model the thermal properties.

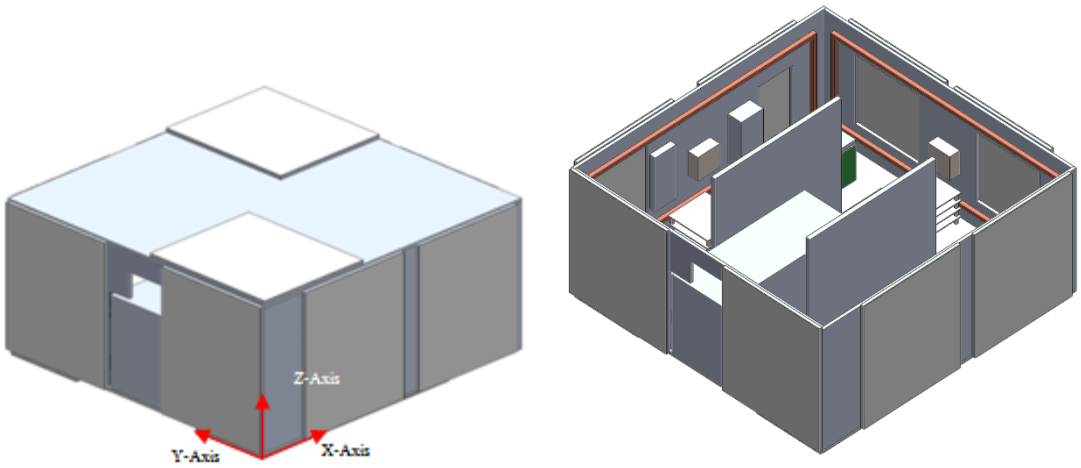

Figure 34: AGS4 Thermal Simulation Model

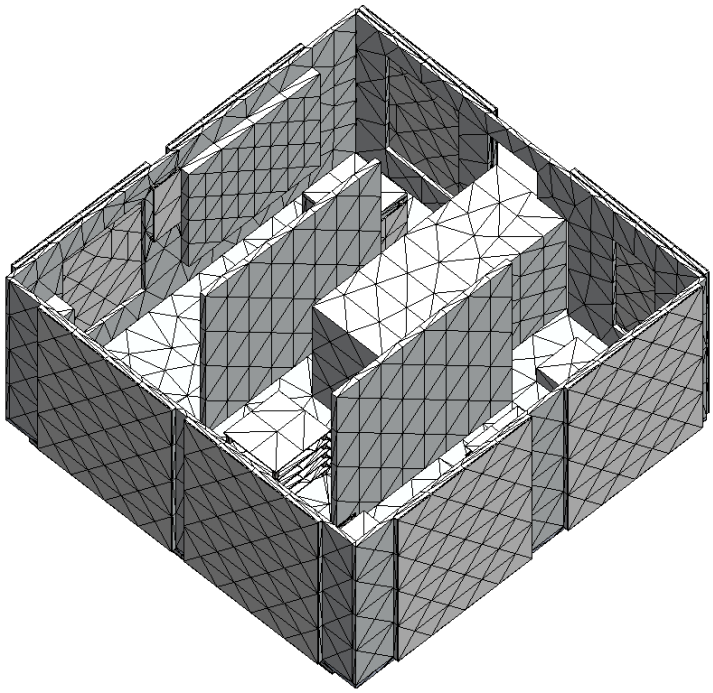

Figure 35: 5 cm Mesh

In a purely radiation heat transfer environment like the vacuum of space, the amount of energy an object absorbs is related to the view factor of the object's face to

the heat source. The view factor is a percentage of the face that is exposed to that source. Assuming a 400 km orbit and that the X+ panel is always facing Earth to simulate the ISS Local Vertical Local Horizontal hold (i.e. rotating to keep one side of the ISS constantly pointed at Earth), the six panels have view factors according to the table below.

Table 12: AGS4 ISS View Factors

Panel	Earth View Factor	Free Space View Factor
+X	93%	7%
+Y	22%	78%
+Z	22%	78%
-X	0%	100%
-Y	22%	78%
-Z	22%	78%

The view factors are significant in that they determine the radiation heat flux to or from that face. There are three primary sources of heat flux in the low Earth orbit (LEO) environment: solar heat flux, outgoing long-wave radiation (Earth blackbody), and Earth albedo (reflected sunlight). These radiation sources have power densities as shown in the table below. Also shown are the Earth and free space temperatures which heated surfaces will radiate to according to their view factor and temperature differences.

Table 13: Radiative Heat Flux Sources and Sinks

Solar Flux	1367	W/m^2
Outgoing Long-wave Radiation	287	W/m^2
Earth Albedo	410.1	W/m^2
Free Space Temperature	2.725	K
Earth Temperature	255	K

Using the above parameters, AGS4 was evaluated over the course of 10.5 hours for three different beta angle cases, 0°, ±60°, and ±75°. The beta angle is the angle between the spacecraft orbit plane and the Earth-Sun vector, which changes with the seasons. The case of $\beta=0°$ is the coldest scenario where AGS4 spends 59% of the time in the sun, while $\beta=75°$ is the hottest case when the orbit is 100% illuminated by sunlight.

SolidWorks® uses radiative heat transfer mechanics to evaluate the external heat flux, and conduction and surface-to-surface radiation to determine the temperatures of each spacecraft component. Each component was monitored to ensure that its temperature stayed within appropriate bounds during the simulations. The primary concern was the lithium ion battery cells which had the smallest temperature range of -20-60°C. The batteries came the closest to their temperature limit of all the components, but stayed within bounds for all three Beta angles. Over the 10.5 hour simulations, they reached a minimum -9.7°C at $\beta=0°$, and a maximum of 27.4°C at $\beta=75°$.

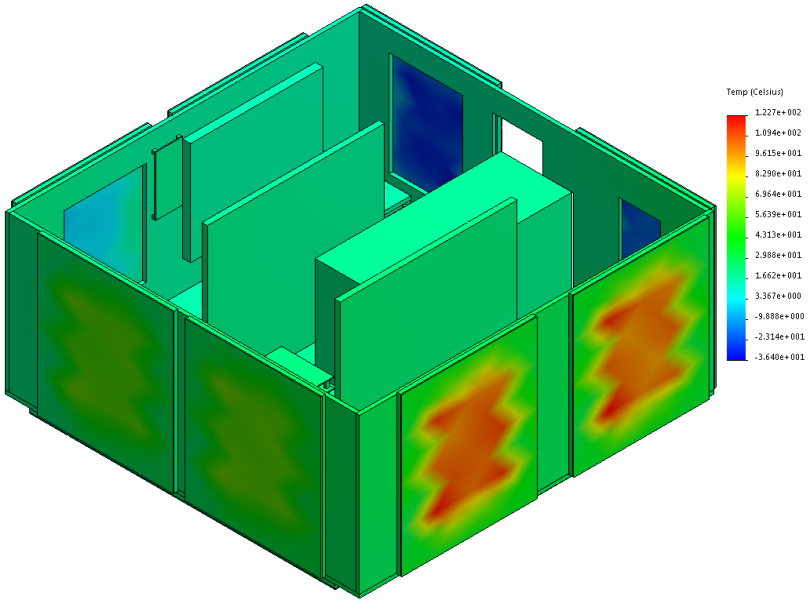

Figure 36: Temperature Model for β= 75°

This analysis indicates that AGS4 will be able to survive the up to 10 hours in an unpowered state while in close proximity to the ISS. Since the orbit will be very similar in shape and altitude for the majority of the spacecraft lifetime, this analysis also indicates that AGS4 should not experience temperature problems during operations.

2.4.2. Command and Data Handling (CDH)

The CDH system is the main computer on the spacecraft, and is responsible for facilitating communications among all subsystems, as well as executing the mission script and performing calculations. AGSL had manufactured the CDH system in-house based around a microprocessor for the less complicated AGS2 mission. Experience from this mission recommended that AGSL upgrade to single board computers for future missions [21] as their more conventional structure and software would ease development and operations.

During the trade study process, there was some trouble finding computer systems that were of the appropriate size and computing power that had sufficient input/output ports to interface with all of the components. CubeSat components usually use the PC104 format which connects stacks of boards with 60+ pin connectors, and do not have ports for traditional components. After several rounds of investigation and trade study, the CDH team found the TS-7800 single board ARM computer from Technologic Systems [22].

Figure 37: TS-7800 Flight Computer

The TS-7800 processor operates at 500 MHz, has 128 MB RAM, and is designed to operate in rough environments. Of particular interest was the computer's ability to accept TS-SER4 serial expansion boards, providing enough ports for all of the AGS4 components. This feature, in addition to the two USB ports needed for the Kenwood radios, and the SD card slot for easy upload and storage of the flight software, made the TS-7800 a computing option that supported the mission and all components.

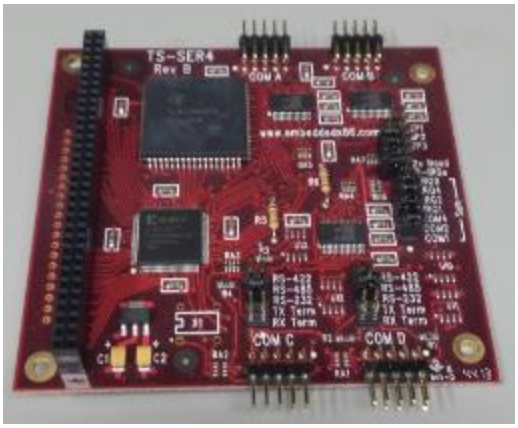

Figure 38: TS-SER4 Serial Expansion Board

A Linux operating system was chosen for its flexibility and customizability to be tailored to the AGS4 mission, and its suitability to work on ARM single board computers.

Figure 39: CDH Stack

2.4.3. Electrical Power System (EPS)

After performing a rough-order-of-magnitude analysis for the power requirements of AGS4, it quickly became apparent that commercially available CubeSat power systems of the day were insufficient to meet the mission needs. Since AGSL had team members with the skill set and previous experience with developing small power systems, the choice was made to fabricate custom designed EPS hardware.

Table 14: AGS4 Power Budget

Subsystem	Device	Voltage (V)	Current (A)	Power (W)	Quantity
ADCS	Vector-Nav	5.00	0.07	0.33	1
ADCS	Reaction Wheel	28.00	0.25	7.00	3
ADCS	Torque Coil	28.00	0.20	5.60	3
CDH	TS-7800 Single Board Computer	5.00	0.80	4.00	1
CDH	TS-SER4 Serial Board	5.00	0.08	0.40	3
COMM	Digi Xtend® TX/RX	5.00	0.73	3.65	1
		5.00	0.08	0.40	
COMM	Kenwood TH-D72A 9600 TX/RX	12.00	1.84	22.08	1
		12.00	0.12	1.38	
COMM	Kenwood TH-D72A 1200 TX/RX	12.00	1.84	22.08	1
		12.00	0.12	1.38	
COMM	High Data Rate – Radio Frequency IC (HDR – RFIC)	5.00	0.02	0.11	1
COMM	High Data Rate – Amplifier (HDR – AMP)	12.00	1.60	19.20	1
DRAGON	DRAGON Board	5.00	0.30	1.50	2
SMTRS	ISIS ISIPOD Deployer	28.00	1.75	49.00	1
VDCS	PSCAM	5.00	1.00	5.00	1
Bevo	Charging Bevo-2	5.00	0.50	2.50	1

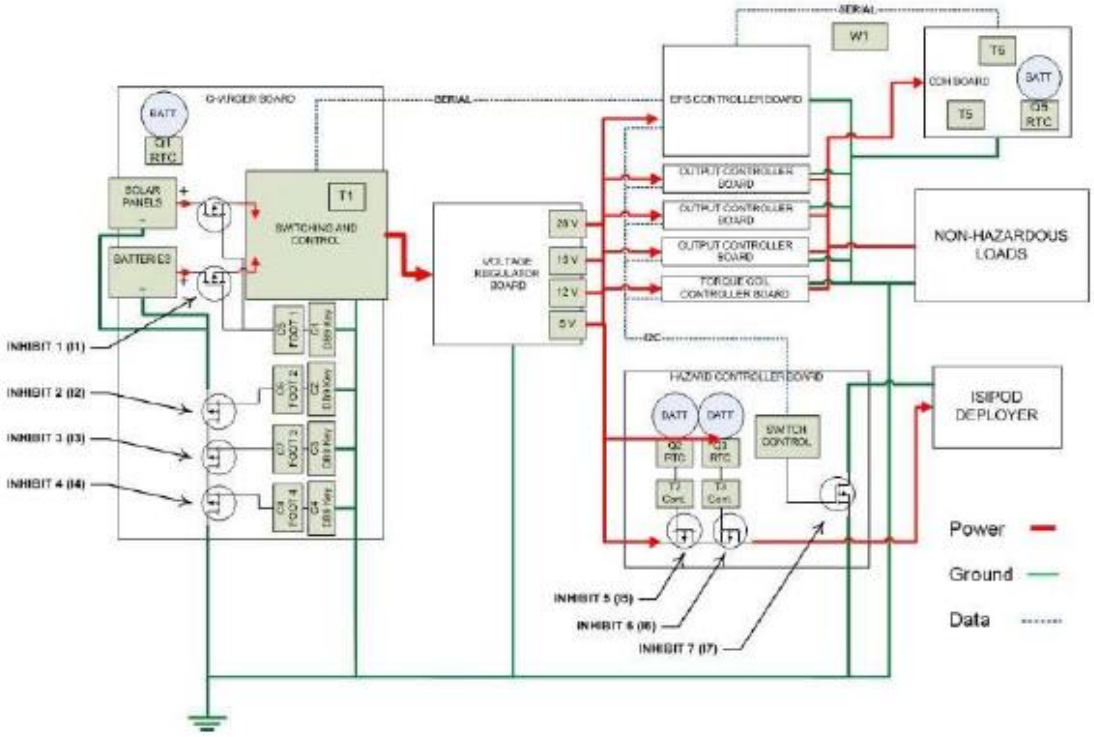

Figure 40: AGS4 Power System Diagram

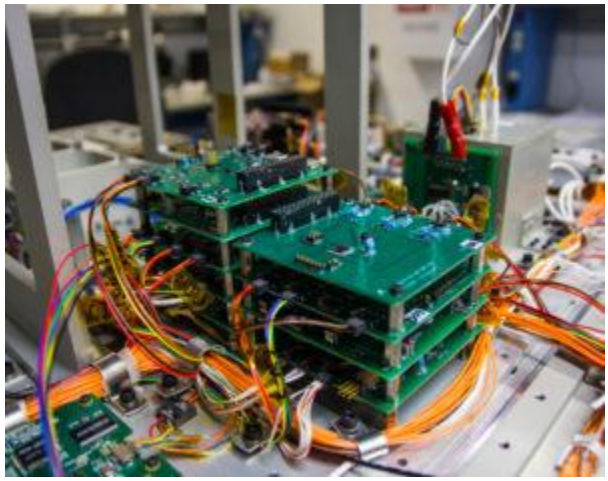

Figure 41: EPS and Battery Installed on AGS4

The EPS consisted of the following custom designed and manufactured components:

2.4.3.1. Battery Charge Regulator

The battery charge regulator board operated as the heart of EPS. In addition to ingesting power from the solar cells, charging the batteries, and distributing solar/battery power to the other EPS stack boards, this board contained a microcontroller to direct all EPS functions across all boards.

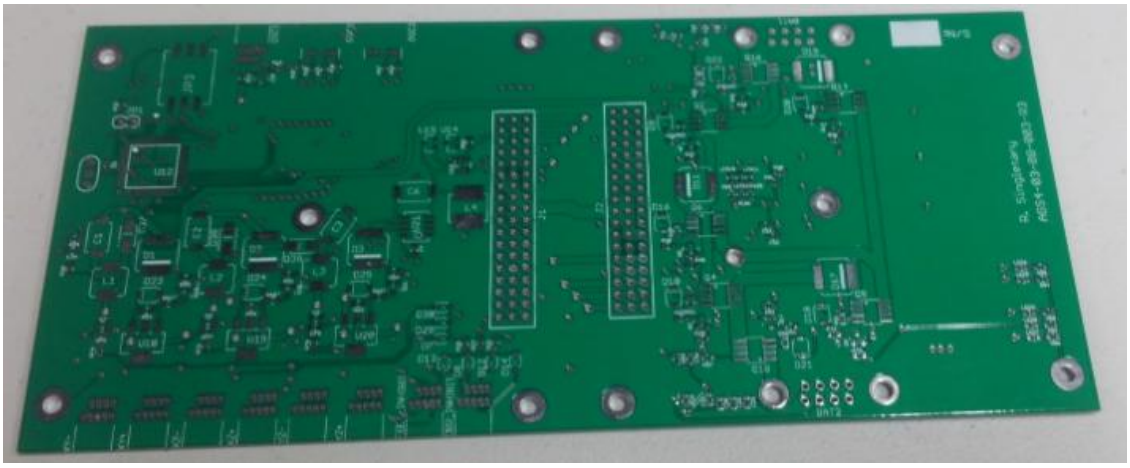

Figure 42: Battery Charge Regulator Board

2.4.3.2. Voltage Regulator Board

The voltage regulator board used a series of regulation circuits and inductors to change solar panel/battery voltage into the various levels the output boards and components require.

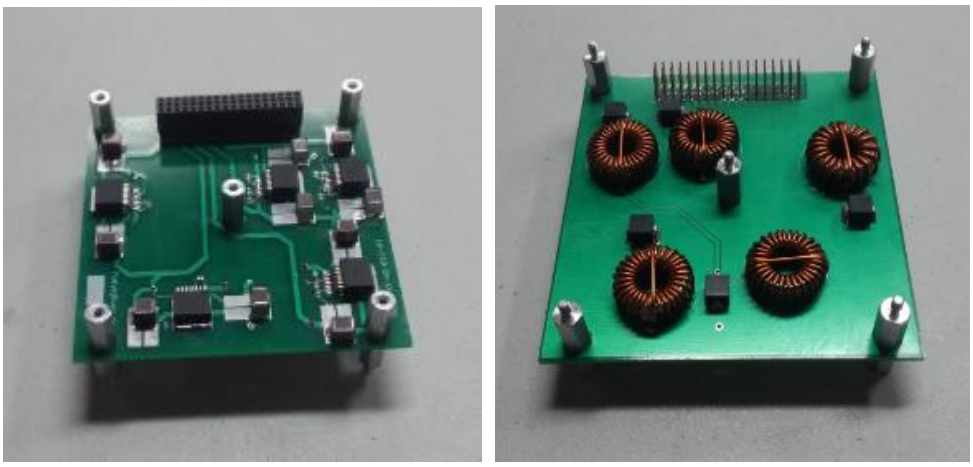

Figure 43: Voltage Regulator Board

2.4.3.3. Torque Coil Control Board

The torque coil control board controlled the 28 V current supplied to each of the three torque coils used for momentum desaturation and coarse pointing of AGS4.

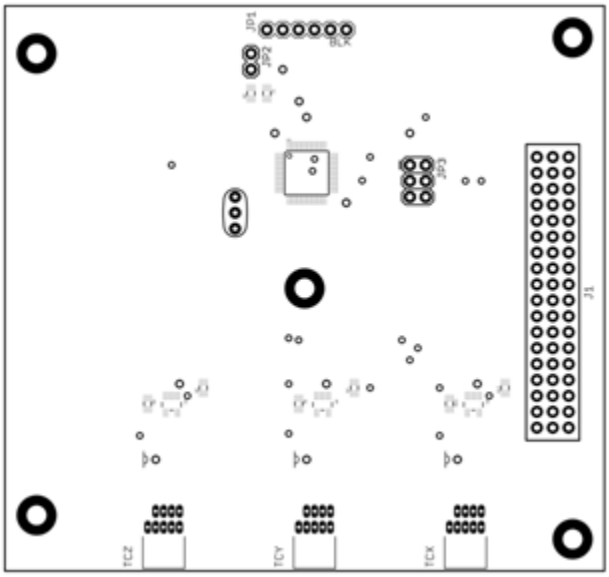

Figure 44: Torque Coil Control Board Layout

2.4.3.4. Output Board

The output board would turn on and off power at specific ports based on commands from CDH. The different voltage levels were produced by the voltage regulator board. The board is capable of being configured for output at 5V, 12V, and 28V. Three of these boards were used to provide the necessary number of output ports at the proper voltage to power the equipment as per the power budget.

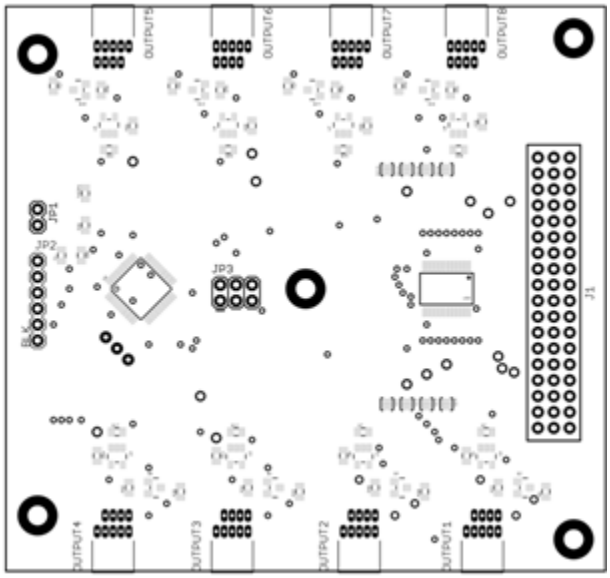

Figure 45: Output Board

2.4.3.5. Hazard Control Board

The hazard control board was designed to prevent CDH from commanding, and EPS from being able to supply power to the ISIPOD release mechanism until a NASA determined time had elapsed. This was to ensure that the release of Bevo-2 could not come back and hit the ISS.

In order to perform this function, this board carried three separate timers powered by independent coin-cell batteries, which would start counting after the inhibits were released. Until all three had shown to have exceeded the predetermined time allotment, relays would remain in the open position physically preventing power from flowing to the release mechanism. The timers would all count up instead of down so that in the event of a power outage they had to start all over rather than immediately being at zero.

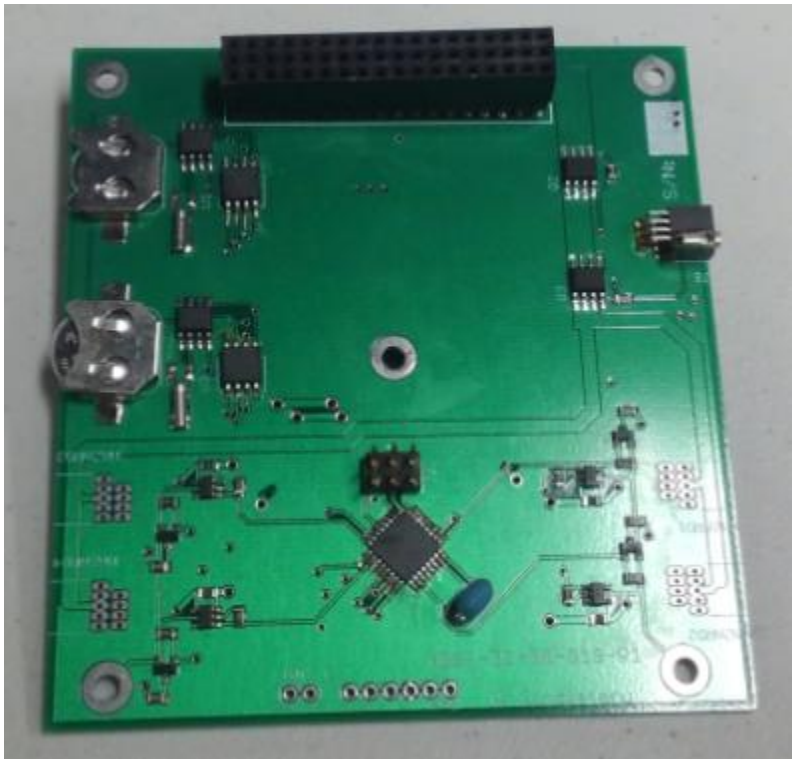

Figure 46: Hazard Control Board

2.4.3.6. EPS Controller Board

The EPS controller board was the means of digital interface between the EPS stack, primarily the battery charge regulator board, and CDH. Control signals for various components are received from CDH, and acted upon by the EPS microprocessor.

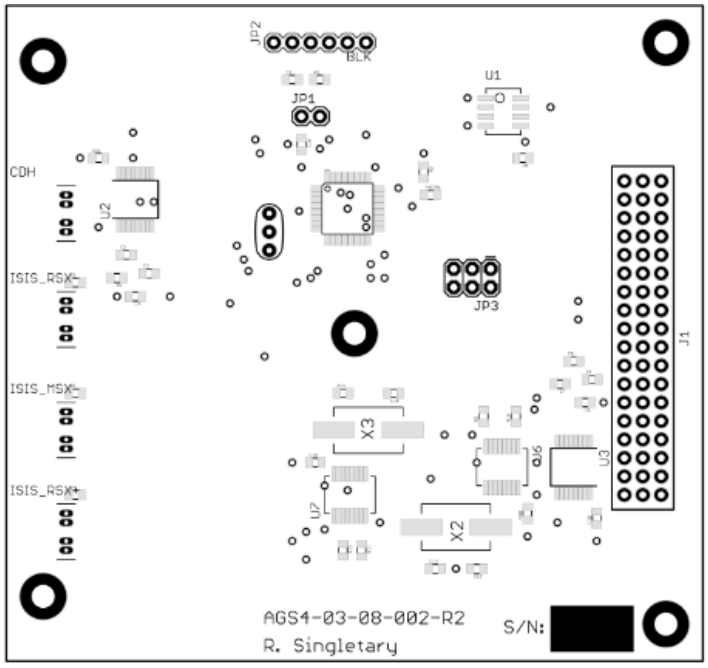

Figure 47: EPS Controller Board

2.4.3.7. Battery and Protection Circuit

As available CubeSat battery packs were not sufficiently large enough for the needs of AGS4, and batteries for larger spacecraft came with a hefty price tag, the decision was made to develop custom battery packs for AGS4. AGSL had gained experience developing small batteries for AGS2, and that experience would be leveraged along with team members experience building Lithium Ion (Li-ion) packs to produce batteries to meet the spacecraft power requirements.

AGS4 would carry two battery packs consisting of nine LG ICR18650C2 Li-ion cells, each with 2800 mAh capacity [23]. The 18650 cell format was used by AGSL on AGS2 for its low mass and high energy density. Nominal voltage was 3.75 V, and when wired in series the pack voltage was 33.75 V.

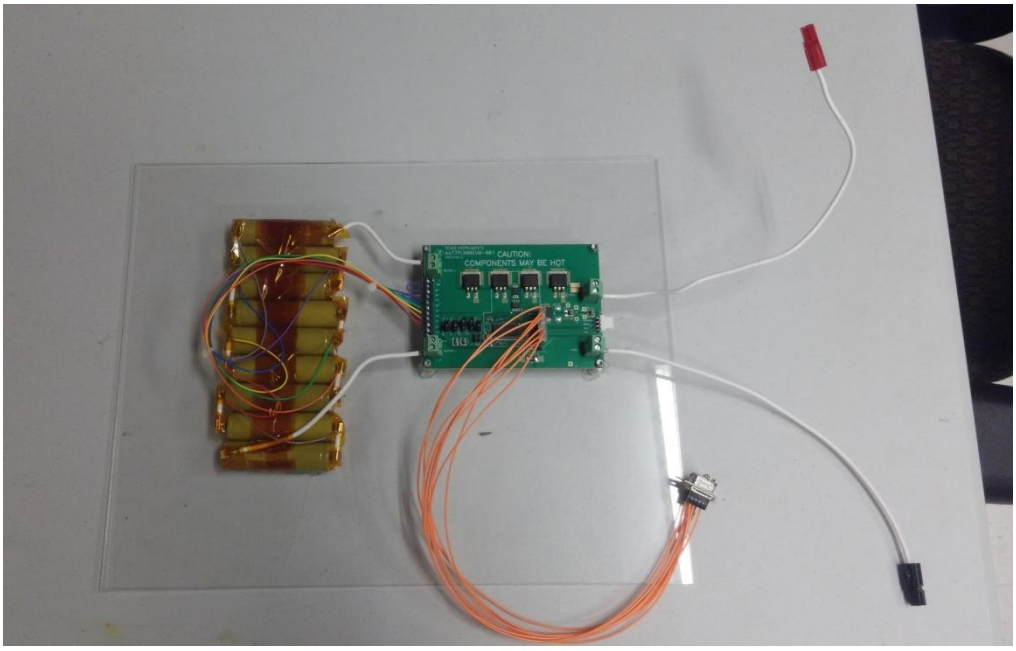

Figure 48: Battery Prototype

As battery explosions are a very real possibility with Li-ion batteries, steps were taken to contain any explosion and protect the rest of the spacecraft, and more importantly the ISS. The nine cells were housed in roughly 3.5x3.5 in. anodized aluminum boxes with divider pockets for each cell. The anodization is intended to passivate the aluminum surfaces, preventing unintended conduction through the box structure, and the box itself is intended to keep any battery explosions contained.

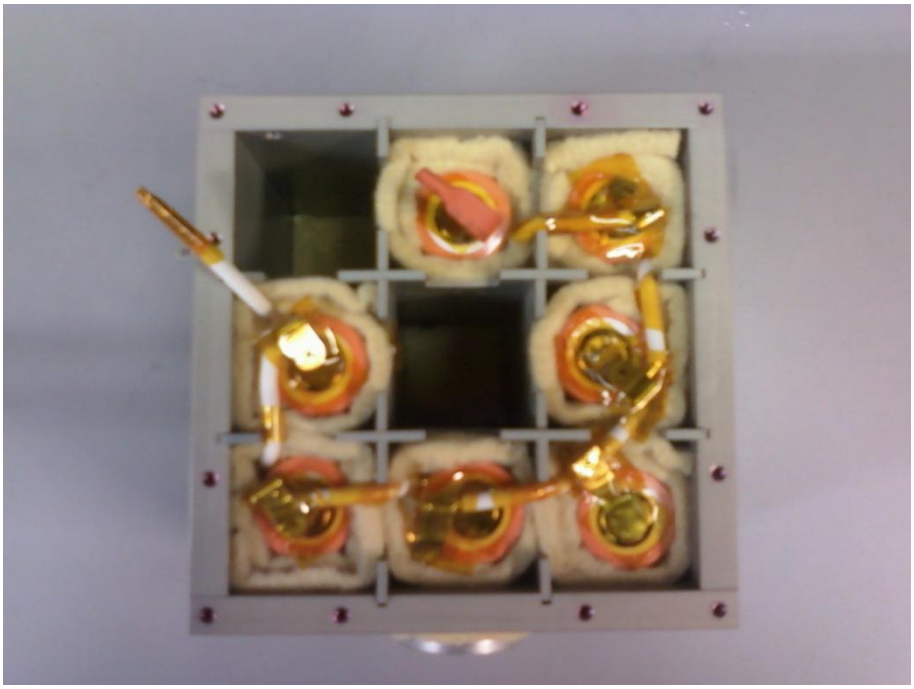

Figure 49: Battery Cut-Away View

The box was lined with, and each cell was wrapped with sheets of Durette® felt, which is a filter material that provides thermal insulation as well as filtration of any liquids that may be released in the event of an explosion. In order to prevent the battery box from becoming a pressurized vessel, whether from atmospheric pressure change or from battery explosion, vent holes were included in one side of the box. These holes were covered with layers of Durette® felt to filter the gas escaping.

Figure 50: Battery Box Vent and Cover

Teflon® insulated 12 ga. wire was soldered to each battery terminal to connect them in series. The wires were routed through the upper gaps in the aluminum dividers, and then they exited the box through two 1/4 in. holes in the lid and ran to the battery protection circuit. Smaller gauge wires were also attached to the positive terminal of each cell, and terminated in a micro DB-9 connector, also in the lid.

The battery protection circuit was necessary to ensure that no individual cell was overcharged or undercharged, conditions that could have destructive results. The circuit was based on the Texas Instruments BQ77PL900 circuit, which used the smaller wires attached to each positive terminal to monitor each cell's voltage, and balance any cells that were over/under voltage from the others.

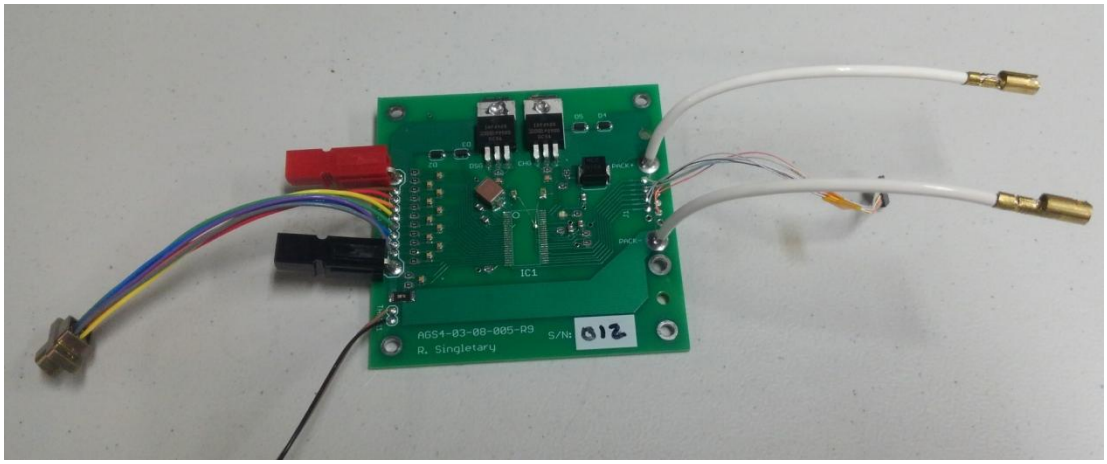

Figure 51: Battery Protection Circuit

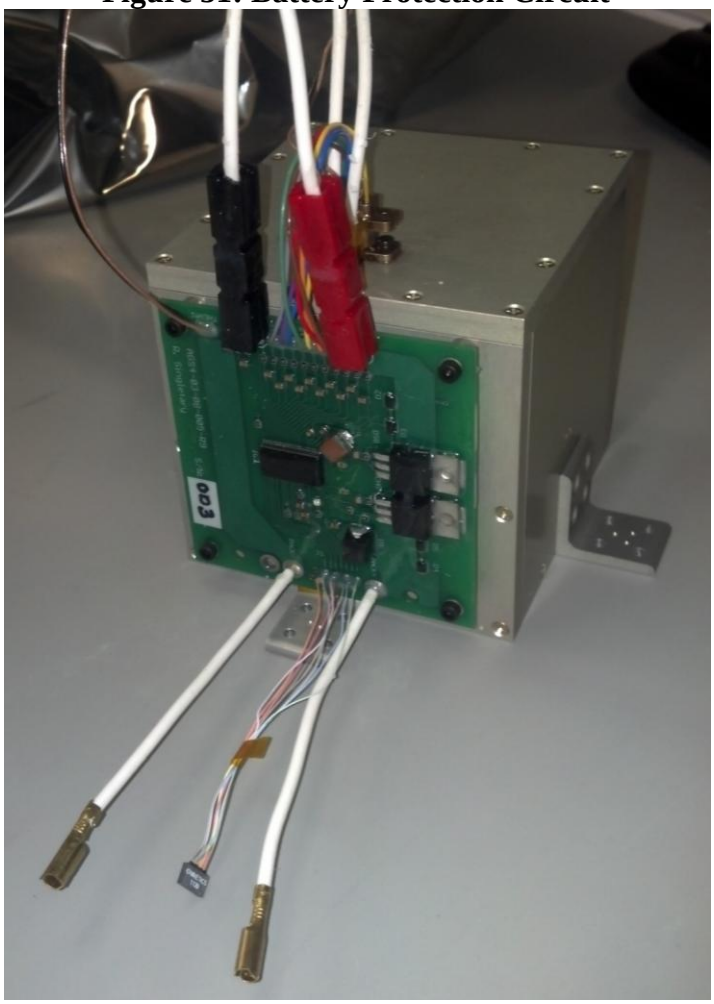

Figure 52: Assembled Battery Box

2.4.3.8. Solar Arrays

The AGS4 team custom designed all of the solar panels using printed circuit boards (PCB) and Spectrolab UTJ solar cells [24]. Custom panels were chosen because body fixed panels can be tailored to the specifics of the vehicle for little cost, and because the offerings on the market were either too large or too small for a spacecraft of this size. Spectrolab UTJ cells were selected as they were one of the highest efficiency cells available at that time, and could be procured in the needed timeframe.

AGS4 had two 6x3 solar panels on each of its faces, except for the bottom face which had three odd sized panels. The 10 panels on the top and side faces were made from white PCB's in order to reduce the amount they would heat up in the sunlight.

Figure 53: Top and Side Solar Panel Configuration

The bottom face had two 3x6 panels and one T-shaped panel containing 18 cells. These panels were shaped this way to accommodate the Cyclops hardware. These panels were green in color because the manufacturer that could print PCB's in this size could only do so in green. All panels on the vehicle had 18 cells to ensure even power generation capability.

AGSL was one of the first spacecraft developers to attach solar cells to the panels using double sided Kapton® tape, instead of the traditional epoxy. This process will be described subsequently in the assembly section.

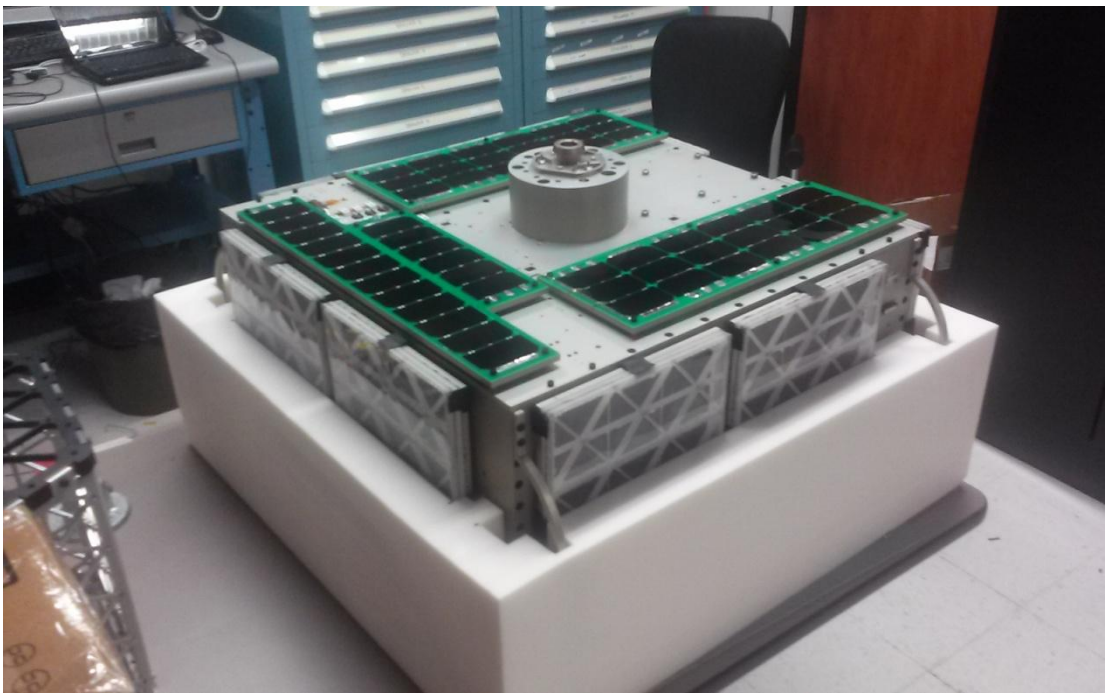

Figure 54: Bottom Face Solar Panel Configuration

2.4.3.9. Wiring Harnesses

All power and data wire harnesses were custom designed. While some were completely handmade to specification using Teflon® coated wire and connectors, most

were custom made by Omnetics, a well respected manufacturer of spaceflight wire harnesses. Some of the Omnetics harnesses were purchased with connections on one end only, so that AGSL could customize the other end to the specific hardware need. Appendix B contains an example of the Omnetics harness specification for a reaction wheel.

2.4.3.10. Inhibits

In order to prevent AGS4 from prematurely activating and potentially releasing BEVO-2 while inside the ISS or prior to release from the Cyclops table, NASA required two sets of three-fault tolerant inhibits.

The first inhibit set was an activation key made out of a Teflon® backed DB-9 connector. Current from the solar panels had to flow through four sets of pins in the connector in order for EPS to be able to activate. Without this key in place, the physical connection is broken preventing current from flowing. When AGS4 was fully installed on the Cyclops table and prepared to enter the airlock, the astronauts removed the key from its "SAFE" storage position, and installed it in the "ACTIVE" receptacle using the screws to prevent it from coming loose.

Figure 55: Inhibit "Active"

In order to keep AGS4 inhibited once the key was moved to "ACTIVE", AGS4 contained four linear pressure switches through which the key current had to flow. When installed on Cyclops, these switches were depressed and held on the open position, preventing current flow. Once released from Cyclops, the switches would depress and allow the activating solar panel current to flow to EPS. The switches were three fault tolerant as they were wired in series so that even if three switches failed to break the circuit, one would still prevent activation.

These four switches were located in the empty space on the inside of the Cyclops knob. They were located here as this was one of the few places where they could be assured to make contact with the Cyclops table and remain depressed.

Figure 56: AGS4 Inhibit Switches

Originally, AGS4 had been designed with four small feet roughly 8 in. outside the knob, and these feet were to house the switches. However, as the Cyclops system was developed in parallel with AGS4, design changes on that system necessitated moving the switches inboard to prevent the possibility of the switch force inducing a spin at release.

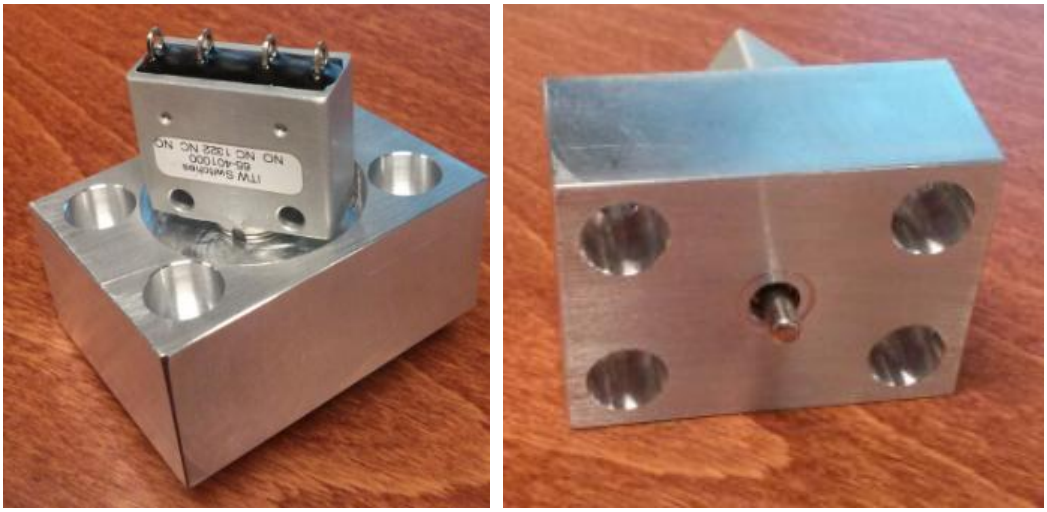

Figure 57: Prior AGS4 Foot Switch Design

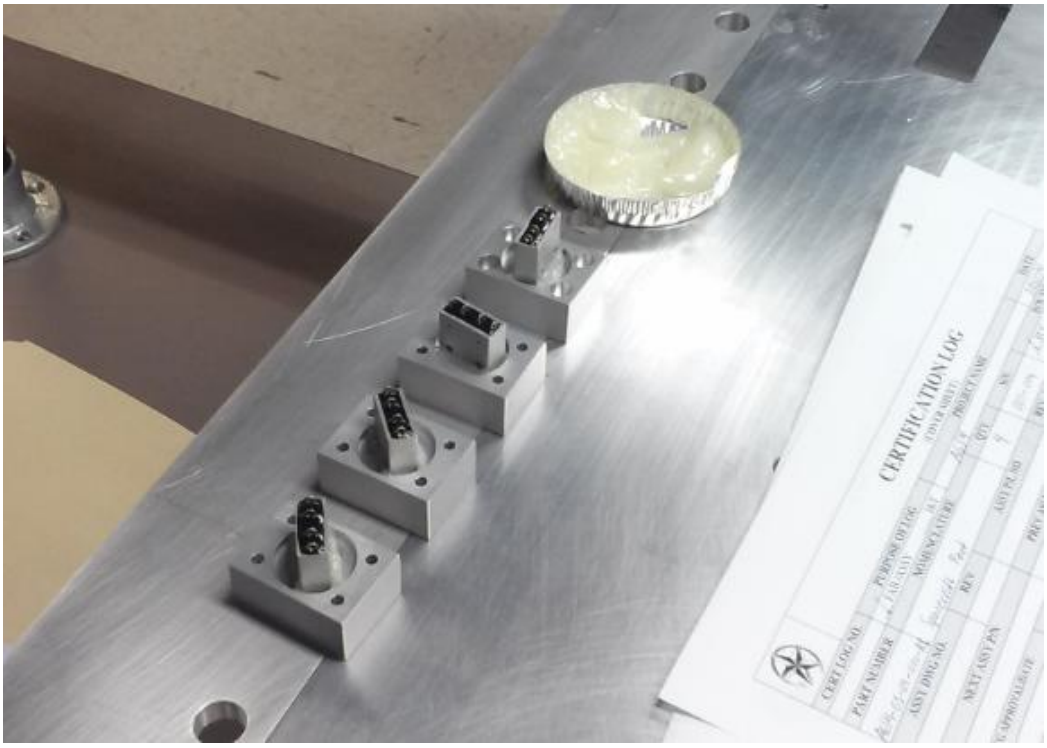

Figure 58: Previous Design Switch Preparation

2.4.4. Communications (COMM)

Lessons learned from the communications troubles on AGS2 were implemented in the communications systems of AGS4. Frequency hopping spread spectrum (FHSS) was avoided for space to ground communications due to its problems compensating for Doppler shift [21]. Instead, it was decided to use redundant lower data rate frequency modulation (FM) radios for simplicity and redundancy.

For reliability, the system design would consist of separate bi-directional uplink and downlink radios. Nominally each would operate only one direction, but had the capability to serve both uplink and downlink roles if needed. Additionally, AGS4 would carry an experimental high data rate transmitter to bring mission data down more quickly if able. Finally, AGS4 would carry a separate crosslink radio to communicate with Bevo-2.

2.4.4.1. Trade Study Criteria

To determine if the candidate hardware was sufficient to meet the mission requirements, various trade studies were performed for each and compared. Factors compared were:

1. Link Budgets: A link budget analysis determines if the signal strength of the transmitters is sufficient to transmit the desired data rate given the receiver equipment, ambient noise level, modulation scheme, etc. Details of link budget calculations are covered in a subsequent section.
2. Environment: All equipment must be rated by the manufacturer to operate within the bounds of the expected environmental conditions,

largely temperature and radiation. As LEO is relatively warm and low radiation, and given the relatively short life expectancy of AGS4, it was determined that commercial grade equipment would be sufficient. Pockets of radiation such as the South Atlantic Anomaly were not understood or accounted for in this analysis, and should be for future efforts before proceeding with this grade hardware.

3. Data Budget: A calculation of data generated over time and mission phase determines how much throughput the communications system will require. By using orbit tracking software, an expected number of communications passes per week can be estimated. Using data from AGS2 regarding personnel availability to monitor passes, weather conditions, and other issues that impeded communications, an adjusted estimate of data per week downloaded was calculated and used to justify the hardware data rates.
4. Cost: Cost of the units compared to capability is a factor in selecting hardware.
5. Frequency and Licensing: Choosing a frequency which has a wide variety of equipment available to operate in that band provides hardware options. Also, selecting a frequency band for which a license will be easily granted reduces complexity and paperwork. AGSL chose to apply for an experimental FCC license using amateur radio frequencies. Experimental licenses are granted for projects to develop hardware and software

capability such as with AGS4, and using amateur frequencies allows radio operators around the world to track the beacons and potentially perform ground passes.

By analyzing the candidate components along these criteria, AGSL converged on a system design of components outlined in the subsequent sections.

2.4.4.2. Data Budget

In order to determine the necessary radio bandwidth to downlink all the required mission data, an accounting of all of the data generated by the spacecraft must be performed. Spacecraft data falls into three main categories: health data, payload data, and subsystem data. Since data transmission is typically in rates of bits and megabits (Mb), this standard is used in the data volume generation calculations as opposed to the traditional storage units of bytes and megabytes (MB).

Health data is generally limited to status data about the spacecraft or subsystem components. These values are constantly monitored by CDH to keep them in the proper bounds, and in the case of AGS4 were stored in memory once every five minutes. With this five minute interval rate, a fairly granular time history of AGS4 could be reconstructed over the elapsed orbits. The state of health (SOH) data packet is listed in the table below, outlining what bits of information were monitored and stored.

Table 15: AGS4 State of Health Packet

	State of Health			
	Bit Size	**Qty.**	**Subtotal**	
Battery Pack Voltage	16	2	32	
Battery Pack Current	16	2	32	
Battery Pack Temp	16	2	32	
Charge Level Indication	16	2	32	
Battery Charge Status	2	2	4	
EPS Board Temps	16	5	80	
Solar Panel Current	16	6	96	
Safety	8	2	16	
State of Components	8	2	16	
CDH Current	16	1	16	
CDH Temp	16	3	48	
Timestamp	64	1	64	
Remaining Data Storage	64	1	64	
Data Remaining to Downlink	64	1	64	
Current Program mode	8	1	8	
COMM Current	16	7	112	
COMM Temp	16	7	112	
Acceleration (x,y,z)	32	3	96	
Angular Velocity (x,y,z)	32	3	96	
Attitude Representation	32	4	128	
Magnetometer Reading	32	3	96	
ADCS Current	16	7	112	
ADCS Temp	16	7	112	
DRAGON Current	16	2	32	
GPS Packet 6F (internal health reading)	272	2	544	
Pos/Vel. Solution (GPS DATA)	384	1	384	
SMTRS Temp	16	6	96	
VDCS Current	16	1	16	
VDCS Temp	16	1	16	
ISIS Current	16	1	16	
Bevo-2 Current	16	1	16	
Third Party Current	16	7	112	
Third Party temp	16	7	112	
			2588	**bits/sample**

At the rate of one sample per five minutes, the total estimated SOH data is calculated in the table below.

Table 16: Health Data Volume

Number of SOH Samples		
Estimated Mission Lifetime (shortest)	3	months
Sampling Rate once per	5	minutes
Samples	25920	
Total State of Health Data	**72.89**	**Mb**

The payloads for AGS4 were the Dual RF Astrodynamic GPS Orbital Navigator (or DRAGON) GPS receiver and the camera system, both described in subsequent sections. The mission requirements call for two orbits of raw GPS data as per MSC-8, and AGSL initially chose one orbit of carrier phase data to satisfy the feed forward requirement of MR-9. This GPS data generated is outlined in the table below. The carrier phase data would be collected during the second raw GPS orbit to utilize data that was already requiring downlink.

Table 17: DRAGON GPS Data Generated

DRAGON Data		
Two Orbits Raw GPS Data, MSC-8	52.10	Mb
Crosslinked Solutions, MSC-10	0.80	Mb
One Orbit Carrier Phase Data, MR-9	78.6	Mb
GPS Data, 8 hr. Tracking	10.1	Mb
DRAGON Download	**141.60**	**Mb**

The mission requirements call for there to be visual confirmation of the AGS4 and Bevo-2 separation event. AGS4 would carry a camera, described in a subsequent section, mounted by the ISIPOD to record the event. This camera would operate in a

medium resolution burst mode to capture the separation, and a slower speed full resolution mode for the Earth imaging phase. Thumbnails of images would be downlinked to reduce data volume, and the best examples selected for full resolution downlink. The table below outlines the image sizes and data generated, though they are likely to be lower with JPEG compression applied.

Table 18: Visual Data Downlink Volume

VDCS Data			
Full Resolution	Full Resolution Image size	46.1	Mb/image
Video	Video Frame Size	7.4	Mb/image
Thumbnail	Thumbnail size	0.26	Mb/image
Release Event	Duration of Video	40.00	sec
	Frame Rate	1.00	frames/sec
	Release Video Image Quantity	40.00	images
	Size of Download	296.00	Mb
Earth Imaging	Duration of Phase	90	sec
	Frame Rate	0.25	Frames/sec
	Earth Image Quantity	23.00	images
	Full Resolution to download	3.00	images
	Thumbnails to download	23.00	images
	Size of Download	144.28	Mb
	Total VDCS Download	**440**	**Mb**

The only AGS4 subsystem that required data recording outside of the state of health readings was the attitude determination and control system (ADCS). This subsystem data was required to verify the spacecraft orientation and control during the crosslink experiment, GPS data collection phase, and Earth imaging phase. The ADCS data packets contain the following information and data sizes.

Table 19: ADCS Data Packet Size

ADCS Downlink Data			
Component	**Bit Size**	**Qty.**	**Subtotal**
Torque Coil (AGSL Manufactured)			
Temperature	16	3	48
Current	16	3	48
Reaction Wheel			
Temperature	16	3	48
Current	16	3	48
RPM	16	3	48
VectorNav (VN-100T)			
3-axis gyros	32	3	96
3-axis accelerometer	32	3	96
3-axis digital compass (magnetometer)	32	3	96
Temperature	16	1	16
Total ADCS Hardware Sample (Bits Per Sample)			**544**

Using this data rate, the ADCS data for each of the mission phases can be totaled as in the table below.

Table 20: Total ADCS Data Generation

ADCS		
GPS Data Logging (2-orbits)	2.94	Mb
Bevo-2 Release	0.05	Mb
Bevo-2 Tracking (8 hr.)	15.7	Mb
Earth Imaging	0.05	Mb
Total ADCS Data	**18.74**	**Mb**

With the data generated for health, payloads, and subsystems totaled, the grand total data required to be downlinked is the sum of these three categories.

Table 21: Total Downlink Data

Total Data			**Notes**
DRAGON	141.60	Mb	Raw GPS data, RelNav exchanged data, Carrier Phase Data, Bevo-2 tracking
Health	72.89	Mb	every 5 min for life
VDCS	440.00	Mb	
ADCS	18.74	Mb	tracking, stabilization, ground pass, imaging
Total	673.23	Mb	

This total downlink data calculation is then used to determine what data rates are sufficient for the downlink radio system. As is further defined in the subsequent sections, two downlink systems are included on AGS4, and the data rates under scrutiny are 9600 bits/second and 153.6 kilobits/second.

Unfortunately, it is not as simple as just dividing the total data by the data rate. Most of the time spacecraft are not within range of the ground station, and even when they are, the highest possible data rate is rarely achieved. In order to determine the opportunities for ground passes, the ISS orbit was propagated over a month using NOVA tracking software, as AGS4 would be in a similar orbit. Passes that never rose 20° above the horizon were not included. The propagations calculated that the AGSL ground station would have an average ground pass time of 12 minutes, 43 seconds as shown in the table below.

Table 22: HDR and LDR Downlink Capacity

TAMU Riverside Downlink Capacity		
Time Per Day per G/S	12	Min
	43	Sec
High Data Rate	153600	Bps
Horizon Data Rate	72000	bps (47% of max)
Packet Efficiency (1-PLR)	80%	
Effective Data Rate	57600	Bps
Pass Efficiency	50%	% available passes taken
% Time Used For Payload Data	50%	% taken pass time used for payload
Per day	11.0	Mb
Low Data Rate		bps
Horizon Data Rate	4500	bps (47% of max)
Packet Efficiency (1-PLR)	80%	
% Time Used For Payload Data	50%	*% taken pass time used for payload
Effective Data Rate	3600	bps
Per day	1.4	Mb

To provide a conservative data rate estimate, the calculations begin by using the data rate at the horizon, where speed of light delays are highest, and require more time for packets and their confirmations to go back and forth. A rate of 47% was estimated [25] for the potential horizon throughput. This data rate will improve as the spacecraft approaches the ground station, and will maximize when directly overhead, only to begin degrading as the spacecraft moves on towards the other horizon. Furthermore, not all packets make it through the first time, requiring the uplink to request resending of the missed packet. This occurs due to noise and other system imperfections. Measurements from radio development showed that roughly 80% of packets can be reliably received [25], and so the effective data rate is reduced by another 20%.

On top of these losses, not every ground pass can be taken due to student schedules or weather, and much of the time taken during successful passes is spent acquiring signal lock initiating the data transfer. Data from AGS2 showed that only about 50% of available passes were attempted or made contact, and that a little more 50% of the pass time was spent downlinking the data, reducing the total time available for the downlink to about 25% of the total available. No pass efficiency was applied to the low data rate system because if that became the only functioning radio, all passes would need to be taken. The conservative margins on the calculations should ease the burden on this high pass efficiency.

These data rates and schedule penalties are more severe than what is expected to occur, and provide a very conservative estimate of data downlink with lots of margin. Using these adjusted daily data rates and schedules, the following table outlines the time required to perform the data downlink.

Table 23: AGS4 Mission Downlink Times

High Data Rate Only		
Time to D/L SOH	6.6	days
Time to D/L ADCS data	1.7	days
Time to D/L VDCS	40.0	days
Time to D/L DRAGON data	12.9	days
	2.04	Months
Low Data Rate Only		
Time to D/L SOH	52.1	days
Time to D/L ADCS data	13.4	days
Time to D/L VDCS	314.3	days
Time to D/L DRAGON data	101.1	days
	16.03	Months

While the estimated time for the low data rate is long, it was within the estimated 24 months maximum lifetime for an AGS4 sized vehicle [11].

2.4.4.3. Uplink System

For uplink, and a low data rate (LDR) backup downlink, a Kenwood TH-D72A [26] handheld transceiver was selected. As this model is a commercial product, it required ruggedization and coating by AGSL. A particularly appealing feature of the D72A was the internal terminal node controller (TNC), a modulator that converts digital data signals into analog radio frequency (RF) for transmission, a feature usually not integrated into amateur radio hardware. Another desirable feature was the transmission (Tx) output power of 5 W, meaning no amplification is required for transmissions to reach the ground station (see link budget). Simple USB serial connections made internal communications and control from CDH straightforward.

Figure 59: Kenwood TH-D72A

One feature that could easily be overlooked was the D72A's ability to power on when DC power is applied to the supply input. Many electronics with a digital power button, and not a physical switch, do not power up when they are plugged in, but instead require activation of the button. The D72A does power up when voltage is applied, making it controllable by the power system.

As uplinking commands does not require much data, the low data rate of 1200 baud (bits per second) was sufficient for command and control. This data rate was selected over the 9600 baud the D72A is capable of as it operates in the 144 MHz band, where the longer wavelength signals experience less loss and arrive at the spacecraft with a higher signal to noise ratio (SNR) than the 440 MHz band signals the unit is also capable of operating with. A higher SNR is desirable on the command uplink to ensure that commands are not corrupted, and can be received when the spacecraft antenna orientation is not favorable.

2.4.4.4. Low Data Rate Downlink System

For the primary downlink and beacon radio, a second Kenwood TH-D72A was selected for all the same reasons as the uplink radio, and it would not require any additional software integration efforts. Additionally, it could be used as a backup receiver for command and control. In order to operate at the 9600 baud rate, the unit would transmit in the 440 MHz band. The 9600 baud downlink would be used as the primary downlink until the experimental high data rate (HDR) radio could be brought online, and continue to be used if there were problems with the HDR.

This LDR downlink system would be used for the spacecraft beacon, transmitted every six seconds. The format of the beacon is outlined below, and it closely resembles the SOH data being recorded.

Table 24: AGS4 Beacon Format

Beacon				
	Bit Size	**Qty.**	**Subtotal**	**Notes**
10 Character Call Sign	80	1	80	
Spacecraft Name (AggieSat4)	72	1	72	
Battery Pack Voltage	16	2	32	
Battery Pack Current	16	2	32	
Battery Pack Temp	16	2	32	
Charge Level Indication	16	2	32	
Battery Charge Status	2	2	4	
Solar Panel Current	16	6	96	
Safety	8	2	16	
CDH Temp	16	4	64	
Timestamp	64	1	64	
COMM Temp	16	7	112	
Position (x,y,z)	32	3	96	
Acceleration (x,y,z)	32	3	96	3 readings, one each axis
Angular Velocity (x,y,z)	32	3	96	3 readings, one each axis
Magnetometer Reading	32	3	96	3 readings, one each axis
Wheel Current	16	3	48	
Wheel Temps	16	3	48	
Torque Coil Currents	16	3	48	
Torque Coil Temps	16	3	48	
			1212	**bits/sample**
			152	**bytes/sample**

2.4.4.5. Experimental High Data Rate Transmitter

As 9600 baud downlink can be painstakingly slow for modern data generation rates, which could result in lost or foregone mission data, AGS4 would carry an HDR radio, but not count on it as the primary due to lessons learned from AGS2 [21]. For this purpose AGS4 would fly an experimental radio unit developed by an AGSL graduate student specifically for AGS4 and microsatellite class vehicles [25].

The radio design consists of an off-the-shelf Texas Instruments CC1101 micro RF transceiver [27] mounted to a custom designed control board. A microprocessor controls serial communications with the CDH, packet handling, and command and control functions for the radio portion. This HDR radio would operate at 153.6 kbaud in the 440 MHz band.

Figure 60: HDR Radio Unit Design (photo by Graves, Dec. 2011)

In order to make the HDR design integrate with the rest of AGS4 systems, a few design modifications were made to the control board by the author of this thesis. The

DB-9 serial port connector was replaced with a latching dual row Omnetics connector, and the power lines split off into a separate two pin latching Omnetics connector. A voltage regulator was built in to convert the 5V power supply from AGS4 down to the 3.3V that the control board requires, as EPS would require another power output board to produce 3.3V for just this device. Finally, the crystal oscillator that sets the serial communication rate was replaced to bring the communications rate with CDH to a supported rate.

Since the CC1101 at the heart of the HDR is only capable of producing a weak RF signal, it would be routed through a 4Watt SM04093-36HS amplifier from Stealth Microwave [28]. This power level would be just sufficient to support the desired data rate (see section 2.4.4.9).

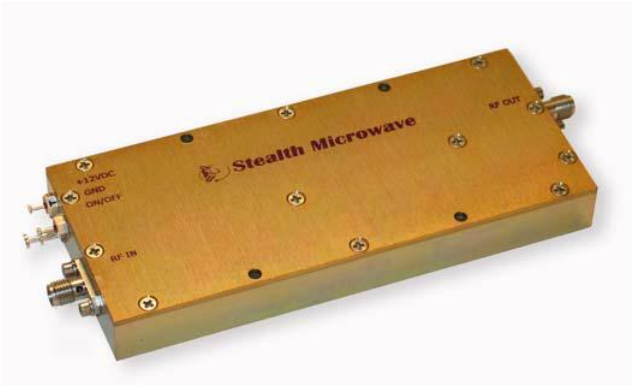

Figure 61: SM04093-36HS Amplifier

While differential carrier phase GPS had been originally selected as the feed-forward technology for MR-9, problems implementing that solution arose as discussed in a subsequent section. As the data budget clearly outlines the need for a high throughput transmitter because of the volume of data these small satellites are

generating, it was decided that this experimental radio system would be AGS4's feed-forward technology.

2.4.4.6. Crosslink

MSC-10 requires each spacecraft to exchange 50 RelNav solutions with the other. In order to exceed this requirement, both vehicles would exchange 100. In order to perform the RelNav calculations, AGS4 and Bevo-2 would need to exchange GPS coordinates with each other. While it would be possible to use both spacecrafts' ground communications radios for this purpose, both teams decided that risk could be reduced by utilizing dedicated point-to-point radios from the same manufacturer, designed to work together. Radio units from Digi International were selected because they are almost plug-and-play, and would require little software integration. As a volume constrained CubeSat, Bevo-2 would carry the Digi Xbee® chip level transceiver, while AGS4 would carry the larger and more powerful (1 W vs. 250 mW) Digi XTend® [29]. Since the XTend® would have a higher transmit power as well as more sensitive receiver and antenna, the communications distance would be increased over both spacecraft using the Xbee®.

Figure 62: Digi XTend®

The packets that each spacecraft would exchange with each other are outlined in the following table.

Table 25: Crosslink Data Packet

Crosslink Nav/RelNav Solution	bits	
X-Position	64	
Y-Position	64	
Z-Position	64	
X-Velocity	64	
Y-Velocity	64	
Z-Velocity	64	
Pitch Rate	64	
Roll Rate	64	
Yaw Rate	64	
Quaternion	256	4 qty 64 bit components
# Space Vehicles in View	16	unsigned short
GPS Week	16	unsigned short
GPS Seconds of Week	64	double
Timestamp	64	
Packet Header	56	7 Byte LONESTAR Packet Header
Total	1048	bits

2.4.4.7. Antennas

Each of the four radios required a dedicated antenna to avoid the need for switches or splitters, which would reduce the signal strength and introduce potential points of failure. The design considerations for antennas were to have sufficient signal gain in a form factor that fits within the dimensions of the airlock.

Flat patch antennas were considered for their high gain RF patterns and nearly surface flush mounting. Unfortunately, their high gain comes at the price of narrow beamwidth, requiring a measure of pointing control to effectively use them. While this may be appropriate in some applications, the AGS4 team wanted communications to be as close to omnidirectional as possible due to lessons learned from communications trouble with AGS2. A successful mission would require that communications be able to proceed even if the spacecraft is unable to actively orient itself. For this reason monopole antennas were selected.

With the monopole design selected, the task became finding antennas with sufficient gain that were short enough to clear the airlock. The antennas that came with the Kenwood radios were too long for the airlock and offered lower signal gain than others on the market.

Antennas that are closer in length to the wavelength of the signal usually have higher gain values [11], with the 144 MHz signal having ~2m wavelength and the 440 MHz signal at ~70cm. In order to effectively lengthen a shorter antenna, manufacturers will sometimes coil a conductor wire around the shaft. SRH815S dual 144/440 MHz band antennas from Diamond Antenna were selected for both the LDR and the HDR

radios because of their 3 dB gain in a 6 in. length package. The 3 dB gain was sufficient to close the communications loop with all systems (see link budget). The A09-HSM-7 antenna (that came with the crosslink radio) was used as it met clearance requirements and was adequate for the experiment range.

A monopole antenna experiences its highest level of signal gain in the plain orthogonal to the pole. The crosslink antenna was installed on the top of AGS4 in order to have the highest signal strength in the same plane that Bevo-2 would be released. The HDR and LDR antennas were installed on the rear face so that the torque coil stabilization would orient their gain lobes towards the ground. The figure below shows the gain pattern for the crosslink antenna. Its highest gain lobe is in the direction of Bevo-2's release trajectory (-180° in this graph).

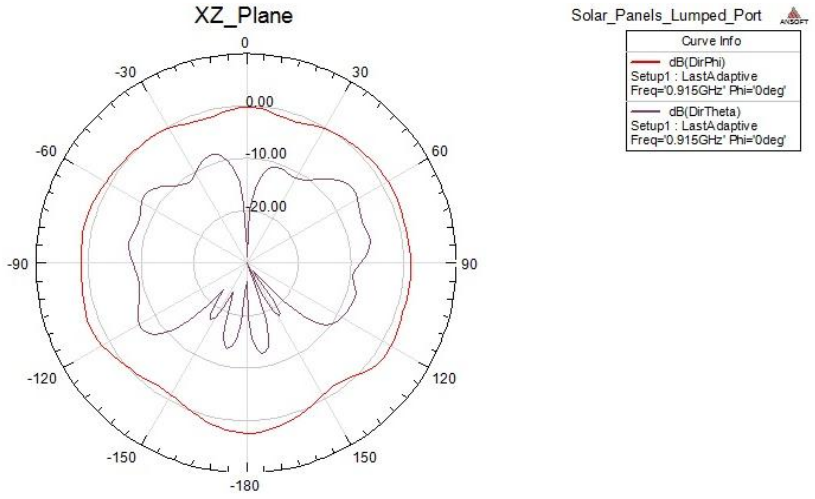

Figure 63: Crosslink Antenna Pattern

Similarly, the HDR antennas pattern is shown in the figure below. The gain is consistent in almost every direction in the plane orthogonal to the antenna, making the

orientation appropriate for ground communications. The patterns for the LDR antennas on the same face are almost identical.

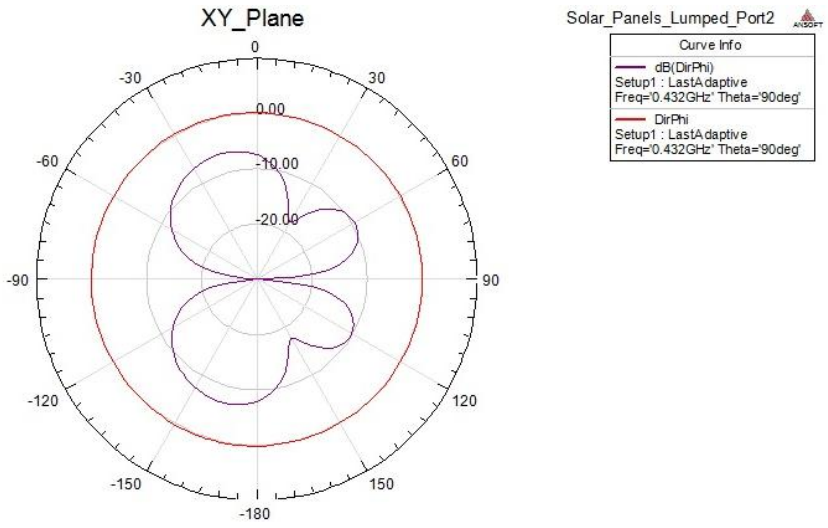

Figure 64: HDR Antenna Pattern

All antennas were installed by ISS astronauts by hand as the SMA style connectors are simple threaded connectors that only require to be finger tight to stay secure.

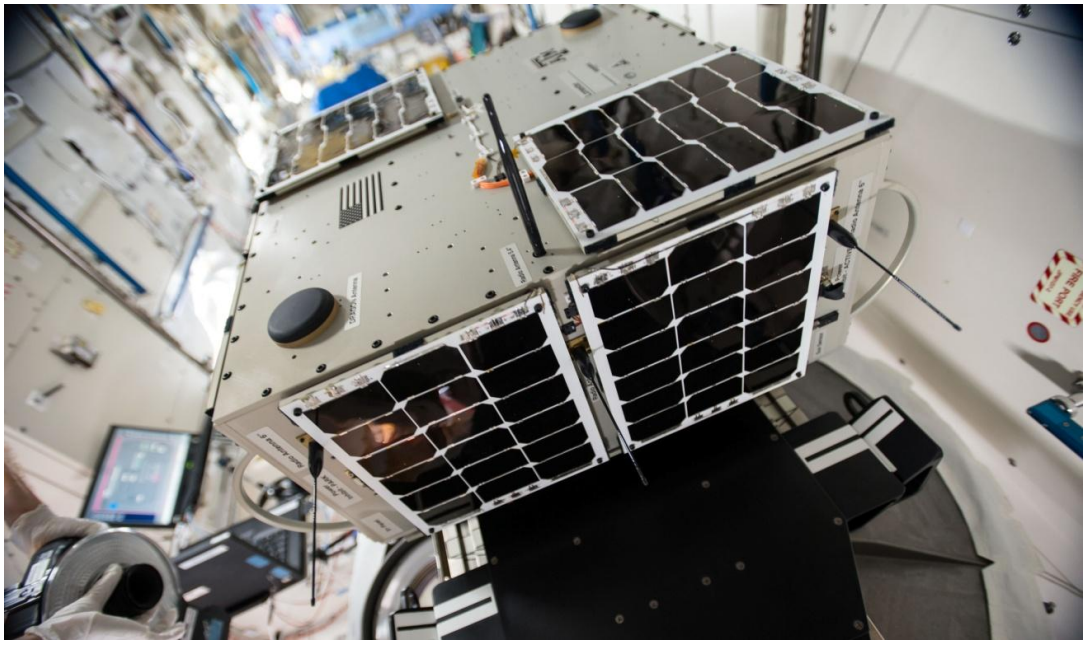

Figure 65: Antennas Installed on AGS4 (Photo by NASA)

2.4.4.8. Iridium® Satellite Network Concept

A concept that was examined and considered for implementation was to leverage the Iridium® satellite telephone communications system for data return. As Iridium® has global coverage, it would be possible to retrieve data from almost any point in orbit rather than waiting for intermittent ground passes, in a similar fashion to the NASA TDRSS satellites. Unfortunately, as development advanced it became apparent that the team did not have all of the skill sets necessary to integrate the satellite modem software into the flight software, and the concept was left to future consideration. Should future AGSL teams have the required skills, implementing satellite telephone communications could prove to be a practical and potent communications method.

2.4.4.9. Link Budgets

The link budget is an analysis to determine the strength with which a signal will arrive at the receiver, and how well it will be received with the equipment being used. If the signal strength is greater than any noise sources, the signal-to-noise ratio (Eb/No) is positive, and communications should be possible. A Eb/No of 3 dB or greater is a good indicator of a strong communications link [11]. However, too high a ratio leads to the communications becoming a source of noise to other users, so excessive power transmissions should be avoided.

The following link calculations were performed while the spacecraft is 10° above the horizon, which is the farthest away it will be during the ground pass. The signal will get stronger as the separation distance closes. This analysis distance provides a conservative estimate of the signal strength. The elevation of 10° was selected as the benchmark for communications based on rough angular measurements of trees and buildings that obscure the horizon.

A complete review of the elements and equations that make up these link analyses is available in Appendix A. Additionally, the calculations for line number 17 in each, the noise temperature, are available there as well.

2.4.4.9.1. VHF (LDR) Uplink

Table 26: Uplink Link Budget

LDR	VHF Uplink				
	Transmit Power	5	W	NOTES	
1		37.0	dBm		
2	Transmit System Losses	2	dB		
3	System Amplification	0	dB		
4	Antenna Gain	3	dB		
5	Pointing Loss	2.37	dB	20	deg
6	VSWR Loss (VSWR of 2)	0.5	dB		
7	**EIRP (1-2+3+4-5-6)**	**35.1**	**dBm**		
	Transmission Frequency, f	140000000	Hz	2.141375	m
	Link Range, R (10 deg, 400 km)	1439650.4	m		
	Propagation Factor, n	1.0			
8	Free Space Loss, Ls	138.5	dB		
9	Atmospheric Absorption Lpa	0.2	dB		
9b	Precipitation Loss Lpp	1.0	dB		
10	**Total Propagation Loss (8+9+9b)**	139.7	dB		
11	Receive Antenna Gain	12.3	dB		
12	Pointing Loss	0.44	dB	4	deg
12b	Polarization Loss	3	dB	Circular	
13	VSWR Loss (VSWR of 2)	0.5	dB		
14	Receive System Losses	2	dB		
15	Tower Cable Loss (RG-6)	2.4	dB	100	ft
16	**Effective Received Power (7-10+11-12-12b-13-14-15)**	**-100.66**	**dBm**		
17	Noise Temperature	30.3	dB	1075.554	K
18	Boltzmann Constant	-198.6	dBm/Hz/K	1.38E-23	J/K
19	Noise Bandwidth	33.8	dB Hz	1200	bps
20	**Noise Power at 140 MHz (17+18+19)**	**-134.48**	**dBm**		
21	**Eb/No (16-20)**	**33.82**	**dB**		
22	minimum for 10^-5 BER	13.3	dB	AFSK	
23	**Margin**	**20.5**	**dB**		

2.4.4.9.2. UHF (LDR) Downlink

Table 27: LDR Downlink Link Budget

LDR	UHF Downlink				
	Transmit Power	5	W	NOTES	
1		37.0	dBm		
2	Transmit System Losses	2	dB		
3	System Amplification	0	dB		
4	Antenna Gain	3	dB		
5	Pointing Loss	2.37	dB	20	deg
6	VSWR Loss (VSWR of 2)	0.5	dB		
7	**EIRP (1-2+3+4-5-6)**	**35.1**	**dBm**		
	Transmission Frequency, f	438000000	Hz	0.684458	m
	Link Range, R (10 deg, 400 km)	1439650.4	m		
	Propagation Factor, n	1.0			
8	Free Space Loss, Ls	148.4	dB		
9	Atmospheric Absorption Lpa	0.2	dB		
9b	Precipitation Loss Lpp	1.0	dB		
10	**Total Propagation Loss (8+9+9b)**	149.6	dB		
11	Receive Antenna Gain	15.5	dB		
12	Pointing Loss	0.44	dB	4	deg
12b	Polarization Loss	3.0	dB	Circular	
13	VSWR Loss (VSWR of 2)	0.5	dB		
14	Receive System Losses	2	dB		
15	Tower Cable Loss (RG-6)	4.5	dB	100	ft
16	**Effective Received Power (7-10+11-12-12b-13-14-15)**	**-109.47**	**dBm**		
17	Noise Temperature	25.3	dB K	341.0674	K
18	Boltzmann Constant	-198.6	dBm/Hz/K	1.38E-23	
19	Noise Bandwidth	42.8	dB Hz	9600	bps
20	**Noise Power at 440 MHz (17+18+19)**	**-130.44**	**dBm**		
21	**Eb/No (16-20)**	**21.0**	**dB**		
22	minimum for 10^-5 BER	13.3	dB	FSK	
23	**Margin**	**7.7**	**dB**		

2.4.4.9.3. HDR Downlink

Table 28: HDR Downlink Link Budget

HDR	UHF Downlink	RFIC			
	Transmit Power	4	W	NOTES	
1		36.0	dBm		
2	Transmit System Losses	2	dB		
3	System Amplification	0	dB		
4	Antenna Gain	3	dBi		
5	Pointing Loss	2.37	dB	20	deg.
6	VSWR Loss (VSWR of 2)	0.5	dB		
7	**EIRP (1-2+3+4-5-6)**	**34.1**	**dBm**		
	Transmission Frequency, f	440000000	Hz	0.681346	m
	Link Range, R (10 deg, 400 km)	1439650.4	m		
	Propagation Factor, n	1.0			
8	Free Space Loss, Ls	148.5	dB		
9	Atmospheric Absorption Lpa	0.2	dB		
9b	Precipitation Loss Lpp	1.0	dB		
10	**Total Propagation Loss (8+9+9b)**	149.7	dB		
11	Receive Antenna Gain	18.9	dB		
12	Pointing Loss	0.44	dB	4	deg.
12b	Polarization Loss	3	dB	Circular	(Max)
13	VSWR Loss (VSWR of 2)	0.5	dB		
14	Receive System Losses	2	dB		
15	Tower Cable Loss (RG-6)	0.1	dB	1	ft
16	**Effective Received Power (7-10+11-12-12b-13-14-15)**	**-102.7**	**dBm**		
17	Noise Temperature	26.7	dB K	469.6618	K
18	Boltzmann Constant	-198.6	dBm/Hz/K	1.38E-23	J/K
19	Noise Bandwidth	54.9	dB Hz	153600	bps
20	**Noise Power at 440 MHz (17+18+19)**	**-117.0**	**dBm**		
21	**Eb/No (16-20)**	**14.3**	**dB**		
22	minimum for 10^-5 BER	13.3	dB	2-FSK	
23	**Margin**	**1.0**	**dB**		

2.4.4.9.4. Crosslink

Table 29: Crosslink Link Budget

	Crosslink				
	Transmit Power	1	W	NOTES	
1		30.0	dBm		
2	Transmit System Losses	2	dB		
3	System Amplification	0	dB		
4	Antenna Gain	2	dB		
5	Pointing Loss	0.59	dB	10	deg.
6	VSWR Loss (VSWR of 2)	0.5	dB		
7	**EIRP (1-2+3+4-5-6)**	**28.9**	**dBm**		
	Transmission Frequency, f	928000000	Hz	0.323052	m
	Link Range, R (100 km)	100000	m		
	Propagation Factor, n	1.0			
8	Free Space Loss, Ls	131.8	dB		
9	Atmospheric Absorption Lpa	0.0	dB		
9b	Precipitation Loss Lpp	0.0	dB		
10	**Total Propagation Loss (8+9+9b)**	131.8	dB		
11	Receive Antenna Gain	2	dB		
12	Pointing Loss	0.59	dB	10	deg
12b	Polarization Loss	3	dB	Circular	
13	VSWR Loss (VSWR of 2)	0.5	dB		
14	Receive System Losses	2	dB		
15	**Effective Received Power (7-10+11-12-12b-13-14-15)**	**-107.0**	**dBm**		
16	Noise Temperature	32.3	dB	1693.341	K
17	Boltzmann Constant	-198.6	dBm/Hz/K	1.38E-23	J/K
18	Noise Bandwidth	42.8	dB Hz	9600	bps
19	**Noise Power at 928 MHz (17+18+19)**	**-123.5**	**dBm**		
20	**Eb/No (15-19)**	**16.5**	**dB**		
21	minimum for 10^-5 BER	13.3	dB	FSK	
22	**Margin**	**3.2**	**dB**		

While a 20^{o} pointing error is assumed for uplink and downlink due to the coarse control of the magnetic torque coil stabilization system, a 10^{o} pointing error is assumed for both spacecraft as they will both be under active reaction wheel control during the crosslink phase, which is a more accurate attitude system with feedback control. The XTend's 2 dB gain antenna was used in the design as the polarity was correct and it was specifically tuned to the frequencies used.

2.4.4.10. Licensing

The United Nations International Telecommunications Union (ITU) requires that all spacecraft be licensed to transmit by the radio communications governing authority of the owner's nation, in this case the Federal Communications Commission (FCC). The ITU then facilitates coordination with all other spacecraft and nations using the same frequency bands.

Since the HDR radio system was itself an experiment to test a new piece of hardware, AGSL applied for and was granted an FCC experimental license (0137-EX-ML-2012). The license call sign was WG2-XFJ, and authorized transmissions at 436.25 MHz, with a channel bandwidth of 406 kHz using frequency modulation (FM).

It was not quite as clear what radio service to file the primary LDR communications systems under, as they were not testing new hardware designed by AGSL. The NASA project management worked with the FCC to understand that, since the AGS4 mission was itself an experiment, radio signals were necessary to facilitate and the LDR and crosslink systems would also fall under an experimental license. AGSL applied for and was granted a second license (0305-EX-PL-2014). The license

call sign was WH2-XGN, and authorized transmissions in three frequency bands. The LDR uplink system was authorized to transmit at 145.98 MHz, with a channel bandwidth of 13 kHz using FM. This would only be used for downlink if there were problems with all other radios. The LDR downlink system was authorized to transmit at 436.25 MHz, with a channel bandwidth of 36.5 kHz using FM. Finally, the crosslink system was authorized to transmit over the range of 902-928 MHz required for FHSS, with a channel bandwidth of 19.2 kHz using FM.

As these two licenses only cover transmissions from the spacecraft, separate licenses are required to operate the ground station. AGSL required that at least one person present during a ground pass hold an Amateur Radio License in order to be the responsible party for the terrestrial side transmissions, and that all applicable regulations are followed.

2.4.5. Attitude Determination and Control System (ADCS)

In order to meet the requirements for 3-axis stabilization and pointing control, AGS4 would need a system of actuators and orientation determination sensors connected by a feedback control system. A series of trade studies were performed to determine the suitability of hardware types for the ADCS system.

2.4.5.1. Attitude Determination Hardware

An ideal attitude determination system would consist of multiple external and internal sensors of varying type for redundancy and to increase accuracy. However, since resources and budgets are constrained, designers need to determine what will be sufficient to meet the mission requirements. It was decided that AGS4 should have at

least two methods for attitude determination, one of which should be able to produce results at all times.

The first type of sensor considered was a star tracker. Star trackers are cameras that take an image of the starfield and compare it against a database of stars and their positions in memory. When the processor has matched the image taken to the database, adjusting for rotation, the star tracker can then determine the orientation vector of the camera boresight and return that value to the spacecraft. The CDH then uses coordinate transformation to gain an external orientation vector for the spacecraft. Star trackers are often considered the best attitude sensors as they produce measurements on the level of arcseconds, but unfortunately carry price tags close to $100k, and were outside the budget for AGS4.

The second sensor type considered were sun sensors. Sun sensors are analog 2-axis photovoltaic sensors that produce voltage based upon the incidence angle of sunlight on them. Each unit is calibrated by the manufacturer and comes with a unique voltage lookup table to translate voltage along each axis into a vector pointing at the sun. Coordinate transformation would be used to calculate the spacecraft vector. While sun sensors are much less accurate than star trackers, on the order of 0.5-1° as compared with 5 arcseconds for a star tracker, they were still sufficient to satisfy the pointing requirement at relatively low cost. For this reason, the decision was made to include one on every face of the spacecraft. SA05 sun sensors from New Space Systems (formerly SSBV) [30] were chosen above others for their size and mass, cost, and ability to be delivered in time for integration.

Figure 66: Sun Sensor Installed

The third type of attitude sensor investigated was Earth horizon sensors. Horizon sensors are cameras that take images and detect where a large transition occurs, usually from the sunlit Earth to black space, or from the dark Earth to the umbra/penumbra on the night side of an orbit. This produces a vector to the Earth's horizon, and is useful for calculating the nadir vector. One drawback is that horizon sensors on their own do not produce a 3-axis solution, but work well when combined with another sensor such as star trackers or sun sensors. The team had planned on using horizon sensors on AGS4 in conjunction with the sun sensors until an additional handling requirement was brought up by NASA. The astronauts and lab technicians would need handles to manipulate AGS4 without touching other sensitive surfaces, and the only good place for them to go

was on the corners of the structure, right where the horizon sensors were located. Given that the horizon sensors were second to the sun sensors, they were removed from the design to make way for the handles, and AGS4 would proceed with only sun sensors as the external orientation sensor.

The team also wanted there to be at least one internal orientation sensor. Gyroscopes, while extremely accurate, are bulky, heavy, power intensive, and expensive, none of which can be tolerated on a university level spacecraft. This left the team examining more cost effective inertial measurement units (IMU). IMU's detect linear and rotational accelerations, and are able to keep track of spacecraft orientation. The accelerometers tend to wander over time, and require an update from an external source, in this case the sun sensors, to recalibrate. The team chose a VectorNav VN-100T IMU [31] for this role as VectorNav was founded by former students of AGSL, and the support that they could give the program would exceed what other manufacturers would. The IMU was capable of determining angular velocity to within 0.01°/s, and also had a magnetic compass which provided another orientation vector, further increasing orientation knowledge.

2.4.5.2. Attitude Control Hardware

In order to facilitate the pointing control of AGS4 to fulfill the mission requirements, a few types of control actuators were considered.

The first was a compressed gas propulsion system, with thrusters angled to provide rotational force. Thrust based attitude control systems have several benefits, namely rapid angular momentum change, and an easy expansion to translational thrust.

However, compressed gas thrusters were quickly removed from the design space as their drawbacks outweighed those of the other component types. Negative aspects are the cost for reliable actuator valves, limited momentum capacity, and safety concerns from having a pressurized vessel in the ISS crew compartment.

The second type of actuator examined was the control moment gyroscope (CMG). CMG's operate by spinning a flywheel, often at high speed, and using gimbals to rotate the spinning flywheel in one or two axes. The equal and opposite reaction from the torque generated by rotating the spinning flywheel is used to point the spacecraft to the desired orientation. CMG's are attractive because they produce a large rotational force for a small mass, and the gimbaled axes allow a bank of CMG's to orient to any attitude even if one or more fail. Drawbacks of CMG's are their complexity with multiple gimbaled axes and moving parts, their high cost, and their continuously high power consumption as they must be run constantly to avoid the stored momentum from coming back into the bus. For these reasons, as well as a lack of appropriately sized options available on the markets, CMG's were not chosen for the AGS4 design.

Instead, the team selected a system consisting of three reaction wheels (RW). An RW is a simple metal flywheel spun about a single axis, without any gimbaling. While RW's do not produce as much torque as CMG's, and are limited to producing torque in a single axis, their reduced complexity, cost, and power consumption fit well with the resources available to AGS4.

Three Sinclair RW-0.06 [32] units were selected to provide the pointing control, as they were calculated to be able to effectively orient AGS4 to track Bevo-2 for the

RelNav experiment. Units from Honeywell were examined, but they were too heavy, too expensive, and could not be procured in the timeframe required. Sinclair also loaned AGSL an engineering model to practice on to reduce risk to the flight hardware. Usually the Sinclair RW would have taken longer to procure, but AGSL happened to be offered units originally built for another customer that cancelled their order.

The equal and opposite momentum generated from accelerating the wheel produces a body torque about the wheel's center. The three RW's were lined up as close as possible with the center of gravity along each of the spacecraft primary axes to reduce the cross-coupling effects that could induce rotation off-axis.

With both RW's and CMG's, there comes a point where the flywheel becomes saturated with momentum, at which point this momentum must be removed in order to be able to continue to use that actuator. Even though the net momentum for orienting the spacecraft from one angle to another is theoretically zero because there is the acceleration to start the slew, and an equal deceleration to stop it, friction on the wheel bearing and minute aerodynamic forces cause losses to occur. These losses require the flywheel to continue to spin, even when holding an orientation, and over time they eventually require the motor to turn at full speed. At this time the momentum must be "dumped" or "desaturated". An obvious method to perform a momentum dump is with a propellant thruster system as is done on the ISS and other large spacecraft. However, this type of system was rejected for the reasons stated in the above section. Instead, the team chose to design a series of electromagnets, one per axis, that would consume power to produce a torque against Earth's magnetic field. These devices are often referred to as

torque coils (TC) or torque rods, depending if they are shaped more like a loop or are composed of a wire wrapped rod. The AGS4 team chose TC's because of the available size of the spacecraft, and because torque produced is proportional to the area of the loops, number of wire loops, and current run through the coils. Each TC was mounted on one of the primary spacecraft axes, and would be able to desaturate momentum from the other two body axes. The figure below shows the construction of the largest torque coil.

Figure 67: Torque Coil

The table below details the torque coil sizes and construction.

Table 30: Torque Coil Construction

	X-Axis	Y-Axis	Z-Axis
Dimensions	1.77 ft x 0.66 ft (0.54 m x 0.2 m)	1.77 ft x 0.66 ft (0.54 m x 0.2 m)	1.64 ft x 1.64 ft (0.5 m x 0.5 m)
Number of Turns	400	400	275
Wire Gauge	26 AWG	26 AWG	26 AWG
Wire Type	Belden Heavy Armored Polythermaleze	Belden Heavy Armored Polythermaleze	Belden Heavy Armored Polythermaleze

Small elements of the control hardware were three 2.35" long, 0.16" diameter metal rods, dubbed "hysteresis rods". What made these metal rods unique was that they were made from HyMu80, a metal with malleable magnetic properties such that it is easily magnetizable. Exposure to a magnet makes the rod a magnet, but it wears off relatively quickly. This property acts as a sort of magnetic drag against the Earth's magnetic field, and serves to dampen long period rotational oscillations. One rod was included along each spacecraft axis to dampen rotation oscillations for that axis.

2.4.5.3. Attitude Feedback Control System

The orientation values from both the sun sensors and IMU, as well as the IMU magnetometer, would be used in a Kalman filter to calculate the best accuracy attitude estimate. A Kalman filter was chosen as it was recommended by the NASA technical advisors to the program, and some AGSL team members had experience in implementing them before. A Kalman filter would be useful because it uses the time history of observations from multiple sources to achieve a more accurate solution than a single measurement. This would be especially useful during eclipse periods where the

sun sensors would not produce orientation data, and the IMU alone would provide the attitude solution. The Kalman filter would be used in conjunction with a negative feedback control system commanding the reaction wheels.

2.4.5.4. ADCS Simulation

The ADCS system hardware, navigation filter, and feedback control system were simulated in MatLab® and Simulink® to verify the system's capability to navigate and control the orientation. Since AGSL did not have access to a full motion feedback control simulator, this analysis was the best way to verify the model. The simulation concluded that the AGS4 control system would be able to orient the spacecraft for Bevo-2 release, image the release, and track Bevo-2 for eight hours after release (battery limited).

2.4.6. DRAGON GPS (DRAGON)

AGS4 carried a dual-channel GPS receiver designed and provided by NASA. Initially, the design was to utilize differential carrier-phase GPS for attitude determination. A single GPS receiver is unable to determine attitude and pointing, but two or more can. If two receivers are spaced sufficiently apart, the orientation vector can be calculated from the position of each antenna on the vehicle. Unfortunately, this only works on very large vehicles like the ISS, and not on microsatellites.

Differential carrier-phase offers a solution for small vehicles. Rather than use the position of each antenna, differential carrier-phase measures the time difference of when a distinct GPS signal or "ping" is received at each of the antennas. Given the position of the receiver and GPS satellite, it is possible to calculate the angle between the antenna

vector and the GPS satellite, providing an attitude solution. This process requires a minimum antenna separation to be able to work, as there needs to be sufficient time for the receiver to distinguish the time difference. The minimum separation was calculated to be roughly 24 inches, which was just enough to implement on AGS4.

Unfortunately, due to personnel changes and the receiver not behaving exactly as expected, AGSL was unable to implement differential carrier-phase GPS attitude determination. Instead, the GPS receiver was used for position determination and to collect the two orbits of GPS data as per the requirements.

2.4.7. Visual Data Capture System (VDCS)

AGS4 was required to carry a camera in order to capture visual evidence of the spacecraft separation event, as well as to verify attitude pointing capability by imaging celestial objects such as the Earth. Additionally, images are great tools to stir student interest in the project.

While using a commercial grade camera was first considered, it was determined that AGSL did not have the skill-set or equipment to ruggedize components like shutters and lenses. Fortunately, AGSL has friends at The Aerospace Corporation through a cooperative agreement to host an Aerospace ground antenna at the AGSL facility, and they donated a PSCAM that they designed and manufactured for the LightSail satellites [33]. This was preferable to the alternative as it was specifically designed for spaceflight. The only development that AGSL had to do was create an interface board to connect the camera's ribbon wire connection to the computer's serial port, and modulate the data into the proper format.

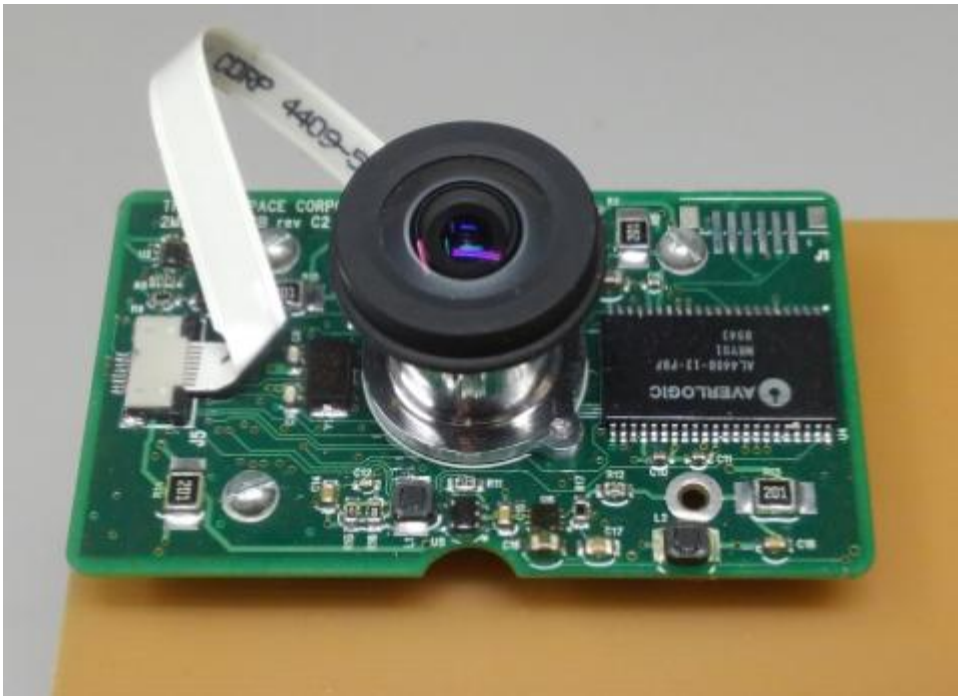

Figure 68: PSCAM

The camera has a 185° fisheye lens, and can operate in two different capture modes, with resolutions and frame rates as laid out in the table below. Each frame for each capture mode has a thumbnail generated to help select desired images for downlink.

Table 31: PSCAM Imaging Capabilities

Full Resolution	Width	1600	pixels
	Height	1200	pixels
	Max Frame Rate	0.4	Frames/sec
Video	Video Width	640	pixels
	Video Height	480	pixels
	Max Frame Rate	1	Frames/sec
Thumbnail	Thumb Width	120	pixels
	Thumb Height	90	pixels
	Max Frame Rate	N/A	Post-processed

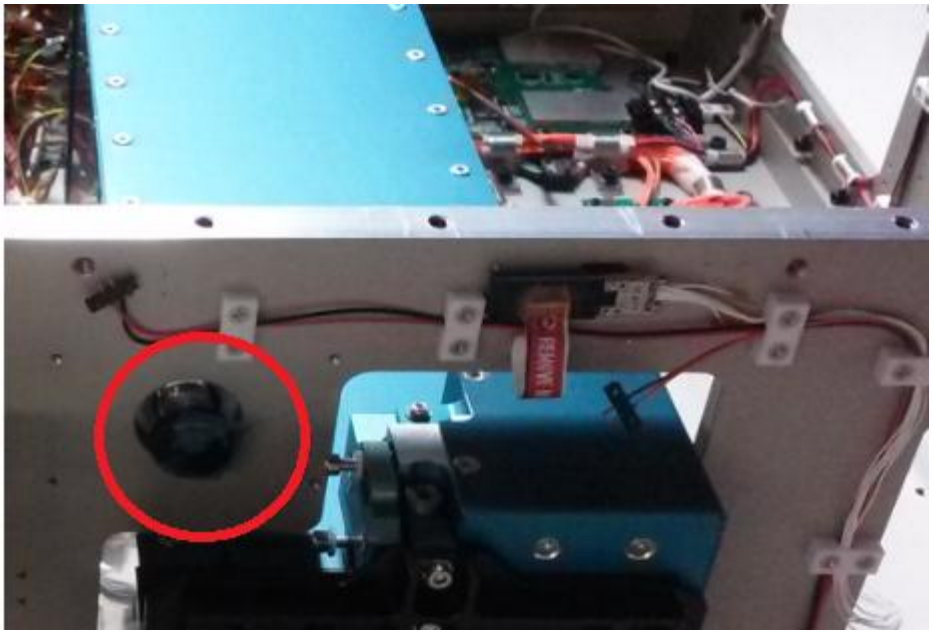

Figure 69: Camera Location (red)

With the camera interface board connected, the final step to prepare for integration was to focus the lens. This was done by taking test images, rotating the lens, and taking another test image. When the test images were focused, the lens was staked in place to maintain the focus setting.

The following images illustrate the size difference between the three image capture modes. The clear blue film lens protector was still on the camera at this point in testing, and was not removed until on the Cyclops table in orbit. While this causes some haziness, the image is still visible, and the fish-eye effect can be seen at the edges. These images were taken after VDCS integration to the bus, prior to panel fold up, so the imagery is of the assembly jig and table.

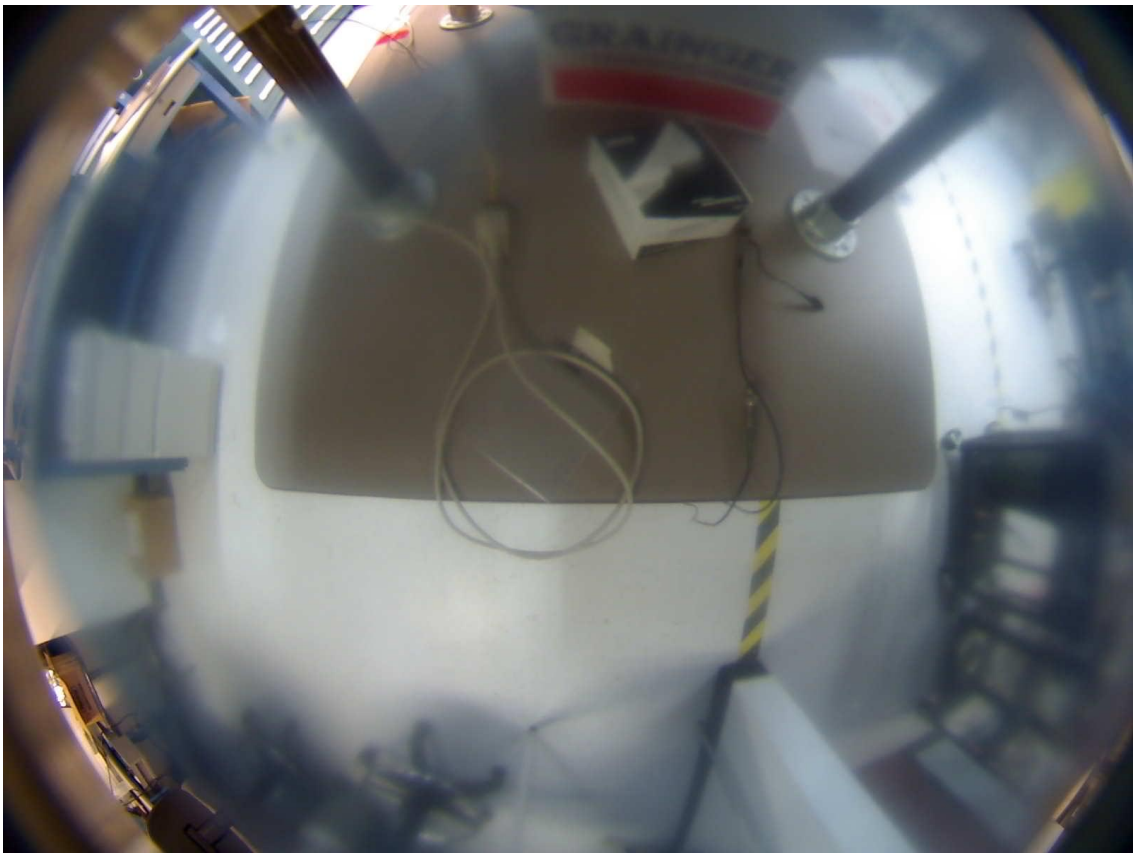

Figure 70: PSCAM Full Resolution

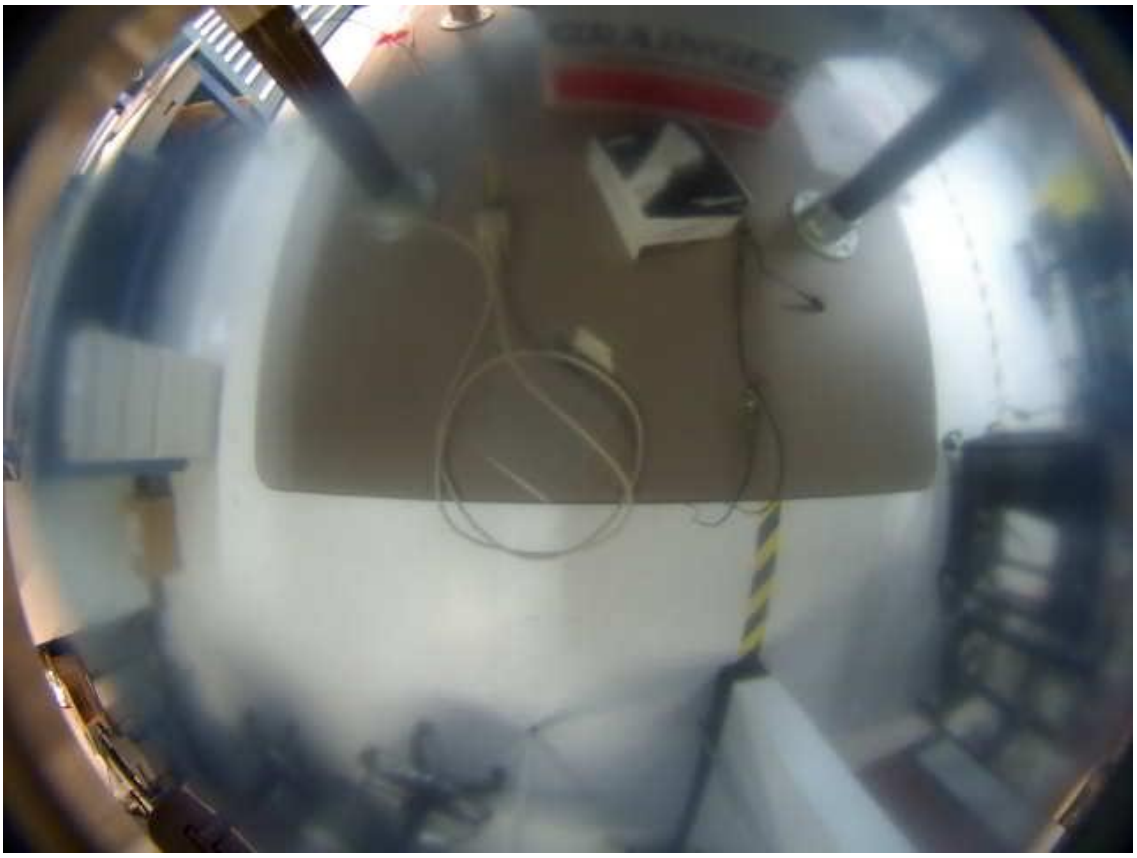

Figure 71: PSCAM Video Resolution

Figure 72: PSCAM Thumbnail

3. ASSEMBLY, INTEGRATION, AND TESTING

3.1. Assembly

3.1.1. Prototyping

Prior to component and vehicle assembly, each subsystem was prototyped using non-flight versions of hardware to verify the system design and capability. Non-flight versions of hardware are used such that wear and tear are reduced for the flight articles, and so that any mistakes destroy less costly hardware. This testing also provides the opportunity to test system interactions and develop the software to ensure that all components are working together. In support of the type of development, prototype level components were assembled into a configuration known as a "FlatSat".

A FlatSat is a desktop representation of the majority of subsystems of the spacecraft that will need to be working together. For AGS4, the FlatSat consisted of a CDH, full COMM system, camera, and emulators for the ADCS system. EPS was not included, and was instead replaced by AC power supplies. EPS to CDH integration would be extensively tested in other phases. This setup allowed AGSL to test all subsystem interactions and develop the interfaces such that CDH can command and control every aspect of the spacecraft. FlatSat was used to test the ability of AGS4 to perform the mission operations and meet the requirements. With FlatSat development and all other systems prototyped, components could begin to be made flight ready, and start the assembly process.

3.1.2. Component Assembly

For each subsystem, the components were prepared for spaceflight separately before being integrated into the final flight configuration. This process included hand soldering electronics boards (where applicable), staking and coating, and function testing of each component.

3.1.3. Soldering

Each electronic circuit board developed by AGSL, and the solar panel PCB's and cells, were hand soldered by team members lab certified to solder. Soldering techniques and quality assurance practices are as per NASA-STD-8739.3 Soldered Electrical Connections [19] and AGSL-3108-200 Quality Management System [34].

Soldering consists of applying heat to the two parts being joined, and flowing a conductive material between them to electrically and mechanically bond them. Many commercially available solders have a high tin content to reduce potential lead exposure. Unfortunately for spaceflight, in the cold, vacuum, microgravity environment being operated in, tin can actually begin to grow "tin whiskers", crystalline structures which branch out and can potentially touch other surfaces causing a short [19]. For this reason, high lead content solder is recommended for space applications, which requires soldering to be performed in a well ventilated environment, preferably with a fume fan.

Electronic board soldering involves placing the part in the correct orientation on the PCB, and forming the appropriate solder connection as per [19]. Smooth, filleted joints are desired.

3.1.4. Staking and Conformal Coating

Staking is the application of a thick epoxy to large soldered components, with the intent of taking the strain of the rocket launch off of the soldered connections, and having the epoxy become the load bearing structure. Conformal coating is the process of applying a thin epoxy resin over the surface of boards and other components to serve as a vapor barrier between components and the environment. It also has the benefit of preventing certain plastics from outgassing [35], or essentially dissolving in the vacuum, and being destroyed in the process. Staking and Conformal Coating are prescribed by AGSL-3105-200-001 Staking and Coating Procedure Rev A [36], which is an application specific adaptation of NASA-STD-8739.1A Workmanship Standard for Polymeric Application on Electronic Assemblies [37]

Prior to applying any polymerics, the PCB must be thoroughly cleaned. Using 100% isopropyl alcohol and an acid brush, the board is cleaned using horizontal strokes and washed down. The board is then rotated 90° and the board cleaned again using horizontal brush strokes. This process is repeated twice more to be sure that all solder residue and debris are removed, and dried with a lint free wipe. The board is then baked at least 30 minutes at 60-65°C to evaporate any solvents.

Staking is performed by mixing a 1:5 ratio of Uralane 5753A and Uralane 5753B, along with silicon dioxide powder to thicken the mixture. After thorough mixing, the mixture is exposed to vacuum of 0.05 Torr for 5-8 minutes. The mixture is then placed into a syringe, the gauge of which is appropriate to the size object being staked. A sample of the mixture is to be saved for analysis if needed. Using the syringe,

fillets of epoxy are applied between the body of large electronic components and the PCB surface, avoiding the soldered connections. After 24 hours the mixture will be cured sufficiently to perform conformal coating.

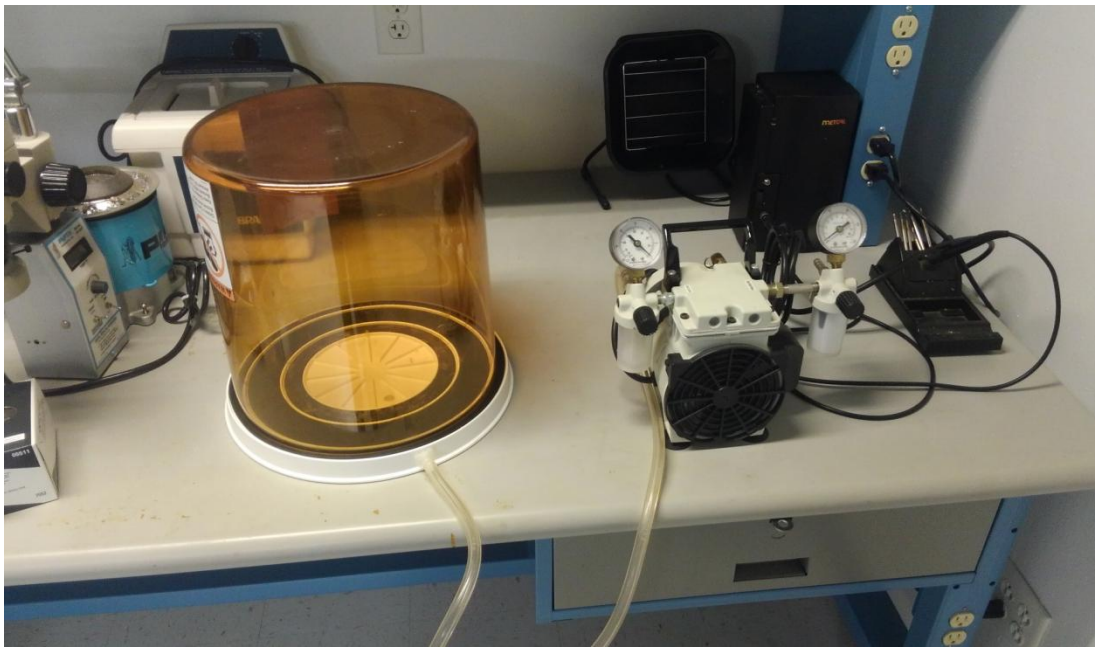

Figure 73: Vacuum Jar Setup

With all of the large components adequately secured to the PCB using staking compound, the conformal coating barrier can be applied. The process of mixing the resin is similar, using a 2.7:15 ratio of Uralane 5750A and Uralane 5750B. No thickening agent is used for this resin. With the components mixed, the mixture is exposed to the same vacuum period as the staking material, and a sample set aside. An acid brush is the used to apply the resin to the PCB, being sure to cover all components and fill every crevice. Care should be taken to avoid creating air bubbles, and apply thin and even layers to both sides of the board. With the conformal coat in place, the

assembly is then exposed to the vacuum again to remove any trapped air bubbles on the parts. The resin will be dry to handle in 24 hours, and fully cured in 5-7 days.

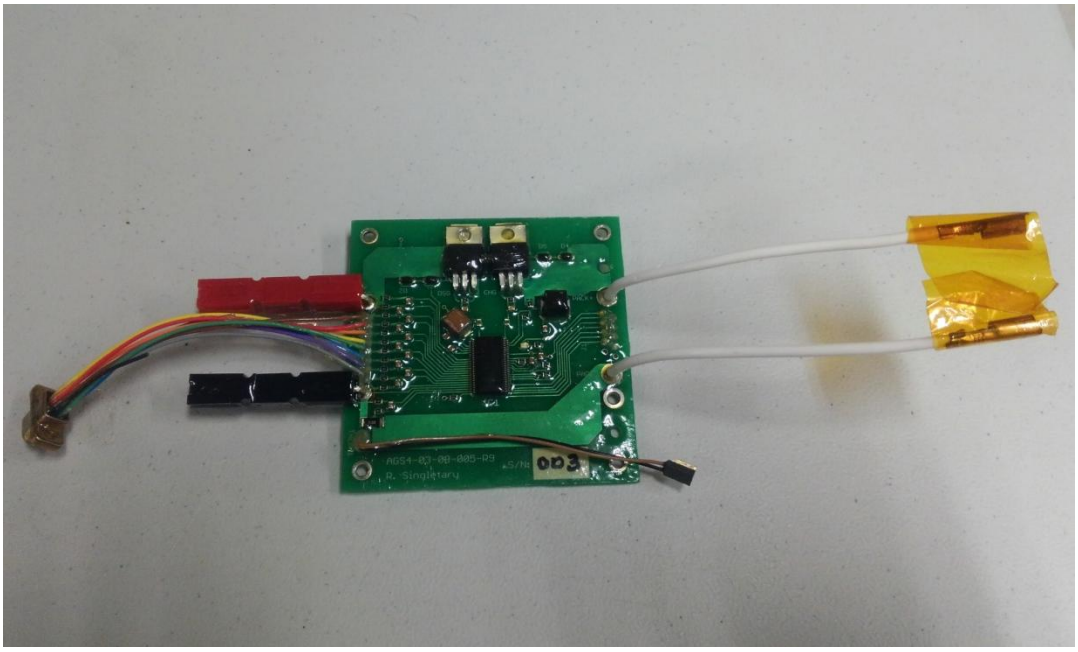

Figure 74: Conformal Coat Visible on Battery Protection Circuit

3.1.5. Locktite® Adhesive

For AGS2, thread locking compound such as Locktite® was not allowed by NASA. By AGS4, NASA had changed this policy and were allowing it to be used. This epoxy was used as back-out prevention for #0 size fasteners, and as a general bonding adhesive on AGS4.

Locktite® was the simplest to prepare adhesive used on AGS4, and is fully described in AGSL-3105-200-002 Thread Locking Compound Procedure [38]. Another two part epoxy, the mix ratio for Locktite® is 100:17 EA9394A and EA9394B by weight. After weighing out the correct quantities, the two are thoroughly mixed until

uniform in color. The working time is 90 minutes, and is best applied by spreading due to the high viscosity. A sample should be kept for future analysis if needed.

3.1.6. SMTRS

As the structural components were fabricated by a machine shop, SMTRS did not have to assemble these pieces. However, the first task upon receipt was to verify that they were fabricated according to the drawings, including each hole and their spacing. This was necessary as it was discovered that the shop that the machine shop contracts to for anodization and Alodine® treatments placed the Alodine® patch for the ISIPOD support block at a 90° angle to desired.

After the part was fixed, the next step was to install the locking Heli-Coils® into every hole that required a fastener. This was done by hand by the AGSL students using the tools in the Heli-Coil® kit for each size fastener.

The other remaining assembly task for SMTRS was to assemble the solar panel covers, and attach Velcro® to the solar panel trusses. The polycarbonate sheets had been cut using a waterjet into a sheet with triangular grid cutouts, and a rectangular spacer piece to keep the grid off of the solar cells. These two pieces were bonded using Locktite® epoxy, and the excess wiped away. After it had cured, a sheet of Mylar® polymer film was bonded to the outside of the grid sheet using staking compound. Originally Locktite® had been specified for this purpose, but prototyping found that the Locktite® was unable to bond to the Mylar®, preventing a seal from being formed and defeating the purpose of the panel covers. Experiments with staking compound showed that it was able to adhere to the Mylar®, and so was selected as a substitute. With the

film in place, the last step was using Locktite® to attach strips of male Velcro® to the edges of the cover. The epoxy was applied to the hook side rather than the flat back of the material so that when cured it could latch the cover to the matching Velcro® on the solar panel. Female Velcro® was applied in matching locations on the solar panel trusses using Locktite®. The adhesive was applied to the back of the material so that the loop side was open for attachments.

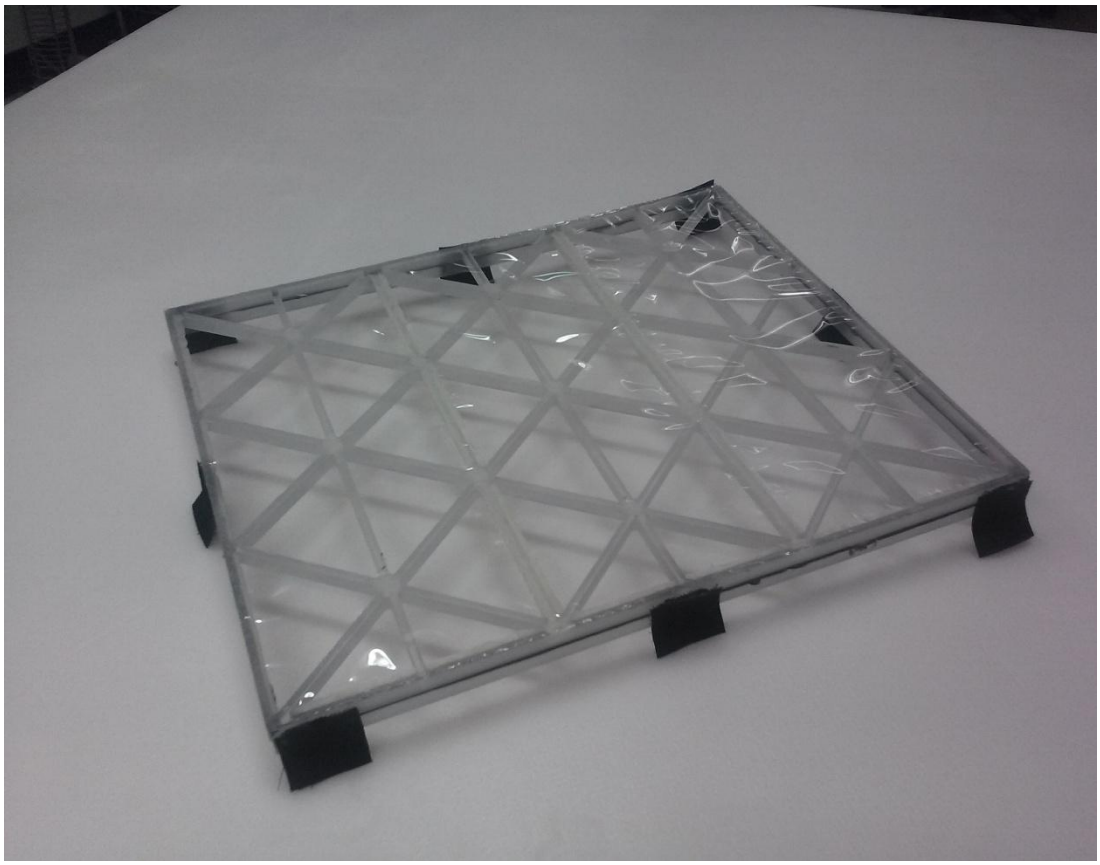

Figure 75: Solar Panel Cover

3.1.7. CDH

As the TS-7800 is a production unit, no soldering was required. The only customization needed was to use the user accessible jumper pins to select the data rate for the serial ports. The flight software and operating system were loaded onto the SD card, and inserted into the slot on the computer. The SD card was then staked in place along with all large components on the TS-7800 and the serial expansion boards. Stake was applied not only to the microprocessors, capacitors, and inductors, but to all of the serial and USB connectors to reduce the load they will experience during launch. After the staking had cured for all boards, they were conformal coated.

3.1.8. EPS

All EPS boards were hand soldered, along with the solar cell connections and battery connections. The boards comprising the EPS stack were all relatively straightforward to prepare. After soldering, they were staked and coated as per the polymerics procedure.

The solar panels were a bit more interesting. Normally solar cells are adhered to the panel using an epoxy. This can be quite messy, and cause excess to wind up on a cell face which cause glass breakage while trying to clean. AGSL learned firsthand from AGS2 how frustrating this process can be. In order to eliminate this source of stress, The Aerospace Corporation suggested that AGSL look into using double sided Kapton® tape for the adhesive, which was a project they were researching. Kapton® tape has a high enough temperature range to handle the direct sunlight and the soldering iron.

AGSL was one of, if not the first spacecraft to utilize this method for attaching solar cells.

After determining that this was indeed a viable solution, cardboard templates were designed for shapes that would provide maximum adhesion surface area while not interfering with the cells' connection tabs. These templates were used to cut out tape for the 234 solar cells by hand. One side of the Kapton® cut-outs was peeled off, and the tape gently placed on the back of each cell, careful to ensure than no air bubbles were trapped.

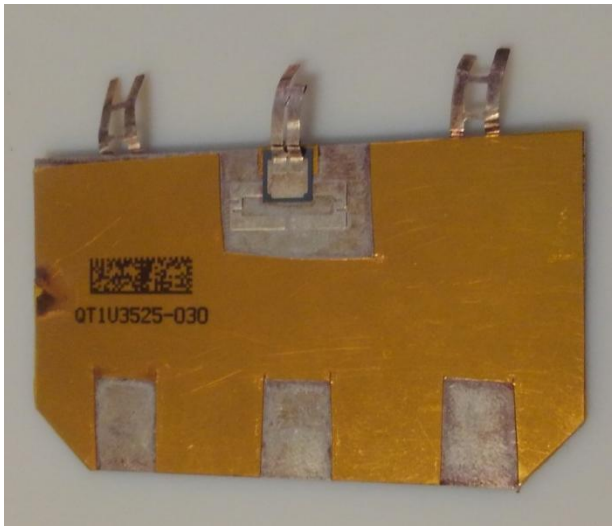

Figure 76: Double Sided Kapton® Cut-Out

Custom solar panel soldering jigs were made to connect the cells in the proper shape and adhere them to the PCB.

Figure 77: Solar Panel Jigs

The cells were placed into the jig, and the tabs from the previous cell were soldered to the base of the next in series. Only a small amount of solder was needed on each tab, as a blob would have created a pressure point that would likely cause cell breakage when pressing down to secure the Kapton® to the panel.

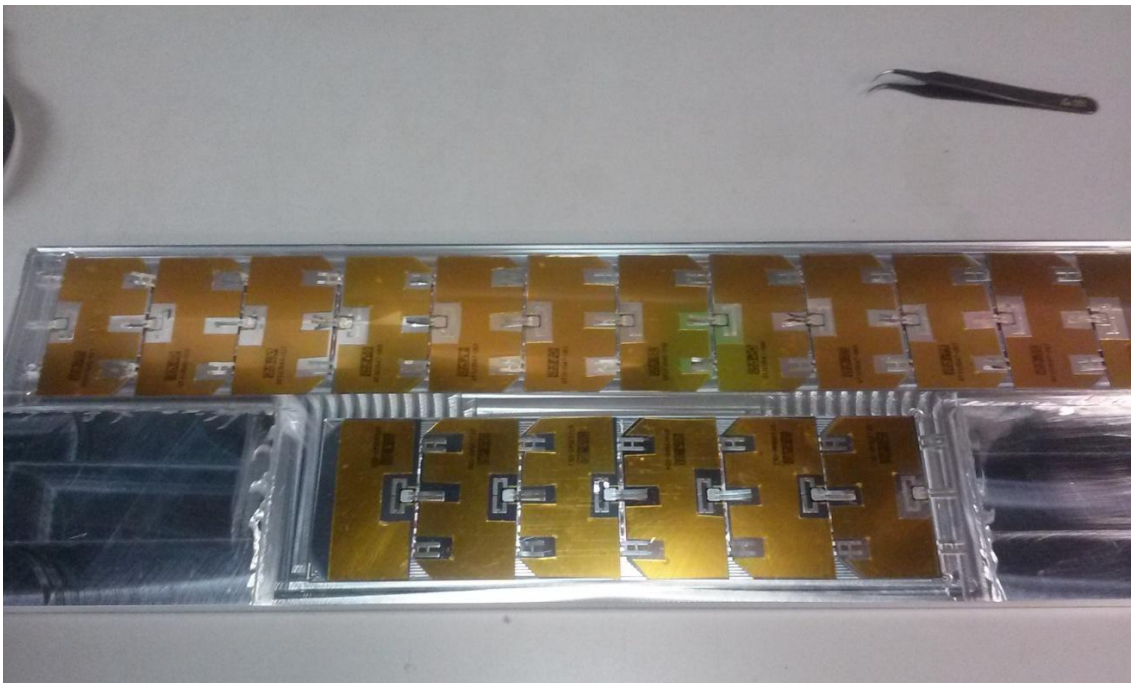

Figure 78: Solar Cells in Assembly Jig

With all of the cells connected, the backs of each of the Kapton® adhesives were removed, and the PCB for each panel was gently pressed into the back of the cells. The jig aligned the PCB such that the cells would be in the proper locations. The PCB was then removed, and all of the cells had adhered to it. Solder was then used to connect the cells at the end of each string to the PCB, creating a series of 18 cells. The short wire harness for the solar panel was soldered to the PCB at the designated terminals. This process was the same for all 13 panels of the three types.

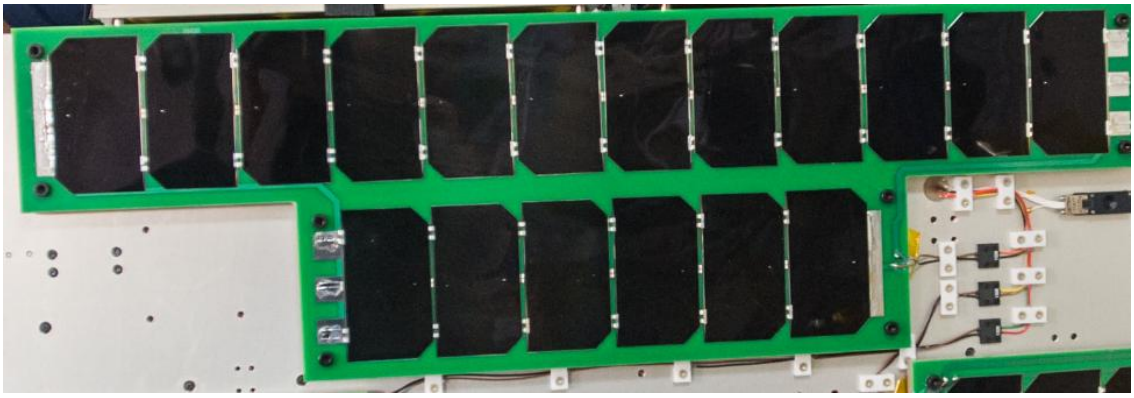

Figure 79: Assembled Solar Panel

The batteries were a bit more difficult to assemble than the solar panels. The first steps were to assemble the box and attach the feet and vent cover. The cell dividers were installed, and small patches of Durette® felt were placed in the bottom of each chamber for padding and insulation. A 4" 12 gauge wire was soldered to the negative tab of each cell, and the cell wrapped in Durette® felt. The cells were then inserted into the chambers such that the soldered lead from one reaches the positive lead of the next and soldered together in series. Kapton® tape was used to insulate all exposed leads. The figure below illustrates the process of cell insertion and connection.

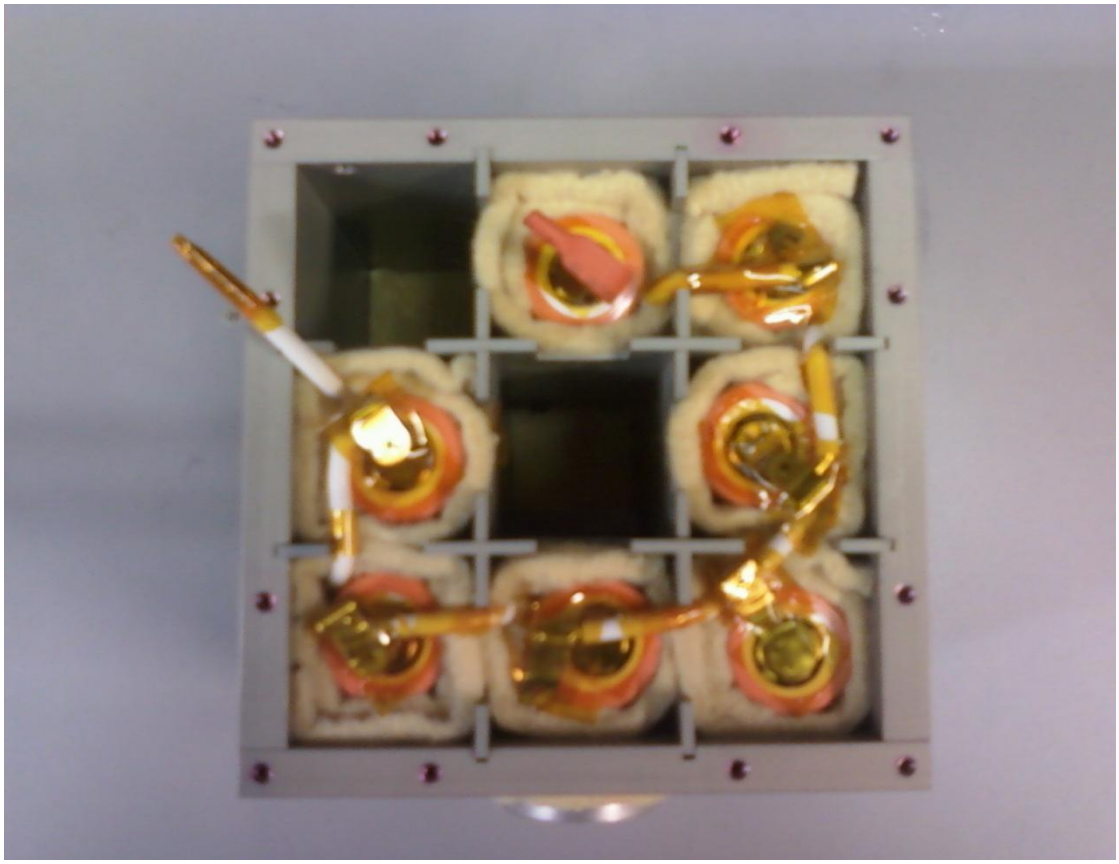

Figure 80: Battery Assembly

A 26 gauge wire from a micro DB-9 connector in the box lid was run to the positive terminal of each cell. This allowed the battery protection circuit to monitor each cell voltage and balance the pack cells. Durette® felt sheets would then cover the top of the cells for more insulation.

What made this design difficult was that originally the 12 gauge wires for the first and last cells in the series were to snake over across the tops of the cells in the pack and take a sharp turn out of the hole near the DB-9 connector. Unfortunately this caused too sharp of a bend for such a thick wire which damaged the wire. While attaching the

lid using the screw driver, these wires were bent beyond their limit and forced into the sharp edge of the box lid and dividers. Although anodized to prevent conductivity, the wires were shoved so hard into the aluminum that they chipped the coating and created a short circuit. This produced a cascade of sparks that shot out of the almost attached lid, dangerously and rapidly depleting the battery.

A thorough investigation discovered that the wires bending too sharply was the cause of the problem, and the design was modified so that the pack lead wires exit the box lid directly above the cell they are attached to. AGSL students drilled new holes in the lid and chamfered the edges to reduce their sharpness. This would eliminate the problems with wire chafing and being bent too far. A Teflon® wire sheathing material was added to further prevent the possibility of these wires rubbing against the edge of the battery box. This redesign proved fairly easy to assemble, and passed all tests.

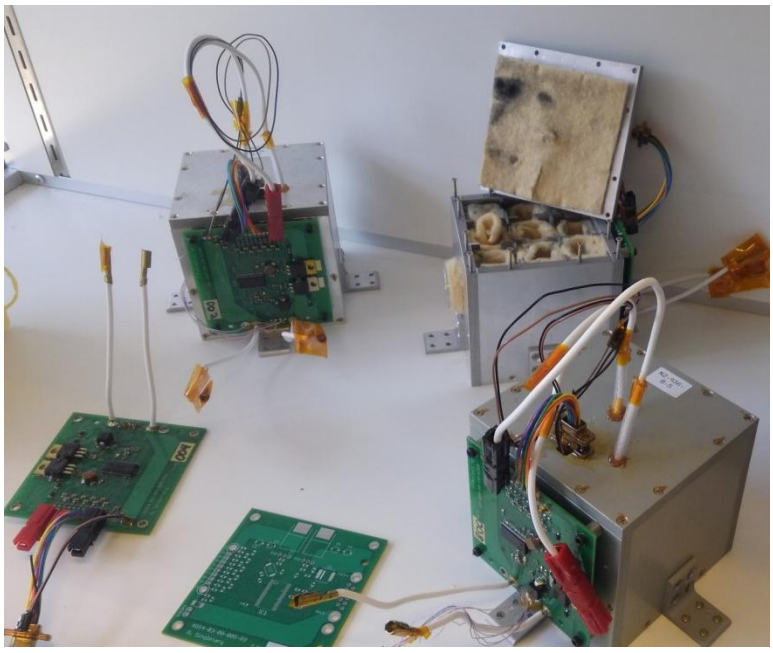

Figure 81: Prototype and Flight Battery Boxes

3.1.9. COMM

Since only the HDR was designed and fabricated by AGSL, this was the only COMM PCB requiring soldering. Coaxial cables to carry the signal from each of the radios to its antenna also had soldered connections.

The HDR amplifier did not require any components soldered, but it did utilize power terminals where the lead wires were directly soldered on. What was unique about the amplifier compared to the other components of AGS4 was that it was thermally bonded to its aluminum housing. Waste heat generated would be carried away from the electronics by conducting to this aluminum "tub" in which it was mounted. This presented a challenge in that the underside of the amplifier could not be brush conformal coated. Fortunately, the staking and coating procedure has an option for this use case. As the housing is a single piece of aluminum, conformal coat could just be poured onto the tub and the amplifier covered in a process called "potting". The assembly is then placed under vacuum to remove all air bubbles. In this manner the amplifier is completely coated, but maintains thermal conductivity to the housing.

As the two LDR radios were commercial units, they did not require any soldering. Their electronics boards however would require staking and coating. After removing the plastic housing, the two electric PCB's sit mounted in a convenient aluminum chassis. By removing the top board, but not disconnecting the ribbon wire connecting the two, staking and coating is a fairly easy procedure. Special attention was given to staking the ribbon wire to ensure it would not come loose. Once cured, the boards were replaced and the fasteners for the chassis were reinstalled using Locktite®.

The crosslink radio did not require any soldering. After opening up the aluminum housing, the electronics just slide out from rails built into the housing. The electronics were removed, and the unit staked and coated. Upon reassembly, Locktite® was used when reinstalling the fasteners.

3.1.10. ADCS

As much of the ADCS hardware is built for spaceflight, the reaction wheels and sun sensors required no additional steps taken. The VectorNav control board and sun sensor interface board were both hand soldered, staked, and conformal coated.

The torque coils were assembled by building a wooden jig with pegs marking the dimensions of the particular coil shape. The jig was mounted to a wire winding device that counts rotations of an object mounted to it. This made it simple to keep track of how many loops of wire had been wound so far to get the desired number. Reference Figure 67 for the build jig. Once the correct number of wire loops had been wound for the particular coil as per Table 30, the wires were bound together into shape by tying loops of lacing tape around them. Self tightening knots were selected to prevent the coils from coming undone, and the knots were staked to provide an extra layer of safety. The leads of the torque coil were then soldered to the wire harness using the Linemans Splice [19]

3.1.11. DRAGON

The DRAGON GPS was built for spaceflight, and did not require any additional steps.

3.1.12. VDCS

As the PSCAM was designed for spaceflight, the only steps necessary to prepare the unit were to focus the lens by taking sample images and adjusting the focus. Once the focus was found, the lens was staked in place.

The camera interface board was designed by AGSL, and so it was soldered, staked, and coated, paying special attention to stake the ribbon wire that connected the PSCAM to the interface board.

3.2. Integration

With all of the subsystem components prepared for spaceflight, the first step to ensure that they survived the assembly process and are ready for integration is a function test. Function tests were developed for each component to test the various aspects of the hardware and ensure that they can communicate with the computer. For instance the COMM system components would undergo a transmit and receive test, and the other systems had similar tests that proved their functionality. Only once a component had passed the function test could it be integrated into the spacecraft.

Integration procedures were developed for each subsystem, divided into two phases. Phase I consisted of components that had to be installed before folding the five lower panels of the structure together, and Phase II covered components on the +Z face that would be the last face to be folded into place. For Phase I an assembly jig was designed and fabricated to elevate the panels off of the assembly table, and hold the five lower panels in their relative positions. Holes were cut in the panels so that exterior components and some wire harnesses could be installed while attached to the jig.

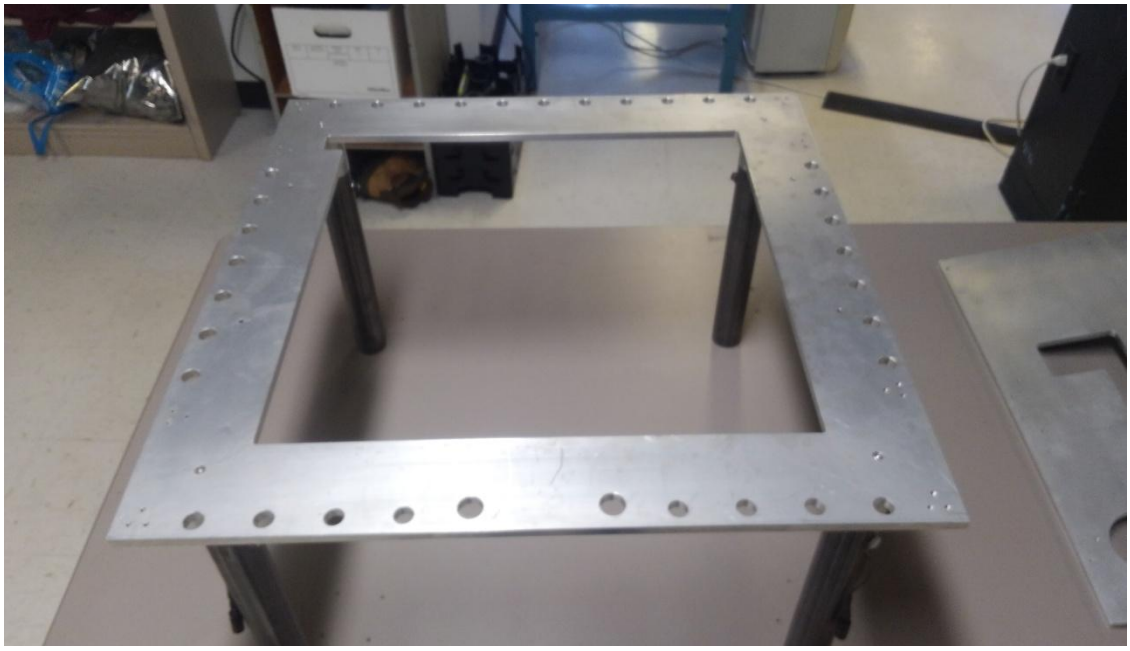

Figure 82: -Z Panel Assembly Jig

Panels were attached to the jig with fasteners to prevent them from slipping off. After attaching the panels to the jig, the Cyclops EAF and spacer block with switches were installed on the underside of the -Z panel as shown in the figure below, followed by the two I-beam supports in the middle (see Figure 84 below).

Figure 83: Cyclops EAF and Inhibit Switches

Within the Phase I & II framework, the first subsystem to be installed was CDH, followed by EPS. The other subsystems could follow in any order with few exceptions. The reason for this order was twofold, the first being that CDH and EPS would be used to function test the component after install, and the second being that it made running the wire harnesses much simpler. Since each component connected to CDH and EPS, their wires were run from one terminus to the other, and gently placed in one of several designated wire corridors. By placing the wires in the corridors one by one, it made it much easier for the technician to keep track of which wire goes where and by what route, rather than having a whole bundle of often identical looking harnesses that had to be sorted through. Labels were made and affixed to each end of each harness as they

were installed just in case they ever had to be disconnected. Harnesses were run through the wire brackets described previously, but were not clamped down until all wires were in place. In order to minimize the number of places that wires cross panels, all the wires running to components on a face were routed through a single corridor. This included the wires that would run to the +Z panel, which passed through the corridor to the +X panel, and then onto the +Z. Care had to be taken to ensure that the bend radius of the corridor when the panel is folded does not exceed that of the thickest wire in the bundle. The figure below shows CDH installed and the beginning of some of the wire harness corridors, as well as the side panels in position.

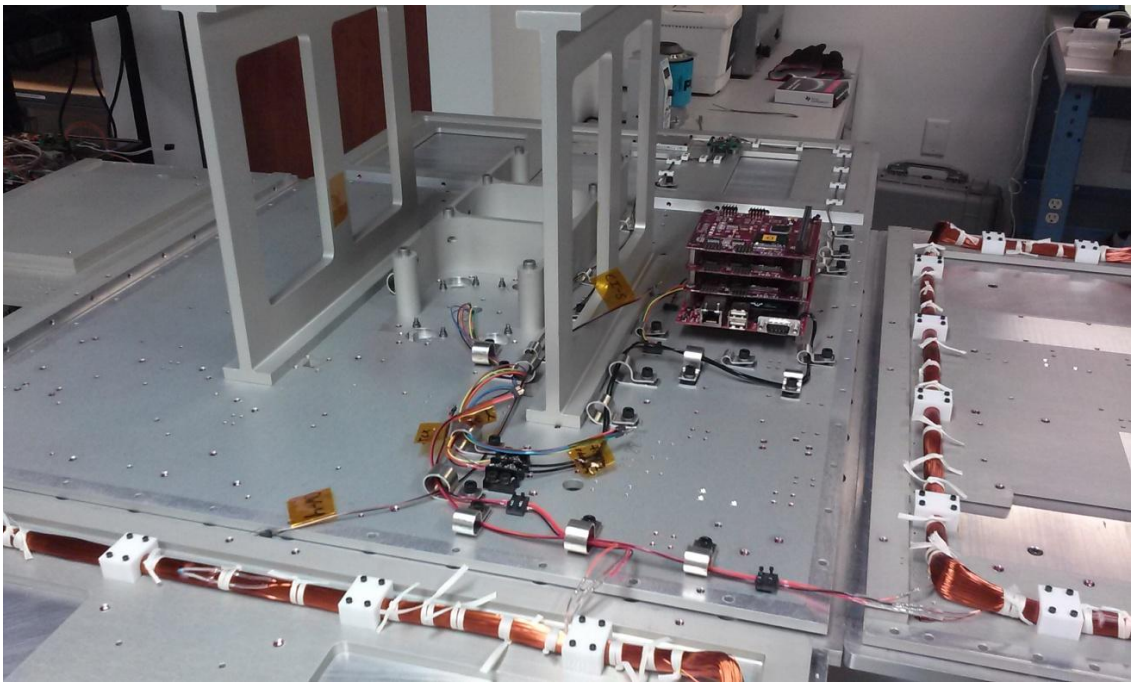

Figure 84: CDH Integration

The torque coils were the first components to be installed on their panels as harnesses for other components would need to run over them and not be pinned down.

They were installed using 3D printed polycarbonate brackets. The other components were integrated as they became available and passed their function/acceptance testing. One by one the components were integrated until all components on the lower five panels had been installed.

Figure 85: AGS4 Pre Fold Up

After all Phase I components were installed, the ISIPOD was installed, and the wire bracket fasteners torqued down. At this stage an integrated system test was performed to make sure that all components installed were functioning and communicating, as the next steps would significantly hamper the ability to remove, repair, and replace troubled components. With all components fully functional, the side panels were folded up, and attached together using #8-32 fasteners.

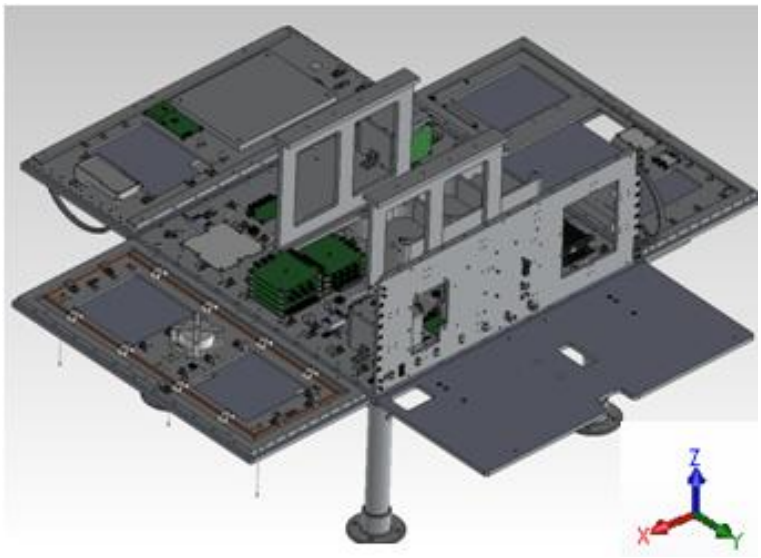

Figure 86: Illustration of +Y Panel Fold Up

Remaining exterior component wire harnesses were installed after each panel was locked in place. The other side panels were folded up in a similar manner, and attached with fasteners such that AGS4 resembled an open topped box. The grab handles attach via the fasteners holding the Y axis panels to the X axis panels, and were installed at this time as the panels were fastened together.

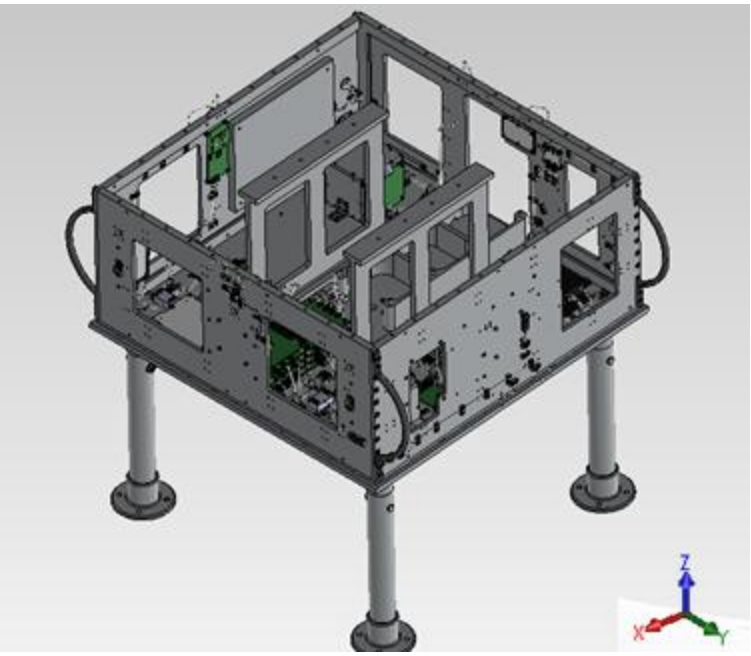

Figure 87: Folded Up Side Panels with Handles on Assembly Jig

With the side panels attached, the next step was to modify the assembly jig to accommodate the +Z panel. A jig would be needed as the panel would be too large and cumbersome to easily manipulate by hand, and since an expensive reaction wheel would be installed, the risk of dropping it was too great. First the side panel jig faces were removed to free up access space. Then the +Z jig panel was attached to the assembly table.

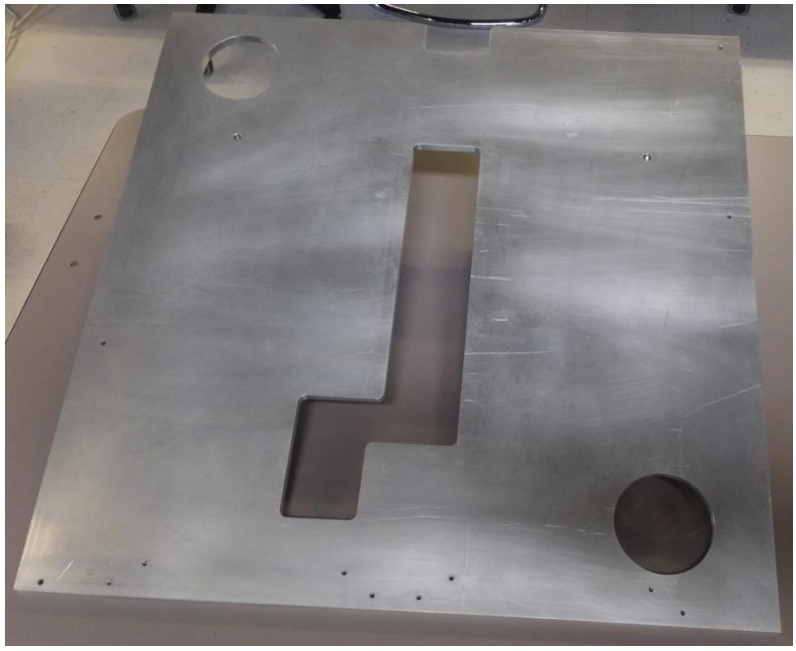

Figure 88: +Z Assembly Jig Panel

This jig panel attached to the +X side panel via a piano hinge, which would allow the +Z panel to be lowered into position slowly and in a controlled fashion.

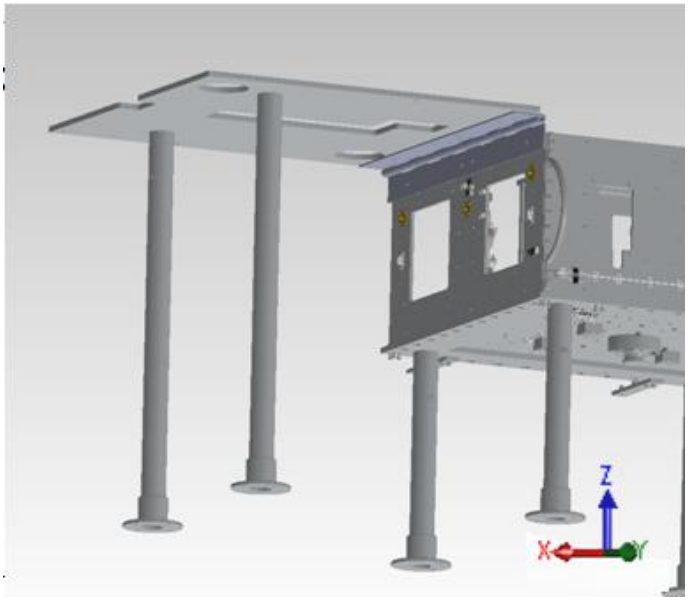

Figure 89: Illustration of +Z Jig Attachment

The +Z panel was attached to the jig plate, and the components for that face were installed. The wire harnesses had previously been run from CDH and EPS through the wire corridors up to the panel. This was the one case where running the wires before the components made sense as there were few enough components that labels were not cumbersome, and there was not sufficient room to maneuver hands inside the bus when the panels were folded up. The wire harnesses were routed to their respective components and attached, and the wire brackets torqued down to hold the wires.

With all components installed and connected, a final full system function test was performed to ensure that all components were not damaged during the integration process, and that the system as designed is fully functional and capable of meeting the mission requirements.

Prior to attaching the +Z panel, a final round of staking compound was applied to numerous locations throughout the bus. Upper management performed this procedure and used their discretion to determine what areas would benefit from it. Any place where wires went through a panel were staked to prevent movement and chafing against the edges. Places where wires had slack such as near panel crossings, and gaps around wire brackets were filled with staking compound to prevent movement. The knots of other locations where lacing tape had been used were also staked, and any other place where wires could potentially rub against a hard surface.

The last step to structural integration was the attachment of the +Z panel. To facilitate this, pins locking the jig structural members to the table were removed, and the entire jig plate hinged over following the piano hinge track. The hinge had been drilled

and cut so that the top panel lined up with the rest of the structure, paying careful attention to the wire crossing the panels.

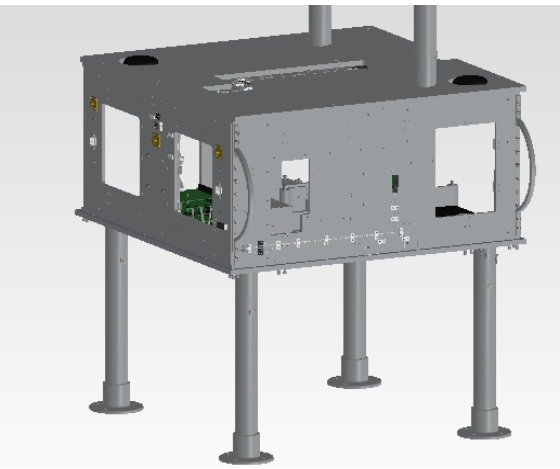

Figure 90: Illustration of +Z Panel Fold Up

The fasteners holding the panel to the jig were removed, and the jig folded away. The panel was then attached to the rest of the structure using 44 #8-32 fasteners, and the piano hinge and jig were detached. All of the structural components were now integrated, and another component function test performed to verify all are functional after the procedure.

The next step was to prepare the solar panels and their truss backing structures. A thin strip of Locktite® was applied to the surfaces of the truss structure that would contact the solar panel PCB in order to bond the two and prevent the PCB from oscillating independently during launch. Bolts and nuts were placed through the mounting holes to properly align the pieces. Once cured, the entire assembly was integrated onto the spacecraft bus in the proper positions, and attached with fasteners. Washers were used to distribute the force of the socket head cap screw over a larger area

of the PCB to reduce stress and help prevent fractures. In one bolt location the solar panel assembly process had shifted the cells approximately 1/32" toward the bolt hole and created an interference between the corner of the cell and the washer. Since the washer was deemed to be a fairly important stress reducer, a Dremmel® tool was used to cut a piece out of the washer such that there was clearance for the cell, and surface area to distribute the fasteners pressure. The wire harnesses were attached to their mating leads and fastened to the spacecraft bus. Staking compound was applied to keep the wire harnesses in place along the positions where they leave the solar panel. With the 10 upper and side face solar panels installed, the covers that had been made were attached using the embedded Velcro® strips.

Figure 91: Bus with Solar Panels and Covers Installed

Since the -Z panel had been unavailable for access as it was structurally supporting the bus, it needed to be flipped over so the bottom panels could be integrated. This would be done using the foam packing clamshell pieces as they provided sufficient protection and supporting area to hold the vehicle without damage. It would also serve as the first fit check for the foam with the solar panels and covers, though a preliminary fit check had been performed once before as shown below.

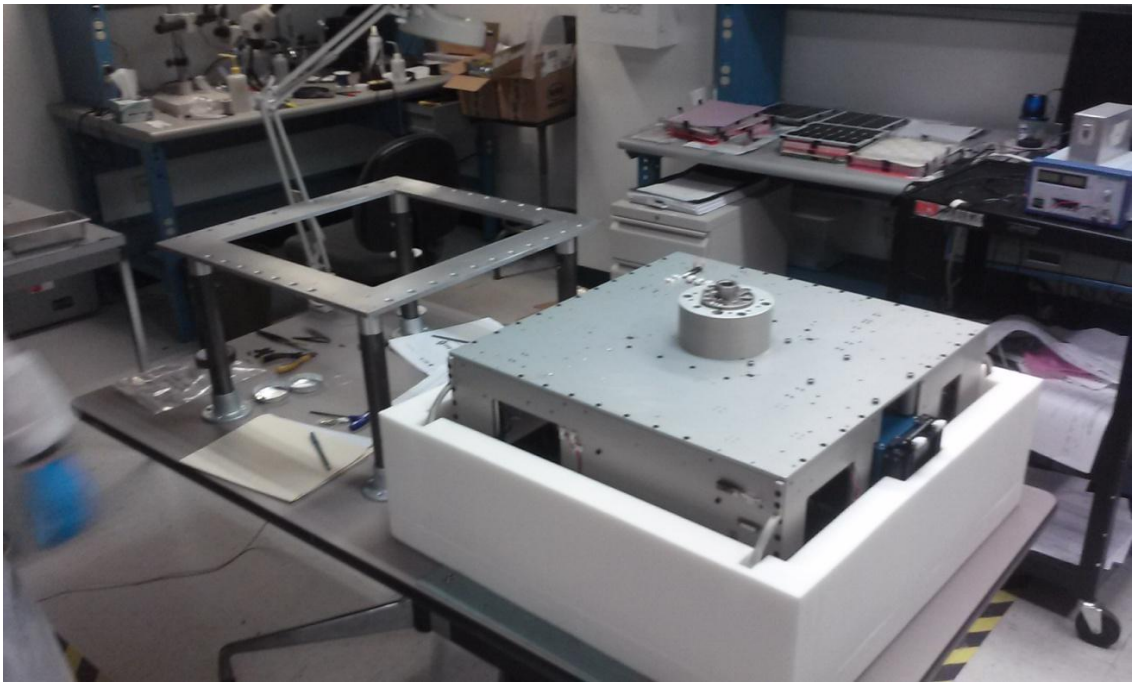

Figure 92: Foam Fit Check

Using four of the stronger AGSL members, a maneuver of lifting AGS4 by the attached handles, rotating it 180° upside down, and gently lowering it into the foam was executed. The biggest problem experienced during this maneuver was that the handles were a bit small to accommodate two peoples' hands during the transition, sometimes

making it difficult to transfer leadership of a particular handle. With AGS4 transferred to the foam packing, the bottom face solar panels were applied.

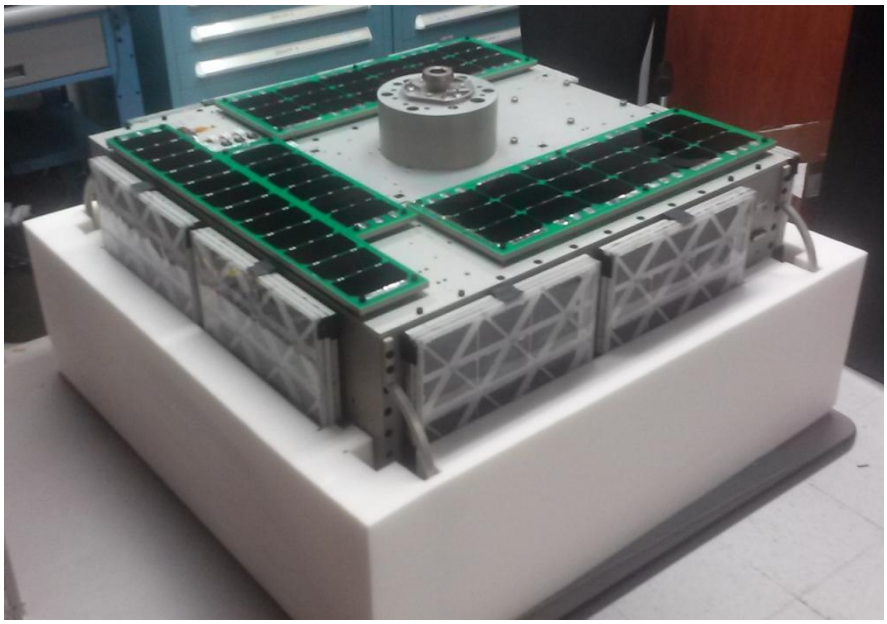

Figure 93: -Z Solar Panels Installed

From this point on, the assembly jig could no longer support AGS4, so it was dismantled to clear the assembly surface. Now, any time that AGS4 was to be removed from the packaging it would reside on the test stand, after being transitioned there by reversing the four person lift and rotate maneuver. The test stand was created by repurposing the prototype microsatellite bus from a previous project, as the triangular grid design gave the aluminum a good amount of strength, reinforced with pipe to prevent sagging. This structure was tested to hold a heavier object than AGS4, and so was deemed safe for use. The structure had an opening at the top that was large enough to allow the Cyclops EAF to pass through, but narrow enough that the Cyclops adapter spacer would rest on the surface supporting the vehicles weight.

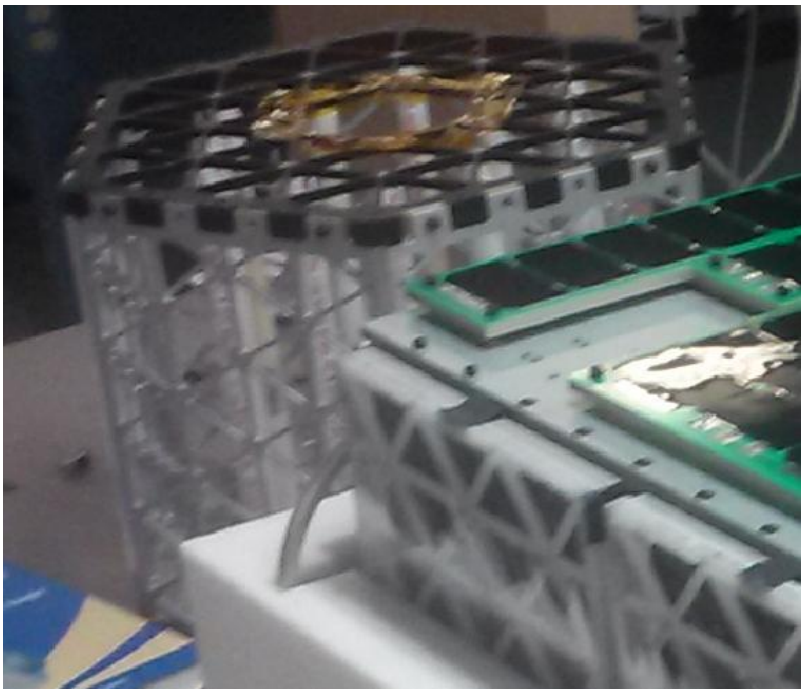

Figure 94: AGS4 Test Stand (behind AGS4)

When running wires through brackets as discussed above, if the number of wires is not sufficient to fill all of the space, the wire bundle was wrapped with Kapton® tape to fill the gap to reduce vibrations. In the case of the steel pipe brackets, the 90° metal edges could easily cut through the Kapton® tape and wire insulation, risking an electric short. To prevent this from happening, wires running through these brackets were wrapped in several layers of 3M® glass cloth tape, which is very abrasion resistant and would protect the wires from chafing. Since the polycarbonate 3D printed brackets had smooth edges made of plastic, this abrasion tape was not necessary. Future projects should consider using 3D printed brackets for reasons such as these, and if there is a printer in-house brackets can be tailored to each bundle without the need for filler wrap.

All load bearing fasteners used on AGS4 were required to be certified of a grade of sufficient strength and temperature durability to meet the loads expected. This certification and chain of custody process increases the price of fasteners orders of magnitude above fasteners from the hardware store. Counterfeit fasteners are a surprisingly big business, and several programs have had to reassemble spacecraft after purchasing them. National Aerospace Standard (NAS) fasteners were chosen from a reputable supplier for all load bearing fasteners because of their traceability and certification process. NAS fasteners follow the U.S. customary system of measurement and fastener specification, #X-YY, where the X represents the diameter of the fastener in 64th of an inch, and Y indicates the number of threads per inch. Hardware store grade non load bearing fasteners were used in some locations, including the metric system fasteners. This was not a problem though as representative samples of every type of fastener used would be destructively tested by NASA to ensure they meet their minimum strength requirement, were made of the appropriate material, and did not have an inappropriate surface treatment.

Each fastener installed into the bus or a component was torqued to a specific value calculated for that application. Under tightening can cause components to vibrate excessively, and over tightening can cause damage to components, strip the threads, or place the system under enough spring tension that causes such as thermal expansion can cause a violent fracture. Unfortunately, calculating the proper torque per fastener is not a straightforward task. Factors such as the mass of the objects being fastened, the temperature extremes the joint will experience, the size and number of fasteners, fastener

length, material types, and whether any lubricants are used are a few examples of the parameters that must be accounted for to calculate the fastener torque. Fortunately, NASA developed a standards manual [39] on how to calculate the appropriate fastener torque. The details of how to perform these calculations are captured in Appendix C. The correct torque was calculated for each fastener, and applied during the assembly process.

3.3. Integrated Testing

With AGS4 fully integrated, the process of testing the assembled spacecraft began. Integrated system tests were performed to emulate the spacecraft functions. For instance, EPS tested battery charge and discharge, torque coil output and magnetic field strength, the hazard control module's ability to prevent Bevo-2's command release before timer expiration, and output boards by providing power to all components for their own system tests. CDH was tested in a similar manner by facilitating the tests of the other subsystems. COMM simulated a crosslink test and data downlink pass. VDCS and DRAGON systems were used to capture images and GPS data to verify their functioning and controllability by CDH, and were downlinked over radio. ADCS systems verified that CDH could command the RPM of the reaction wheels, activate the torque coils, and get accurate readings from the Sun sensors and IMU, however, a full feedback control test was not possible in the lab environment. With AGS4 fully built and functional, the process of integrating Bevo-2 could begin.

A full crosslink test had been successfully performed by the AGSL and UT teams previously using prototype hardware. Now, the UT team brought Bevo-2 to AGSL

where the test would be repeated using the flight articles. The test was successful, as the process had worked out all the issues during the prototype tests, and both vehicles were now ready for final preparations. Prior to installing Bevo-2 into the ISIPOD, its thruster fuel tank needed to be filled with chlorofluorocarbon refrigerant. This operation was performed by the UT lab.

With Bevo-2 fueled and ready, both spacecraft could now be integrated. A wrench was used to actuate the manual release of the ISIPOD door, and gravity as well as spring force held it open. Bevo-2 was loaded onto a custom designed Teflon® tray that lined up exactly with the ISIPOD. While one UT student held the tray in place, another pushed the CubeSat into the ISIPOD opening, compressing the deployment spring. The spring was strong enough that it could eject Bevo-2 in microgravity, but on Earth there was significant resistance making it easier to hold in place. With Bevo-2 sitting flush with the ISIPOD opening, the door was closed and forced shut. The latching mechanism locked the door into place, and Bevo-2 was integrated. ISIPOD contained zero separation force connectors on the inside that connected Bevo-2 to a DB-9 and DB-15 port on the outside of the deployer structure.

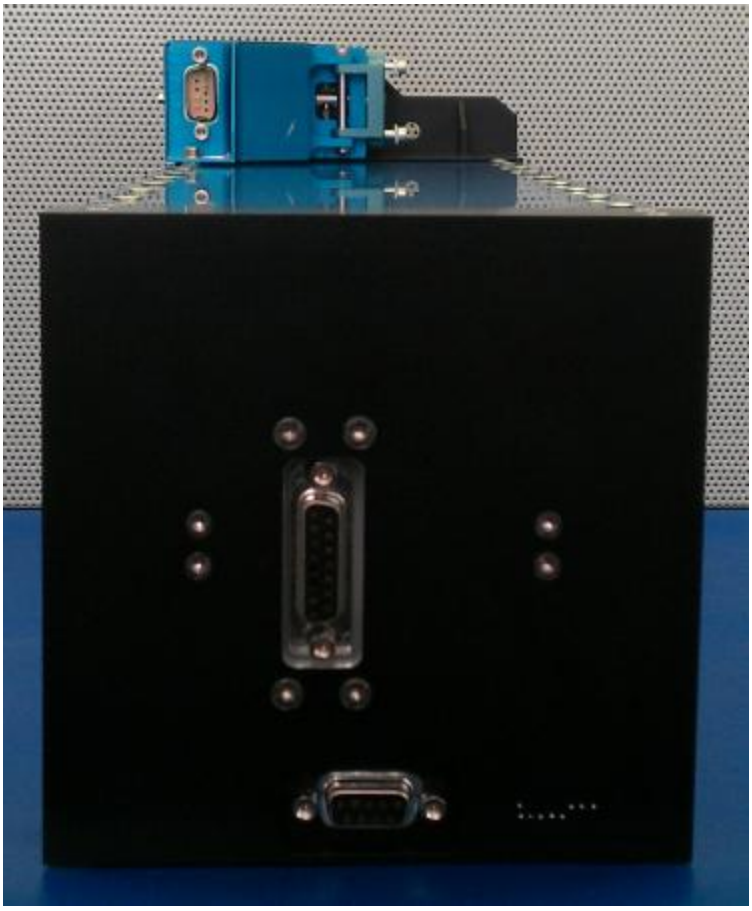

Figure 95: ISIPOD Payload Access Connectors

AGSL had installed a wire harness that brought these pins out to a second computer access port on the side of the AGS4 bus. This test port was used to connect with Bevo-2 and verify that the computer system could be communicated with after install, and that the batteries could be charged externally or by AGS4. All other systems of Bevo-2 were three fault tolerant inhibited for safety just like AGS4. The test ports on the spacecraft are shown in the figure below. The ISIPOD door was the held shut using a locking cable tie to mechanically ensure Bevo-2 could not be released, and the tie would be cut off on

-orbit prior to release. With the two spacecraft integrated, the unit could now undergo final NASA acceptance testing.

Figure 96: Computer Access Ports for AGS4 (Circular) and Bevo-2 (DB-9/DB-15)

With the LONESTAR spacecraft fully assembled and integrated, human factors specialists came to AGSL to verify that the post-launch preparations could be performed by the astronauts on orbit without injury or damage to the vehicle or station. In case of a failure of the ISS deployment equipment, AGS4 would have to be retrieved by spacewalk, so making sure that nothing would damage a space suit was critical. This process was also used to verify and refine the astronaut handling procedure and preparation. Keep out zones such as the solar panel surfaces and ISIPOD release mechanism were identified. First, the specialists followed the preparation procedure to install the antennas, and remove the solar panel covers. They then wiped down the corners, edges, and all other surfaces with a soft cloth looking for any places that it

might snag, potentially cutting an astronaut or space suit. They also verified that the covers were sufficiently transparent to identify any cell breaks.

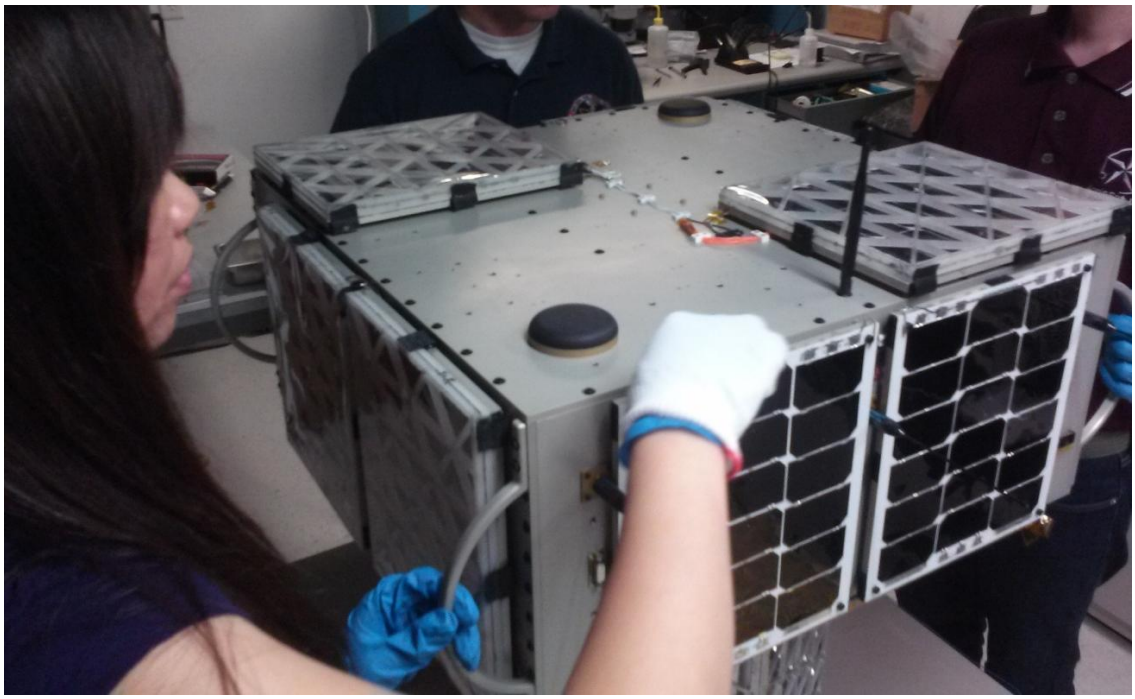

Figure 97: Human Factors Testing

The handles were checked to verify that a space suit gloved hand could adequately use the maneuvering handles, with or without the solar panel covers in case any had to be left on for deployment. They also tested the ability to reattach the covers in case there was the need to abort deployment and re-stow AGS4 in the foam packaging and M01 cargo bag. After passing all of these tests, the unit could proceed to vibration testing to implement the simulations performed in section 2.4.1.5.

In order to verify workmanship and structural integrity, the integrated AGS4 and Bevo-2 would be vibrated along each axis to the loads and duration outlined in section 2.4.1.5. The spacecraft, packaged in the foam clamshell and wrapped in the M01 cargo

bag, was strapped down to the shaker table using cargo straps. Since the table only moves in one axis, the test was repeated three times, rotating which face was in contact with the table. The figure below shows one of the tests being performed.

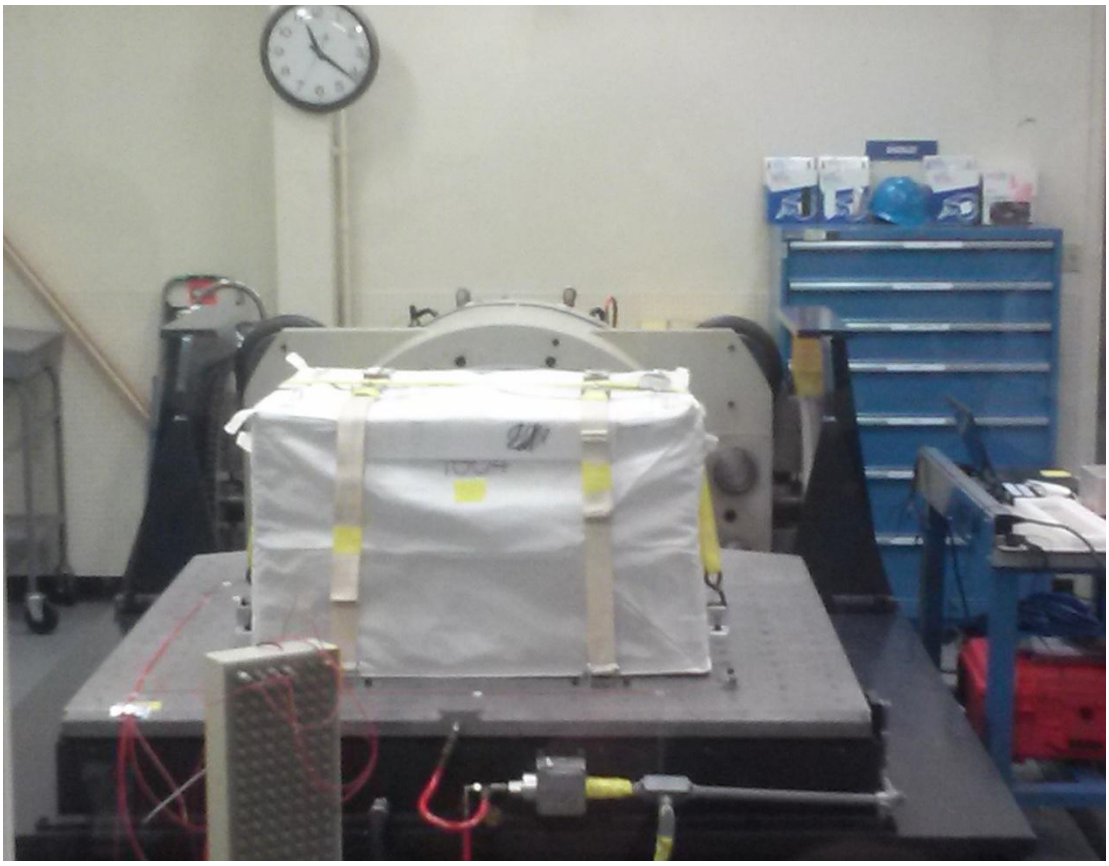

Figure 98: Dynamic Random Vibration Testing

Basic function tests of each component were performed on AGS4 after every axis run, and the UT team checked Bevo-2's functionality as best as able with the limited functionality available while in ISIPOD. For the Z-axis and X-axis runs both spacecraft performed flawlessly. Unfortunately, after the last run on the Y-axis the HDR radio was unresponsive, indicating a problem. As there were no loose pieces inside the bus, it was believed to be either a wire issue or an electronics issue with its control board.

Having been given a passing grade from a safety standpoint, AGSL brought the vehicle back to AGSL to investigate. Removing the +Z panel was not possible as doing so would break the "as tested" configuration and void the testing results. Non structural members such as the solar panels could be removed to investigate. When investigating, no wire damage could be found to repair, and the HDR failure deemed to be a problem with the control board. As there was insufficient room to maneuver tools and hands inside to remove and replace it, the decision was made to proceed with only the LDR radios as the mission could still be completed with a longer downlink period.

AGSL continued to refine and test the flight software up until it was time to bring AGS4 to NASA Johnson Space Center (JSC) in Houston for delivery. The software was installed using the computer access port. AGS4 was taken to JSC in foam and an M01 bag, where it was transferred into fresh foam and a different cargo bag. This was done as a precaution since these items had been outside of NASA care, and they needed to ensure that their properties were as modeled. NASA took possession of the package for transport out to Kennedy Space Center, where it was integrated into the cargo launch vehicle.

4. LAUNCH, DEPLOYMENT, AND OPERATIONS

4.1. Launch

AGS4 was launched to the International Space Station (ISS) aboard the Orbital ATK commercial resupply vehicle OA-4 (Cygnus) inside the foam packed soft-stow M01 bag as cargo. The rocket was the ULA Atlas 5, which experienced 3 scrubbed launch attempts before finally being able to liftoff on the morning of December 6, 2015. OA-4 rendezvoused with ISS three days later on December 9, where AGS4 was unloaded with the other cargo.

4.2. Deployment

AGS4 was removed from the M01 bag and packing foam to be installed onto the Cyclops payload deployment system on January 27, 2016. Astronauts Scott Kelley and Tim Peake donned gloves and static electricity grounding straps to begin the AGSL unboxing and installation procedure.

First, the upper half of the packing foam was removed and the lower solar panels inspected for cracks and breaks during launch. If breaks had been found, the Mylar® covers would have been left in place to avoid introducing tiny glass shards into the weightless cabin environment. After verifying that there were no cell breaks, the Mylar® coverings were peeled away, and AGS4 was removed from the lower half of the foam packaging. During this process, one of the astronauts received a static discharge when touching the metal structure of AGS4, due to the charge buildup from rocket vibrations and the foam packing. It was determined that since the flow of charge was

from AGS4 to the astronaut rather than the other way around, that it was unlikely that this spark caused any damage.

Figure 99: Astronauts Removing Lower Solar Panel Covers (Photo by NASA)

Figure 100: AGS4 Removed from Packaging (Photo by NASA)

With the bottom cells uncovered, the astronauts carefully placed the Cyclops knob into the Cyclops table and locked it into place. When firmly seated, the four inhibit switches in AGS4's Cyclops attachment knob are engaged and prevent activation.

Figure 101: AGS4 Install onto Cyclops Table (Photo by NASA)

With AGS4 secured to the table, the astronauts carefully inspected the other 10 solar panels for cell breaks. Again, if any had been found broken that cover would remain in place for deployment to prevent cabin contamination. Finding no breaks, the covers had their Velcro® attachments undone and the covers removed. With the covers removed, the four communications antennas were threaded onto their attachment points by hand.

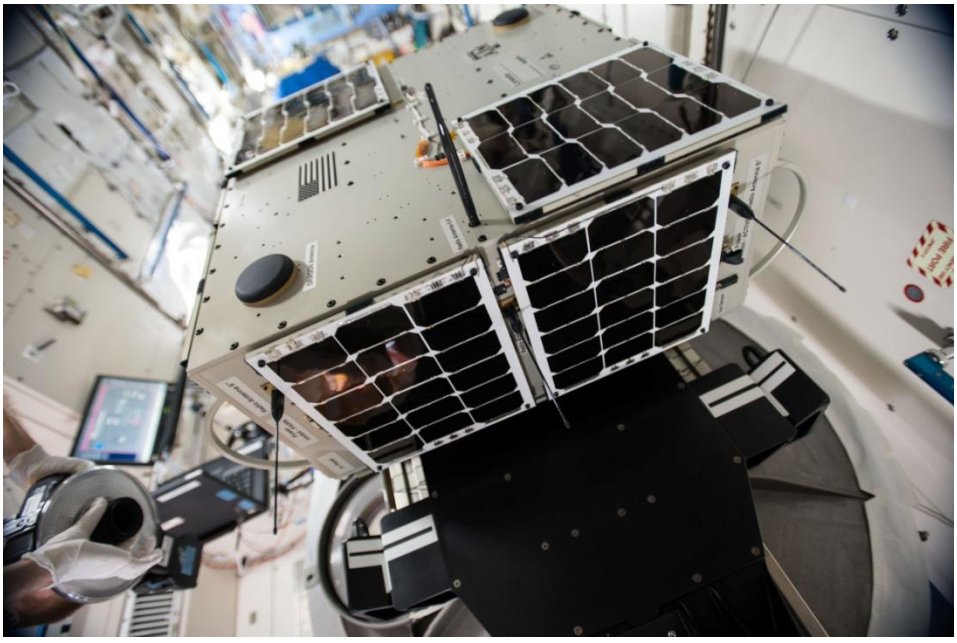

Figure 102: AGS4 Solar Panel Covers Removed and Antennas Installed (Photo by NASA)

With the antennas in place, the last step to prepare AGS4 for deployment was to move the inhibit key from "SAFE" to "ACTIVE". An Allen wrench screwdriver was used to attach the two captive #2-56 screws in the inhibit to prevent it from coming loose on-orbit and de-activating the spacecraft. With the inhibit key now in place, the only thing preventing AGS4 from activating were the four inhibit switches in the knob, which would close on separation. A custom timer board would then activate and begin a clock that counts up, and closes another electric inhibit switch upon expiration allowing the remainder of the spacecraft to power up. This timer is to prevent AGS4 from activating in proximity to the ISS. The timer counts up instead of down so that in the event of a power fluctuation and the clock resetting to zero, the count restarts rather than suddenly thinking that time has elapsed.

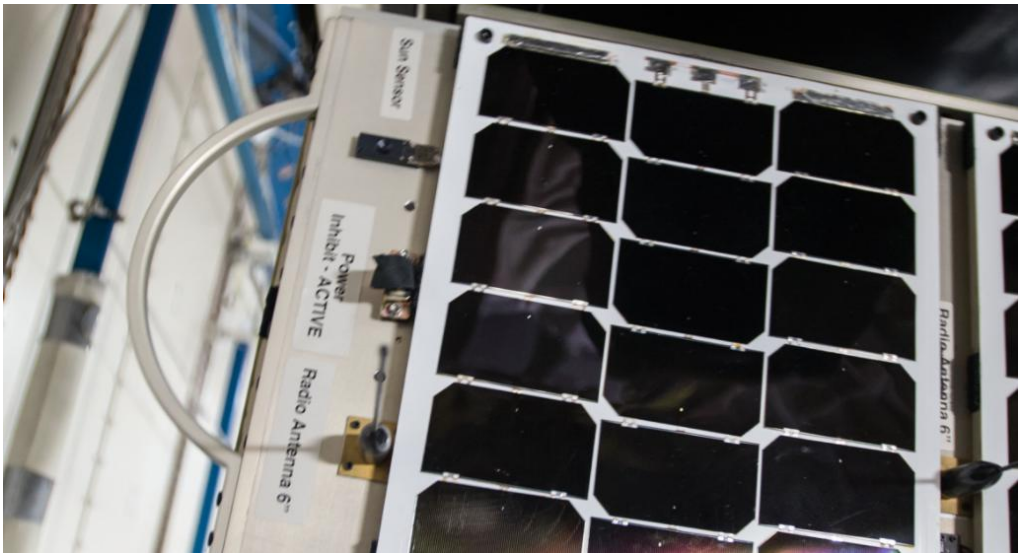

Figure 103: Inhibit "Active" (Photo by NASA)

With the inhibit key installed, the Cyclops tray with AGS4 was slid into the Japanese Space Agency JEM Airlock, where it would remain for the next two days. The delay was to accommodate the ISS crew schedule.

Figure 104: AGS4 Insertion into JEM Airlock (Photo by NASA)

Figure 105: JEM Airlock (Photo by NASA)

When two days had elapsed (January 29, 2016), the JEM was depressurized, and AGS4 moved outside into an area called the "porch". Over the next several hours, the Special Purpose Dexterous Manipulator "Dextre" maneuvered into position, attached to the Cyclops table, and moved AGS4 into deploying position.

Figure 106: AGS4 and Cyclops Table Moved onto Porch (Photo by NASA)

Figure 107: Dextre Moving AGS4 to Deploy (Photo by NASA)

Figure 108: AGS4 Pre-Deploy (Photo by NASA)

NASA determined that the proper release angle for payloads is 45° down (radial) and 45° to the side (cross-track) off of the ISS velocity vector to ensure that released objects will not come back and possibly conjunct ISS on the next orbit. Once Dextre had AGS4 in this orientation, the Cyclops table was activated, and the pre-loaded spring force shoved AGS4 away from Cyclops.

Figure 109: AGS4 Release (Photo by NASA)

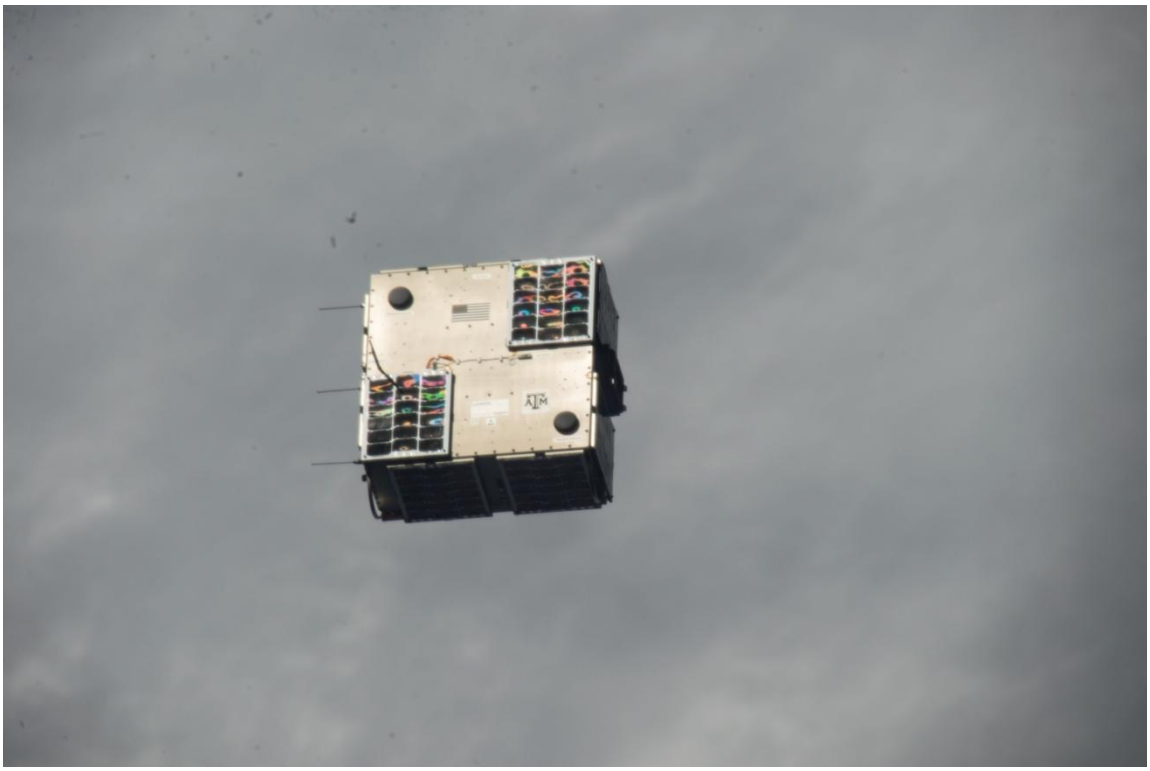

Figure 110: AGS4 Free Flying (Photo by NASA)

4.3. Operations

After release from Station, NORAD began tracking AGS4 within a few days, and Dutch Amateur Radio operators were the first to track and detect the beacons. Unfortunately, the AGSL team was having trouble compensating for Doppler shift at low elevations, and was unable to establish communications in a timely manner. It was calculated that tuning the receiver down by 15 kHz while the spacecraft was approaching (blueshift), and up by an equal amount when departing (redshift) during a ground pass, or also widening the receiver channel, that the Doppler effect could be overcome. This proved easier in theory than in practice with the manually controlled ground station radio being used.

NORAD had begun tracking two distinct space objects, with the only likely answer being that Bevo-2 had been prematurely and inadvertently released. A fault tree analysis was begun to determine the cause of this unintended release, focusing on the release control electronics, and the structural integrity of the ISIPOD. The analysis came up with six options that could have caused the release.

Option 1: Release command prematurely sent. This was deemed unlikely because the timers on the hazard control module create an open circuit condition for power to be applied to the release mechanism, and the required 31 days had not elapsed.

Option 2: Timer values changed due to bit flips. The time value that had to elapse before the hazard module would close the circuit, 2,678,400 s, was stored in four separate memory locations to prevent the value from being changed. Testing with the hardware showed that even with one memory value changed, the highest time value must still be reached before the transistors can close, and so this scenario was deemed unlikely.

Option 3: All four timer memory locations were changed to lower values by high energy particles. In order for this to occur, the spacecraft would have to be exposed to a significant amount of radiation, and it is estimated that this amount would have also damaged the transistors, causing them to become stuck in the off position. This situation was deemed unlikely because this would have caused the system to fail safe, and Bevo-2 would never have been able to be released.

Option 4: Sneak short circuit to ground. This was deemed unlikely as ISIPOD was inhibited on the ground leg by the hazard control module, and by EPS on the

positive side. Even if there was a sneak ground path, power would have still had to have been applied by EPS . As this system was designed to be three fault tolerant, this was deemed unlikely.

Option 5: Thermal expansion and contraction caused the ISIPOD door mechanism to fail. This was deemed unlikely as the ISIPOD design was thermal vacuum tested for six cycles at -40-+90 °C, and flight articles are tested to two cycles. This acceptance testing showed that the design will not fail due to expansion and contraction.

Option 6: Repeated thermal cycles caused stress on the ISIPOD latching mechanism, causing it to fail. This scenario was deemed the most likely cause of failure as the roughly 34-38 thermal cycles experienced before the release were well in excess of what it was tested for. ISIPOD type dispensers are usually mounted to the outside of the launch vehicle, and only experience a handful of thermal cycles before activation. Additionally, the UT team cycled the mechanism several dozen times for analysis, testing, and video demonstrations, which far exceeds what AGSL policy dictates could be done with flight hardware. These factors combined make release mechanism due to thermal stress the most likely cause of the unintended release.

Unfortunately, the trouble for AGS4 did not stop there. After six days of receiving and tracking the beacons, AGS4 went silent. Re-boot commands, and attempts to switch radios were unsuccessful. Data from some of the beacons indicated that there may have been some data corruption issues due to radiation effects. The FlatSat was used to duplicate the problem, and it was found out that AGS4 had a critical software

flaw. After about 52 hours the memory would fill up, forcing a re-boot. EPS would also power cycle CDH if it did not receive signals after an hour. This memory filling problem, combined with the potential radiation corruption of memory, put CDH into an unrecoverable state. This problem could have been caught in ground testing, but tests had never been run for more than 24 hours. Future missions should run the whole mission end-to-end on the ground before launch, not piecemeal and stitching segments together.

After it was deemed unrecoverable, AGS4 operations ceased, and the process of identifying all of these potential faults and failures began to help the lab learn from past mistakes and apply them to future programs.

5. CONCLUSIONS

Even though AGS4 was unable to complete the Relative Navigation experiment, and subsequently experienced total loss, the students of AGSL learned more from the design and assembly processes than in much of their college classes. Working under NASA supervision to produce a product that had to stand up to all the real-world requirements and constraints gave AGSL students a leg up when competing for employment, and helped to produce more qualified engineers with design and hardware experience beyond the theoretical to improve the capability of the U.S. aerospace industry.

5.1. Requirements Design Evaluation

The students designed AGS4 to meet the mission requirements derived from the mission objectives set forth by NASA. While unable to implement most of them on-orbit, they are the design criteria that shaped the design of AGS4, and the following summarizes how the spacecraft design criteria would satisfy these mission requirements.

MR-1 was satisfied by the modeled dimensions of AGS4, including antennas and solar panel covers, fit within the NASA provided CAD envelope of the JAXA JEM airlock, and was verified by the deployment through that airlock.

MR-2 was satisfied by the design mass of both spacecraft being under their allowances, resulting in a combined configuration of <100 kg. This value was verified by NASA at acceptance.

MR-3 was satisfied by AGS4 coming in under the allowance of 50 kg including solar panel covers, excluding Bevo-2. This was verified by weighing AGS4 prior to Bevo-2 integration.

MR-4 was satisfied by the Bevo-2 spacecraft weighing significantly less than the allowed 35 kg, verified by weighing the spacecraft prior to integration with AGS4.

MR-5 was satisfied by both labs developing a program schedule, and adhering to it with alterations, delays, and changes as dictated or approved by NASA management.

MR-6 was satisfied by student management from both labs having a weekly teleconference with NASA management to provide updates and make requests of their partner or management.

MR-7 was satisfied by the AGS4 design utilizing reaction wheels and magnetic torque coils to stabilize and actively orient the spacecraft.

MR-8 was satisfied by both labs developing and establishing a format and protocol for crosslinking between the two spacecraft, verified by the crosslink test and demonstration.

MR-9 was satisfied by the inclusion of a high speed radio modem developed by AGSL, which would be necessary to downlink the large volumes of data generated by ARD maneuvers in future missions.

MR-10 was satisfied by AGS4 utilizing the RelNav solutions exchanged between both spacecraft to actively track Bevo-2 as it separates from AGS4, testing algorithms and capabilities to orient a spacecraft for rendezvous and docking in subsequent missions.

MR-11 was satisfied by the inclusion of multiple radios in the communications system, two capable of bi-directional communications, and one high speed downlink only radio. This system was verified by testing prior to launch.

MR-12 was satisfied by the inclusion of a dedicated crosslink radio on both spacecraft for communications with the partner, verified by the crosslink demonstration tests.

MR-13 was satisfied by developing a protocol and format for exchanging GPS position states with the partner spacecraft using the crosslink radio, verified by the crosslink demonstration tests.

MR-14 was satisfied by AGS4 carrying the PSCAM and developing the sequence to image Bevo-2 as it was deployed. Space in the data budget was dedicated to downlink this data.

MR-15 was satisfied by the inclusion of the DRAGON GPS receiver in the design, and its use as the means of position determination for RelNav calculations, and in the active tracking of Bevo-2 to test GPS usefulness for ARD.

MR-16 was satisfied by the mission concept of operations dedicating a portion of the mission to capture and downlink two orbits of DRAGON GPS data.

MR-17 was satisfied by the inclusion of the ISIPOD mechanism built into AGS4, and verified by the testing of AGS4's ability to actuate the release mechanism.

MR-18 was satisfied by the inclusion of the PSCAM in the design of AGS4, and the mission concept of operations including the capturing of the Bevo-2 release, as well as tracking and imaging the Earth and Moon.

MR-19 was satisfied by development of the RelNav protocol and exchanging of GPS solutions via crosslink radio, and verified by the crosslink demonstration tests.

MR-20 was satisfied by the development of the data plan including the stored spacecraft health data to be downlinked and beaconed from AGS4.

As demonstrated above and in this document, AGS4 and the mission it would fly were designed to satisfy these 20 mission requirements.

5.2. Mission Summary

To meet the mission requirements, AGS4 would perform a series of actions. After release from the ISS, AGS4 would collect orbits of raw and carrier phase GPS data, and downlink as able. After charging Bevo-2, it would be released, and the two spacecraft would exchange navigation solutions with the other. The release would be captured on video. Additionally, AGS4 would track Bevo-2 using the exchanged navigation solutions to demonstrate attitude control for future ARD missions. The remainder of the spacecraft life would be spent downlinking the data and images from the experiment.

5.3. Spacecraft Design Summary

To meet the mission requirements, the final design was based around a 24x24x11" box shaped bus containing a CubeSat deployment mechanism. The complete power system was made in-house, to include battery packs, solar panels, regulation, and distribution systems. Command and data handling was performed by a single board computer with supplemental serial expansion boards. Communication with the ground was facilitated by two bi-directional commercial handheld radios and a custom made

high speed downlink radio, while communications with Bevo-2 were handled with a commercial point-to-point radio. Spacecraft attitude control and stabilization was facilitated through three single axis reaction wheels and magnetic torque coils. Attitude determination was handled through a system of six sun vector sensors, and a three axis linear and rotational accelerometer/magnetometer IMU. Position navigation solutions were generated from the NASA provided DRAGON GPS receiver. Finally, visual imagery for the mission would be captured through the PSCAM provided by the Aerospace Corporation.

5.4. Assembly Summary

AGS4 was assembled on a panel by panel basis after the components for that panel had been assembled and prepared for spaceflight. After the -Z panel, and X and Y panels had their components installed, the panels were folded together and fastened such that it made an open top box. The +Z panel was then assembled, and folded into position and attached once complete. Then, the solar panels and their covers were installed on the outside of the spacecraft. Testing was then performed to ensure that the spacecraft was functional and spaceworthy, including the random dynamic vibration testing. AGS4 was then transferred to foam packaging and delivered to NASA for launch vehicle integration.

5.5. Lessons Learned and Recommendations

This section is a list of lessons learned that others developing their own space mission or designing their own satellite might find useful. The topics are presented in no particular order.

1. As much as possible, have external interfaces identified and fully defined before designing hardware. The Cyclops table and EAF were developed in parallel with AGS4, which caused delays and necessitated design changes and modifications.
2. If using commercial grade computer components, at the very least use radiation hardened or tolerant data storage.
3. During integration and testing, unshielded power wires were producing electromagnetic interference on data wires, preventing communications. This was remedied by twisting the power wire conductors into a helix so the ground wire provided some shielding. If possible, use shielded wires for power and data, or run them in separate corridors. If unable to do either, at least twist the wires of each harness together to provide some shielding.
4. Always be cognizant of the bend radius of a wire bundle, as exceeding this can cause wire damage.
5. 3D printed wire brackets are an inexpensive and easy way to secure wires and cables. If the design lab can obtain their own printer capable of printing a suitable material like polycarbonate, then brackets can be sized to the particular location, eliminating the need to wrap the wires with tape and such.
6. Perform full end-to-end mission script testing, rather than testing each segment separately, and saying that the flight software will implement

each segment. Doing this would have exposed the memory allocation flaw in AGS4, which could have been addressed.

7. Take high quality pictures of every component at every stage in development, not just final pictures, label them, and categorize them appropriately. This can help to track down when problems occurred.
8. Adhering solar cells with double sided Kapton® tape is a significant time saver compared to traditional epoxies, and is far less likely to break cells. Several of the 24 cells for AGS2 were broken during fabrication and had to be replaced, while only one of the 234 cells on AGS4 broke during fabrication.
9. Create an easy to track system for the number of times a soldered connection has been re-worked. AGS2 and AGS4 simply wrote it in the certification log, which did not make it easy to keep track of.
10. Using a disposable polypropylene cup instead of a glass or polypropylene beaker eliminates the need to clean and wash the beaker after mixing epoxies, as it can simply be thrown away when done.
11. The experimental radio license is probably the simplest to apply for and be granted, and is a good avenue to investigate for communications licensing.
12. Make software and people capable of writing it an early and integral part of the design process. The AGS4 team was almost entirely aerospace engineering students, and as such there was a distinct lack of software

knowledge, especially around embedded hardware systems. Having more software focused team members with hardware experience could likely have prevented the satellite from becoming unresponsive.

13. If re-using the HDR radio design, redesign the control board such that the CC1101 is either integrally mounted to the control board, or mechanically fastened. On AGS4 it was attached using the friction of the pin connectors and epoxied, which is believed to have been the most likely reason that the HDR did not survive vibration testing as all other electronics had no problems.

5.6. Personal Contributions

The author worked at AGSL from Fall 2008 through Summer 2015, and had the opportunity to work on both AGS2 and AGS4. For the AGS4 program, he filled the roles of communications subsystem Team Lead, Chief Engineer, and Graduate Lab Manager. This thesis outlines the decision making process and system design for all aspects of the spacecraft, where the more detailed sections represent areas where the author had significant input. These areas, along with other significant roles, responsibilities, and contributions are outlined in the list below:

1. Oversee subsystem and vehicle design, integration, and testing.
    a. Oversee and verify thermal and structural analysis.
    b. Verify EPS system designs.
    c. Lead redesign and retrofit efforts for battery boxes after the short circuit accident.

d. Design the solar panel covers.
e. Develop the method used to attach solar cells to the PCB panel using Kapton tape.
f. Design the concept of using 3D printed wire brackets.
g. Develop communications architecture and apply for FCC licensing.
h. Modify the HDR design to interface with AGS4.
i. Review and verify schematics and mechanical drawings.
j. Develop the fastener torque calculation procedure and calculator.
k. Perform and oversee integration of components into the vehicle assembly, and the performance of integrated testing procedures..

2. Oversee Lab quality assurance and requirements verification
    a. Train students in soldering techniques, polymerics, and other lab procedures.
    b. Oversee Lab safety practices.
3. Interface with NASA management to execute tasks and recommendations.
    a. Responsible to ensure AGS4 compliance with NASA safety requirements.
    b. Interface with UT team on crosslink and other interfaces.

5.7. Final Evaluation

Participating in the design and fabrication of AGS4 provided students the unique opportunity to work on an actual spacecraft in a real world engineering environment with NASA. Students learned how to distill mission requirements into a spacecraft design and concept of operations to satisfy those requirements. They also learned how to perform trade studies to narrow design choices to those that best satisfy the requirements, and how to perform engineering analysis on real-life systems which is the next leap forward from the theoretical analyses taught in engineering classes. Students learned how to fabricate components and systems according to designs and specifications, learning how to perform the roles of the technician. And very importantly, students were exposed to the regulatory environment involved when working with NASA or other Government entities, how to adhere to necessary design standards, and that such standards exist for almost every aspect of spacecraft design. Students from AGSL are more prepared to go into the workforce and hit the ground running than their counterparts, as they have real world engineering and space mission experience under their belt. Such prepared workers are vital to the United States continued leadership in space, and ensuring freedom of action in space for all.

My time at AGSL remains some of the best and most influential of my life, where I was able to learn by doing, and sometimes failing, which shaped me into the engineer I am today. Where else does one have the opportunity to participate in designing, building, and flying two spacecraft missions while at college? Being allowed to make mistakes and learning from them teaches one far more than any textbook ever

could. AGSL is a true gem of the Texas A&M engineering program, and every student across the country should be so lucky to get to participate in such a program.

Figure 111: Signatures and Aggie Rings of AGSL Members and NASA Management displayed on AGS4. Also shown (top) is the Aggie Ring of Civil Engineering graduate Patrick Brand ('81) whose father, Vance D. Brand, carried it into space as commander of Space Shuttle Columbia Mission STS-5 in November 1982.

REFERENCES

1. Butow, Brig. Gen. Steven J., et al. *State of the Space Industrial Base 2020*, United States Space Force, Jul. 2020.
2. Mattis, Jim. "Summary of the National Defense Strategy of the United States of America." U.S. Department of Defense, Jan. 2018.
3. Harrison, Todd, et al. *Space Threat Assessment 2019*, The Center for Strategic and International Studies, Apr. 2019.
4. Garamone, Jim. "Esper: Air Force, Space Force Leading Charge to New Technologies." *DOD News,* U.S. Department of Defense, 16 Sept. 2020, https://www.defense.gov/Explore/News/Article/Article/2349408/esper-air-force-space-force-leading-charge-to-new-technologies/
5. Erwin, Sandra. "Raymond calls out Russia for 'Threatening Behavior' in Outer Space." *SpaceNews,* SpaceNews, 12 Feb. 2020, https://spacenews.com/raymond-calls-out-russia-for-threatening-behavior-in-outer-space/
6. National Academies of Sciences, Engineering, and Medicine. 2016. *Achieving Science with CubeSats: Thinking Inside the Box.* Washington, DC: The National Academies Press. doi:10.17226/23503.
7. California Polytechnic SLO, *CubeSat Design Specification*. San Louis Obispo, CA: California Polytechnic

8. NASA CubeSat Launch Initiative, *CubeSat 101: Basic Concepts and Principles for First-Time CubeSat Developers*. NASA, Oct. 2017.

9. Reed, Helen L., *Final Report: NNJ06HG15G AggieSat2: Autonomous Rendezvous and Docking*, Texas A&M Engineering Experiment Station, Dec. 2016.

10. Fury, Kris. "Launching Traffic Cameras Into Space." *Lawrence Livermore National Laboratory Science & Technology Review*, Apr. 2012, pp. 4-10.

11. Wertz, James R, David F. Everett, and Jeffery J. Puschell. *Space Mission Engineering: The New SMAD*. Hawthorne, CA: Microcosm Press, 2011. Print.

12. "STARE (Space-Based Telescopes for the Actionable Refinement of Ephemeris)." *STARE - EoPortal Directory - Satellite Missions*, https://directory.eoportal.org/web/eoportal/satellite-missions/s/stare.

13. Vincent Riot, Willem de Vries, Lance Simms, Brian Bauman, Darrell Carter, Don Phillion, Scot Olivier, "The Space-based Telescopes for Actionable Refinement of Ephemeris (STARE) mission," Proceedings of the 27th AIAA/USU Conference, Small Satellite Constellations, Logan, Utah, USA, Aug. 10-15, 2013, paper: SSC13-XI-11.

14. NASA, *NASA-ESPC-2903-B JEM Payload Accommodation Handbook*, NASA, Mar. 2014.

15. NASA, *JSC 27301F Materials and Processes Selection, Control, and Implementation Plan for JSC Flight Hardware*, NASA, Aug. 2009.

16. NASA, *SSP 50835D ISS Pressurized Volume Hardware Common Interface Requirements Document*, NASA, Apr. 2013.
17. Destain, Adelin. AGS4-05-05-004-R0 Structural Analysis Report, AggieSat Lab, 15 Jul. 2015.
18. NASA, "Cargo_Tool_revK-Dragon Environment.xlsx", JSC Engineering Technology & Science Contract, March, 2015.
19. NASA, *NASA-STD 8739.3 Soldered Electrical Connections*, NASA, 6 Jun. 2008.
20. Cooper, Jake. *AGS4-05-05-006-R0 Thermal Analysis Report,* AggieSat Lab, 16 Jun. 2015.
21. Graves, John Thomas, et al. "AggieSat2 Student Satellite Mission." *50th AIAA Aerospace Sciences Meeting including the New Horizons Forum and Aerospace Exposition,* AIAA, 9-12 Jan. 2012, AIAA 2012-0434.
22. Technologic Systems, *TS-7800,* Technologic Systems Inc., 5 Feb. 2021, https://docs.embeddedarm.com/TS-7800
23. Kim, Bong Tae, *Rechargable Lithium Ion Battery Model: ICR18650 C2 2800mAh,* LG Chem, 10 Apr. 2014.
24. Spectrolab, *Ultra Triple Junction,* Spectrolab, 16 Jul. 2014.
25. Graves, John Thomas. *Small Satellite Applications of Commercial Off the Shelf Radio Frequency Integrated Circuits,* Texas A&M University, Dec. 2011.
26. Kenwood Corporation, *TH-D72A Manual,* Kenwood Corporation, 15 May 2011.
27. Texas Instruments, *CC1101 Low Power Sub-1 GHz RF Transceiver,* Texas Instruments, Nov. 2011.

28. Stealth Microwave, *SM04093-36HS,* Stealth Microwave Inc. Jul. 2014.
29. Digi International, 9*Xtend -PKG-R RS232/422/485 RF Modem,* Digi International, Mar. 2007.
30. NewSpace Systems, *Sun Sensor Datasheet,* NewSpace Systems, 2020.
31. VectorNav, *VN-100 User Manual,* VectorNav, 2015.
32. Sinclair Interplanetary, *Microsatellite Reaction Wheels (RW3-0.06),* Sinclair Interplanetary, 2019.
33. Davis, Jason. *LightSail update: Of booms and Pretty Pictures,* The Planetary Society, 1 Jul. 2014.
34. Perez, Joe. *AGSL-3108-200-001Quality Management System,* AggieSat Lab, 27 Mar. 2006.
35. NASA, *NASA-STD-6001B Outgassing Standards,* NASA, 26 Aug. 2011.
36. Tucker, Andrew L. *AGSL-3105-200-001 Staking and Coating Procedure Rev A,* AggieSat Lab, 30 Jun. 2014.
37. NASA, *NASA-STD-8739.1A Workmanship Standard for Polymeric Application on Electric Assemblies,* NASA, 4 Mar. 2008.
38. Tucker, Andrew L. *AGSL-3105-200-002 Thread Locking Compound Procedure,* AggieSat Lab, 18 Aug. 2014.
39. NASA, *NSTS 08307 Revision A Criteria for Preloaded Bolts,* NASA, 6 Jul. 1998.
40. Davidoff, Martin. *The Radio Amateur's Satellite Handbook, 4th ed.,* The American Radio Relay League, 2003.

41. U.S Department of Commerce, *Man-Made Noise Power Measurements at VHF and UHF Frequencies,* Department of Commerce NTIA Report 02-390, 2001.

APPENDIX A

LINK BUDGET COMPONENTS AND EQUATIONS

Units

This link budget is based in the decibel milliwatt (dBm). Transmit power in Watts is converted into the logarithmic dBm, and all gains and losses of the system are added. The final result, the signal-to-noise ratio (Eb/No), tells how much signal strength is left once all processing has taken place, and indicates how well the transmissions will go through. Power is converted into dBm through the equation:

$$\boldsymbol{dBm = 10 * \log(1000 * Transmit\ Power[W])} \quad \textbf{(1)}$$

EIRP

The equivalent isotropic radiated power (EIRP) is how much power the signal has after the initial gains and losses from all components (in dBm) between the transmit radio and antenna have been added together. It is calculated through the following equation:

$$\boldsymbol{EIRP\ (dBm) = 10 * \log(1000 * Transmit\ Power\{W\}) - System\ Losses + System\ Amplification + Antenna\ Gain - Pointing\ Loss - VSWR\ Loss} \quad \textbf{(2)}$$

This number is the starting power when the signal leaves the antenna. System loss was estimated [11], while pointing losses were calculated as explained in the following section. Gain values are determined by the selected hardware.

Pointing Loss

Pointing loss occurs when the main lobe of the antenna radiation pattern does not point at the receiving antenna. There is an angle called the half power beamwidth (HPB), at which the loss is 3 dB. For monopoles, this is roughly 45^o, 21^o for Yagi's, and 80^o for patch antennas [11]. The equation to calculate the pointing loss is [11] :

$$\boldsymbol{Pointing\ Loss = -12 * (\frac{Pointing\ Error}{HPB})^2\ dB} \quad \textbf{(3)}$$

The HPB is the "cone" inside which the signal is still above half strength. The actual pointing offset at which the signal drops to half power is actually 0.5*HPB. Pointing error for the ground station antenna rotor was measured to be approximately 4^o, which yields a ground station pointing loss of 0.44 dB.

The current mission plan is to use the ADCS torque coils to prevent the spacecraft from wildly tumbling through its orbit, and keep the antennas at an orientation suitable for ground passes. While not as efficient as actively pointing with the reaction wheels, it is believed from experience with magnetic control on AGS2 that adequate spacecraft control can be maintained for ground communication, though some pointing loss will be incurred. The 20^o used for spacecraft pointing loss in the budgets below comes from an initial estimate of pointing ability from the ADCS team.

The pointing loss from the LDR and beaconing will likely be significantly higher when not performing an HDR pass. For monopoles, depending on the pointing error, pointing losses can range from 0-48 dB, with 48 dB occurring at a pointing error angle

of 90^o. With the current setup, the UHF downlink can tolerate a pointing error of up to 47.6^o before the link margin drops to 0 dB. Similarly, the VHF uplink system link margin drops to 0 dB when the pointing error is 66.5^o. These values are calculated using the signal margin at 10^o elevation, and as the spacecraft range decreases through the pass, the signal strength increases and more pointing error is tolerable.

Free Space Loss

The propagation loss is the combined loss from free space losses (the natural loss in signal strength over distance) and atmospheric and precipitation losses. Free space loss is calculated through the following equation [11]:

$$\boldsymbol{Free\ Space\ Loss = 20 * \log\left(\frac{4\pi R}{\lambda}\right)\ dB} \qquad \textbf{(4)}$$

where R is the link range in meters, and λ is the signal wavelength in meters. In the above budgets, the link range used the distance from the ground station to a point 10 degrees above the horizon at the mean altitude of the ISS (400 km). This is an estimate for the furthest feasible distance for communication with the satellite due to line of sight limitations. The effective received power (ERP) is the value of the signal strength after propagation loss.

Atmospheric and Precipitation Loss

Atmospheric losses were calculated with the help of [11] through the equation:

$$\boldsymbol{Atmospheric\ Loss = 0.3/\sin\beta} \qquad \textbf{(5)}$$

where β is the elevation angle and 0.3 is the loss in dB at 90 degrees elevation. Loss due to precipitation, or moisture in the atmosphere, is based on numbers from [11].

Polarization Loss and Antennas

Total polarization loss occurs when a linearly polarized transmitter and receiver are oriented at 90^o with respect to each other. When they are at this orientation, the loss is practically infinite because no part of the sinusoidal shaped signal can enter the receiver. When their orientation is at 0^o, there is no polarization loss, and the loss varies with their orientation angle. A circular to linear scheme, and vice versa, avoids these problems, since the signal always has an appropriate path to follow on the receiving antenna. To avoid the possibility of this infinite loss, and to remove the need for attitude control in one axis of stabilization, circularly polarized antennas were selected for the ground station. Circular polarization allows the signal to travel essentially in a corkscrew pattern, which means that some portion of the signal will always enter the receiver no matter the orientation angle. Because of this, the maximum polarization loss is 3 dB, and is reflected in the link budgets [40].

To get this circular polarization pattern and a high gain, a Yagi antenna with elements positioned at 90^o to each other will be used for all systems. M2 Antenna makes such products, and their model 436CP42UG offers 18.9 dB gain for UHF frequencies. This antenna was used for the AGS2 mission, was already installed at the Riverside ground station, and will be used for the HDR downlink because of its high gain. The M2 2MCP14 was selected for the LDR VHF antenna because of its short length (to avoid guy wire interference) that delivers 12.3 dB gain. The M2 436CP30 was selected for the LDR UHF system antenna since it is smaller in form factor than the HDR antenna, but still provides adequate gain, 15.5 dB. A reason that all of these antennas were selected is

because they are circularly polarized. Three separate antennas were selected to avoid switching problems and signal loss.

Receive Amplification

In calculating the gains and losses for each system, it became apparent that the radio systems would need amplification to have good margin. Low noise amplifiers (LNA) condition the signal such that the noise downstream of the amplifier is quieted so the received signal is not dwarfed by noise losses. The Amplitech 00250050-0810-D4 offers 25 dB gain to the amateur UHF frequencies, and has been used by AggieSat Lab in previous tests. This LNA will be used for the HDR and LDR UHF systems.

Noise Temperature

Noise temperature values detailed in this section feed into the noise power calculations in the following section.

The first step in calculating total noise temperature is to calculate the receiver noise figure (NF). The formula to calculate the NF is as follows [25]:

$$\boldsymbol{Rx\ Sensitivity = P_{BER} + RxNF + Noise\ Floor} \quad \textbf{(6)}$$

where P_{BER} is the decibel margin required for transmissions with 10^{-5} bit error rate (BER), and the noise floor is calculated through the equation [25]:

$$\boldsymbol{Noise\ Floor = -173.8\ dBm + Noise\ Bandwidth\ dB} \quad \textbf{(7)}$$

Noise bandwidth and its requirements are discussed in the following section. The value -173.8 dBm is the noise temperature value of a 50 Ohm resistor at 290 K,

which approximates a standard radio receiver at room temperature, and the noise bandwidth is a function of the data rate (as discussed in section 3.9 [25]).

The two equations above are solved to find the Rx NF in dB. With the Rx NF known in dB, it is converted out of logarithmic scale by

$$\boldsymbol{NF = \frac{10^{(NF)}}{10}} \quad \textbf{(8)}$$

The non-logarithmic NF is then converted to noise temperature through the *noise figure equation* [11]:

$$\boldsymbol{NF = 1 + \frac{T_R}{T_o}} \quad \textbf{(9)}$$

where T_R is the receiver noise temperature, and T_o is the reference temperature of 290 K. The noise temperature for the low noise amplifier (if used) is calculated in the same manner (with the manufacturers NF). The system noise temperature for a single amplifier is the given by the *Friis equation* stated below [11]:

$$\boldsymbol{T_{system} = T_{LNA} + \left(\frac{T_{RX}}{G_{LNA}}\right)} \quad \textbf{(10)}$$

This temperature is then converted back into the system NF through the *noise figure equation.* **Note***:* This value will be in non-logarithmic form.

The ambient NF value is converted to non-logarithmic form, and then is added to the system NF. This total NF can then be converted to temperature through the *noise figure equation*. This total noise temperature is the effective temperature, and is used in calculating the total noise power (section 3.9 [25]).

In the calculation of link margin, the ambient NF used for the ground station is that of a residential area (3 dB) [41]. Due to its location away at the Riverside Campus, it is believed that the NF will actually be closer to that of a rural setting (-3 dB) [41]. Crosslink assumes the average noise temperature of the Earth, 290 K (3 dB NF) [11], is being seen by the crosslink antenna.

Noise Power

The noise power is the effect of losses due to system components and how they operate. The noise power (No) is calculated through the equation:

$$\boldsymbol{No = 10 * \log(1\,000 * k) + 10 * \log B + 10 * \log T} \qquad \textbf{(11)}$$

where k is the Boltzmann constant (1.38*10^-23 J/K), B is the signal bandwidth (Hz), T is the system noise temperature in Kelvin. The Boltzmann constant is multiplied by 1000 to convert into dBm, which allows the units to match up with those used in the transmit portion of the link budget. Because the VHF and UHF systems operate on AFSK and FSK respectively, their noise bandwidth is twice the data rate [11].

Signal to Noise Ratio Calculations

First, the transmit power is converted to decibel-milliwatts, and used to calculate the EIRP. Then the propagation loss is calculated, and subtracted from the EIRP. The receive system gains and losses are added and subtracted to obtain the effective received power (ERP). The signal-to-noise ratio (Eb/No) is defined as:

$$\boldsymbol{E_b/No = ERP - Noise\ Power} \qquad \textbf{(12)}$$

The Eb/No's required to ensure a bit error rate of 10^{-5} for each system were obtained from [11] based on the modulation scheme, and are listed in the budgets below. The system margin is how much signal strength is left over once the required Eb/No is subtracted from the received Eb/No. The higher the margin, the better the signal strength will be, and the likelihood of transmission errors is lower.

Noise Temperature Calculations

Table 32: LDR VHF Noise Temperature

LDR VHF				
Receiver Noise Calculation				
Sensitivity = P(BER) + Rx NF + Noise Floor				
Sensitivity	-121.00	dBm		
Noise Floor	-140.00	dBm		
Req. P(BER)	13.30	dB		
Rx Noise Figure	5.70	dB		
	Rx NF (dB)	Rx NF	Tr (K)	Gain
Receiver	5.70	3.713546	786.9282	
System Noise Temperature	786.93	K		
System Noise Figure	3.71			
Residential Noise Figure	3.00	dB		
	2.00			
Total Noise Figure	4.71			
Total Noise Temperature	**1075.55**	**K**		

Table 33: LDR UHF Noise Temperature

LDR UHF				
Receiver Noise Calculation				
Sensitivity = P(BER) + Rx NF + Noise Floor				
Sensitivity	-121.00	dBm		
Noise Floor	-130.97	dBm		
Req. P(BER)	13.30	dB		
Rx Noise Figure	-3.33	dB		
	Rx NF (dB)	Rx NF	Tr (K)	Gain (dB)
LNA	0.80	1.202264	58.65669	25
Receiver	-3.33	0.464193	-155.384	
System Noise Temperature	52.44	K		
System Noise Figure	1.18			
Residential Noise Figure	3.00	dB		
	2.00			
Total Noise Figure	2.18			
Total Noise Temperature	**341.07**	**K**		

Table 34: HDR Noise Temperature

HDR				
Receiver Noise Calculation				
Sensitivity = P(BER) + Rx NF + Noise Floor				
Sensitivity	-95	dBm		
Noise Floor	-118.93	dBm		
Req. P(BER)	13.3	dB		
Rx Noise Figure	10.63	dB		
	Rx NF (dB)	Rx NF	Tr (K)	Gain (dB)
LNA	0.8	1.202264	58.65669	25
Receiver	10.63	11.54992	3059.475	
System Noise Temperature	181.04	K		
System Noise Figure	1.62			
Residential Noise Figure	3.00	dB		
	2.00			
Total Noise Figure	2.62			
Total Noise Temperature	**469.66**	**K**		

Table 35: Crosslink Noise Temperature

Crosslink				
Receiver Noise Calculation				
Sensitivity = P(BER) + Rx NF + Noise Floor				
Sensitivity	-110	dBm		
Noise Floor	-130.97	dBm		
Req. P(BER)	13.30	dB		
Rx Noise Figure	7.67	dB		
	Rx NF (dB)	Rx NF	Tr (K)	Gain
Receiver	7.67	5.843846	1404.715	
System Noise Temperature	1404.72	K		
System Noise Figure	5.84			
Earth Background Noise Figure	3.00	dB		
	2.00			
Total Noise Figure	6.84			
Total Noise Temperature	**1693.34**	**K**		

APPENDIX B

CUSTOM OMNETICS WIRE HARNESS EXAMPLE

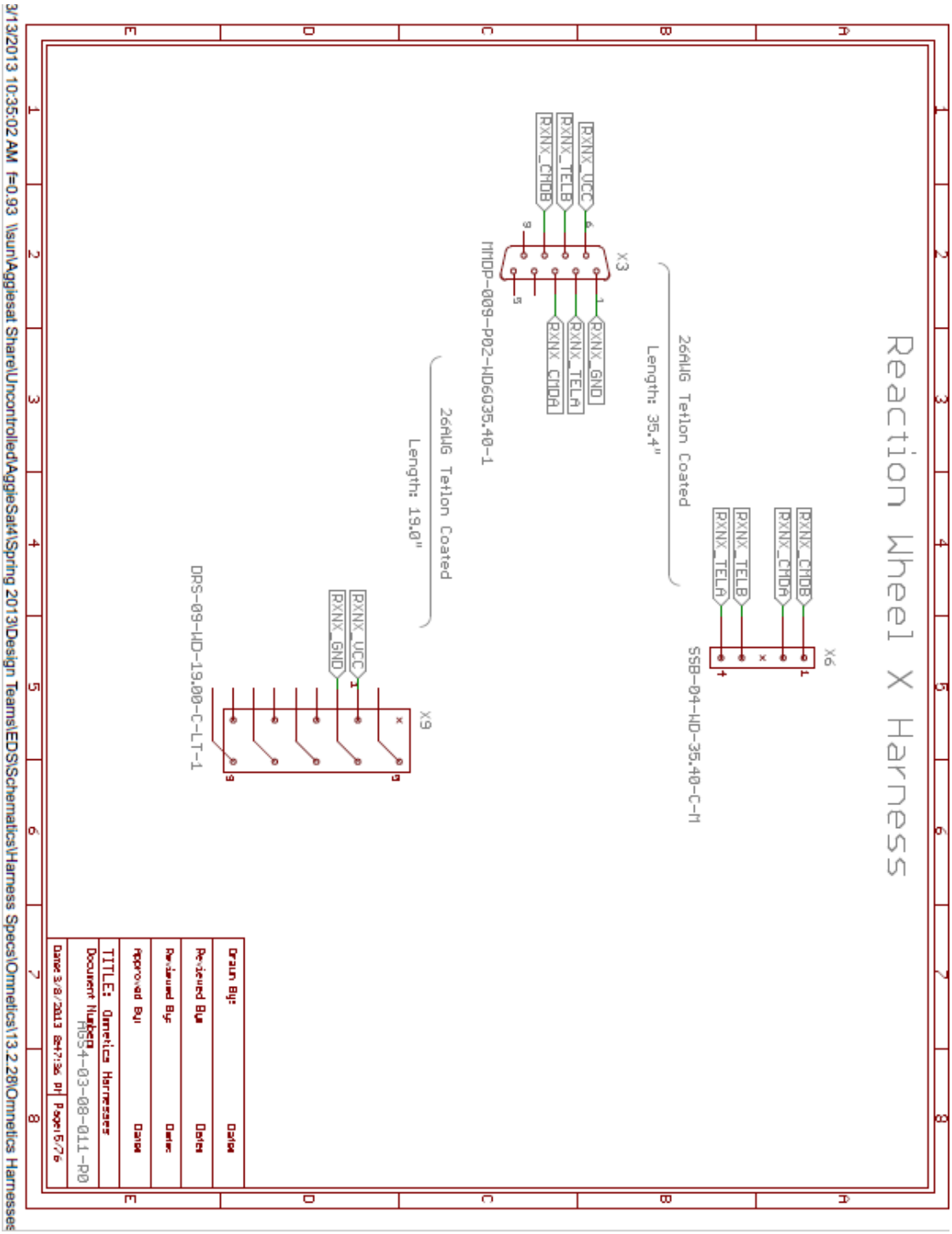

APPENDIX C

FASTENER TORQUE CALCULATION

This appendix details how threaded fastener torque levels were calculated for AGS4, and is based on material from the NASA standard NSTS-08307 Criteria for Preloaded Bolts [39]. This section provides an example for calculating the torque necessary to hold the battery boxes to the AGS4 bus.

Variables

Table 36: Fastener Properties

Variables	Name	Example	Note
TPI	Threads Per Inch	#4-40 has 40 threads per inch	
D	Major Diameter	0.112" for #4-40	
TP	Thread Pitch	1/TPI	
K_b	Bolt Stiffness (Shear Strength)	11000 ksi for Stainless Steel	Fastener material property
E_b	Young's Modulus	$2.92*10^7$ psi for A-286 Steel	Fastener material property
α_b	Coefficient of Thermal Expansion	$9.11*10^{-6}$ /°F for A-286 Steel	Fastener material property
UTS	Ultimate Tensile Strength	87000 psi for A-286 Steel	Fastener material property
A_t	Tensile Area	$0.00616in^2$ for #4-40	$\pi/4*(D-0.938194*TP)^2$
PA_t	Max. Bolt Load		UTS * A_t

Table 37: Heli-Coil® Properties

Variables	Name	Example	Note
L_{hc}	Heli-Coil® Length	0.224" for an MS21209-C0420	Found in Heli-Coil® manual
D_{pmin_ext}	Pitch Diameter	0.1283" for an MS21209-C0420	Found in Heli-Coil® manual
T_P	Locking Torque	48oz-in for #4-40 Heli-Coil®	Found in Heli-Coil® manual

Table 38: Joint Properties

Variables	Name	Example	Note
F_{su}	Ultimate Shear Strength	Aluminum 6061-T6 30000psi	Joint material property
nL_1	Force Application Point Distance	Application specific	1/2 of each pinched material
L_1	Total Joint Thickness	Application specific	Pinched material + Thread engagement length
K_j	Joint Stiffness (Shear Strength)	3770 ksi for 6061-T6	Joint material property
E_j	Young's Modulus	$1.00*10^7$ psi for 6061-T6	Joint material property
α_j	Coefficient of Thermal Expansion	$1.31*10^{-5}$/°F for 6061-T6	Joint material property

Calculating External Loads

The external loads that any fastener on an assembly could experience should be determined from the root mean square acceleration load the mass being fastened will experience, in this case that of the launch vehicle. This resultant force is then divided over the minimum number of fasteners that secure the joint.

Load Calculation Formula/Method

The external load P(lbf) is calculated through the following equation:

$$\boldsymbol{P = m * g * 3 * G_{rms} / N_s} \quad \textbf{(13)}$$

m - Assembly mass (kg)

g - Earth gravitation acceleration (9.8 m/s^2)

G_{rms} - Root mean square acceleration of launch vehicle, (3.2 g's)

N_s – Number of screws (dimensionless)

The "3" in the above equation represents the 3σ distribution from the SpaceX PSD curve, in order to account for the statistical highest loads that could be seen (~ 9 g's).

Thermal Loads

Thermal loads depend on the temperature extremes the spacecraft will experience, as well as the temperature at which the bolts were fastened into the assembly. Temperature change will cause the fastener and joint to expand or contract, increasing or decreasing the load on the bolt. In order to determine the temperature extremes experienced on orbit, a basic thermal analysis must be performed. These temperature changes are used to determine how much the bolt load changes.

Thermal Analysis

The thermal analysis performed for AGS4 was modified to calculate the effects of a worst case scenario, with AGS4 directly between the Earth and Sun, with the Sun shining directly on the -Z panel where the batteries are mounted, and the reflections from Earth striking the +Z panel. Panels were allowed to radiate to the Earth and free space as described in the thermal analysis, and the internal components and panels were allowed to radiate to each other. To model the worst case scenario where thermal stresses are highest, this configuration was allowed to reach steady state conditions. SolidWorks® allows the user to probe locations in the model to find the calculated temperature at that point.

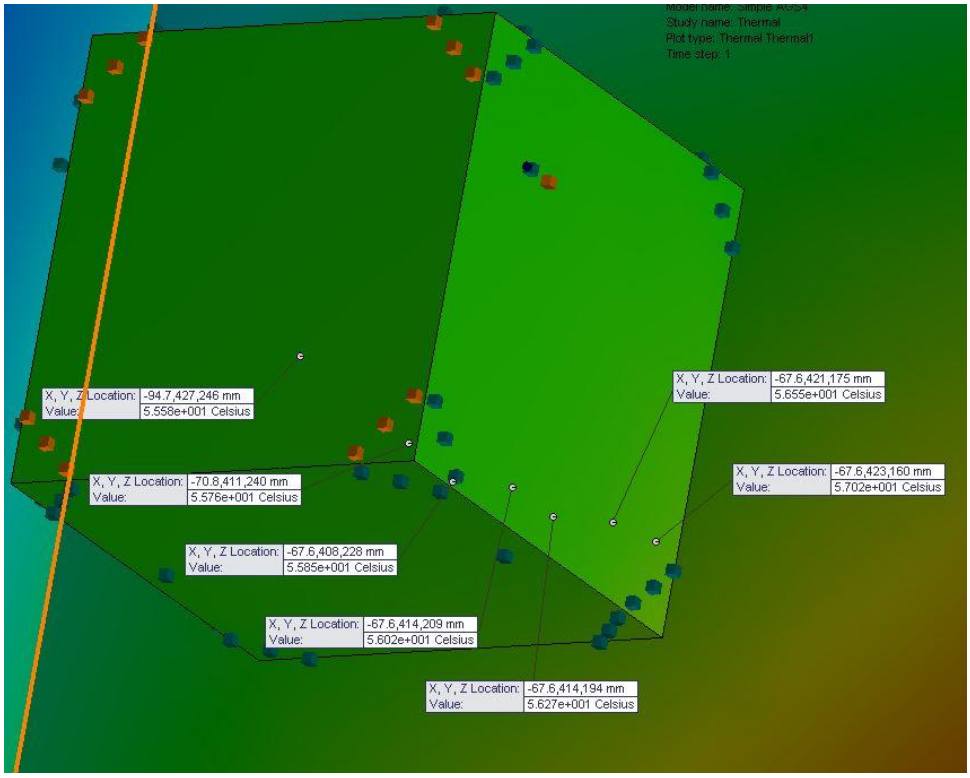

Figure 112: Battery Box Thermal Analysis Probing

Data of immediate usefulness to bolt load calculations is the total temperature the fasteners in the assembly will reach. Probing the results determined that the maximum temperature reached by the boxes and fasteners was 57 °C (134.6 °F). This value is within the survivable range for the batteries and operation. The worst cold case from the dynamic thermal analysis calculated that the lowest temperature these boxes should experience is -9.7 °C (14.5 °F).

Thermal Preload Calculation

An important factor in determining thermal bolt loads is the temperature at which the fastener was installed. They should be at the same temperature of AGSL at

installation, which was roughly 70°F (21°C), approximately room temperature. Since NSTS 08307 uses U.S. customary units, these calculations will be in that system as well.

$$\Delta T_{hot} = T_{hot} - T_{Assembly} = 134.6 - 70 = 64.6°F \quad (14)$$

$$\Delta T_{cold} = T_{cold} - T_{Assembly} = 14.5 - 70 = -55.5°F \quad (15)$$

These temperature differences are used in the following equations to find the positive and negative thermal loads respectively.

$$P_{thr}^{pos} = E_b * A_t * \left((\alpha_1 - \alpha_b) * L_1 + (\alpha_2 - \alpha_b) * L_2\right) * \Delta T_{hot}/(L_1 + L_2) \quad (16)$$

$$P_{thr}^{neg} = E_b * A_t * \left((\alpha_1 - \alpha_b) * L_1 + (\alpha_2 - \alpha_b) * L_2\right) * \Delta T_{cold}/(L_1 + L_2) \quad (17)$$

L_1 and L_2 represent the thickness of materials being clamped, and are depicted in the figure below. Both have a value of ¼" for the battery boxes.

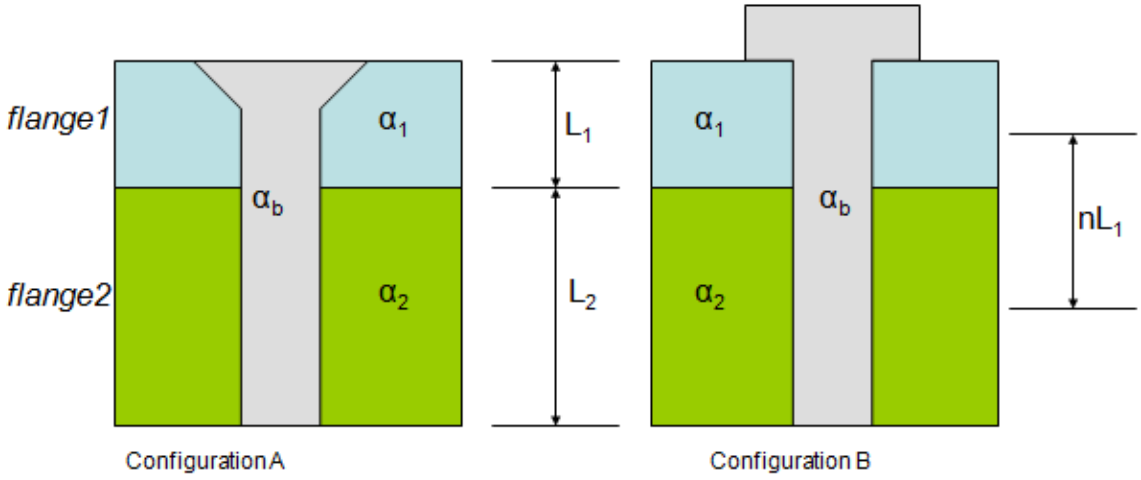

Figure 113: Fastener Dimension Diagram

Using the above equations and the material properties listed in Table 36, Table 37, and Table 38, the resultant thermal loads are as follows:

Table 39: Battery Box Thermal Preload

Thermal Preload		
L_1	0.25	in.
L_2	0.25	in.
P_{thr}^{pos}	46.35	lbf
P_{thr}^{neg}	-39.82	lbf

Calculating Preload

Based on the thermal loads, major diameter of the bolt, uncertainty coefficients, and arbitrary torque values, the preload minimum and maximum values can be determined. A spreadsheet was used to calculate these values over a wide range of torque values according to the following equations, as preload depends on the applied torque. This method will prove useful for calculating other parameters detailed in following sections.

$$\boldsymbol{PLD_{max} = \frac{(1+\Gamma)T}{K^{typ}D} + P_{thr}^{pos}} \quad \textbf{(18)}$$

$$\boldsymbol{P_{loss} = 0.05 * PLD_{max}} \quad \textbf{(19)}$$

$$\boldsymbol{PLD_{min} = \frac{(1-\Gamma)(T - T_p)}{K^{typ}D} + P_{thr}^{neg} - P_{loss}} \quad \textbf{(20)}$$

where:

PLD_{max} - Maximum preload (lbf)

PLD_{min} - Minimum preload (lbf)

P_{loss} - Preload loss

Γ – Uncertainty factor (0.35 used for unlubricated bolts)

K^{typ} - Nut factor – generally 0.2 for most applications

T - Applied torque value

Table 40: Uncertainty Factor Γ

Torque Measurement of Unlubricated Bolts	±35%
Torque Measurement of Cadmium Plated Bolts	±30%
Torque Measurement of Lubricated Bolts	±25%
Hydraulic Tensioner Installation	±15%
Preload Indicating Washers	±10%
Ultrasonic Measurement Devices	±10%
Bolt Elongation Measurement	±5%
Instrumented Bolts	±5%

Spreadsheet Calculation

A spreadsheet was created that listed torque values incremented in tenths of an in-lb ranging from 1.0 to 10.0. Other values should be attempted depending on the application. The formulas for maximum, loss, and preload were used with each torque value to calculate a maximum and minimum preload at that torque. The margin of safety (see subsequent section) was calculated for each of these preloads to determine the acceptable range of torque values for installation of the bolts.

Hole Shear Out Force Calculations

Knowing that the ultimate shear strength of aluminum is 30000 psi, a rough but conservative estimate for the maximum hole shear out strength (PA_s) is as follows:

$$\boldsymbol{PA_s = F_{su} * \pi * D_{pmin\_ext} * L_e * \frac{1}{3}} \quad \textbf{(21)}$$

where L_e is the length of thread engagement, which is determined by:

$$\boldsymbol{L_e = L_{hc} - 1.5 * TP} \quad \textbf{(22)}$$

The 1.5 factor in the above equation is due to the length of the locking feature of the Heli-Coil® (1 thread width), and the distance from the top of the tapped hole to the Heli-Coil® threads (0.5 thread width). Adding the values from both of these factors yields the resultant 1.5 threads.

Using the above equations for a #4-40 screw and Heli-Coil®, and the material properties listed in Table 36, Table 37, and Table 38, the hole shear out strength is calculated.

Margin of Safety

Two tensile margin of safety (MS) criteria must be met for each bolt in the assembly:

$$\boldsymbol{MS_{T1} = \frac{PA_t}{(SF*P)} - 1 \geq 0} \quad \textbf{(23)}$$

$$\boldsymbol{MS_{T2} = \frac{PA_t}{P_b} - 1 \geq 0} \quad \textbf{(24)}$$

where SF is the desired factor of safety, P is the external load, and PA_t is the maximum allowable tensile strength of the bolt. A SF = 3 was chosen to ensure that the load could be handled. P_b, the axial bolt load is determined by:

$$\boldsymbol{P_b = PLD_{max} + n * \Phi * (SF * P)} \quad \textbf{(25)}$$

$$\boldsymbol{\Phi = \frac{K_b}{K_b + K_j}} \quad \textbf{(26)}$$

$$\boldsymbol{n = \frac{nL_1}{L_1}} \quad \textbf{(27)}$$

In the spreadsheet described above, additional columns were added for both margin of safety criteria and the value of P_b. These also change with the incrementing torque values, with the exception of the MS_{T1}, which is constant with torque.

In addition to the tensile margin of safety, two hole shear out margin of safety criteria must be met for each joint in the assembly:

$$\boldsymbol{MS_{S1} = \frac{PA_s}{(SF*P)} - 1 \geq 0} \quad \textbf{(28)}$$

$$\boldsymbol{MS_{S2} = \frac{PA_s}{P_b} - 1 \geq 0} \quad \textbf{(29)}$$

Calculation and Results

The above equations are used to calculate the following results for the fastener joint parameters.

Table 41: Joint Calculation Results

Battery Box Mass	M	2.9 (1.3)	lbf (kg)
Number of Fasteners	N_S	14	
External Load (per fastener)	P	1.96	lbf
Positive Thermal Load	P_{thr}^{pos}	46.35	lbf
Negative Thermal Load	P_{thr}^{neg}	-39.82	lbf
Hole Shear out strength	PA_s	761	lbf
Tensile Margin of Safety-1	MS_{T1}	89.9	lbf
Shear Margin of Safety-1	MS_{S1}	128.2	lbf

With the above quantities calculated, the preload, axial bolt force, and two remaining margins of safety for each fastener torque value can be calculated. These quantities are investigated over a range of torque values to find a value where both remaining margin of safety values are greater than zero, and both PLD_{max} and PLD_{min}

are positive. The range of acceptable values often encompasses several in-lb. From personal experience in automotive applications, a value towards the upper third of acceptable values is usually chosen as it helps to make sure the fastener stays tight, while leaving margin. The table below shows some of the torque values investigated and the associated margins. A value of 7 in-lb was selected as it meets the criteria mentioned above.

Table 42: Preload and Margin of Safety for Fastener Torque

Torque Value (in*lbs)	**PLD_{max}**	**Pl_{oss}**	**PLD_{min}**	**P_b**	**MS_{T2}**	**MS_{S2}**
4	287.4169	14.37085	-10.661	288.267781	0.858414498	1.640229959
5	347.6848	17.38424	15.34344	348.535638	0.537062397	1.183688405
5.5	377.8187	18.89094	28.34567	378.669567	0.414745389	1.009913916
6	407.9527	20.39763	41.3479	408.803495	0.310460967	0.861758132
6.5	438.0866	21.90433	54.35013	438.937424	0.220495211	0.733944727
7	468.2205	23.41103	67.35237	469.071352	0.142088556	0.622553217
7.5	498.3544	24.91772	80.3546	499.205281	0.073147749	0.524609736
8	528.4884	26.42442	93.35683	529.33921	0.01205619	0.4378176
8.5	558.6223	27.93111	106.3591	559.473138	-0.042454432	0.360374931
9	588.7562	29.43781	119.3613	589.607067	-0.091393143	0.290848219